BODLEIAN LIBRARY OXFORD
DEPOSITED
THESIS
1-4-68

THERMODYNAMIC STUDIES OF DISORDER IN INORGANIC SOLIDS

A thesis submitted for the degree of

Doctor of Philosophy in the University of Oxford

by

R. G. LINFORD B.A.

New College.

October, 1967

Inorganic Chemistry Lab.,

South Parks Road,

Oxford.

I would like to thank all my colleagues, especially Robert Clay and Charles Waterfield for their help, patience and humour. I would also like to thank my typist, Elizabeth McAlinden, for wrestling with my illegible writing, and the laboratory technical staff for frequent and kindly assistance.

I am most grateful to Dr. G. R. Wilkinson of Kings College, London, for making available unpublished data on the lattice vibrations of calcite, and to Dr. R. A. Robie of the U.S. Geophysics survey for help in calculating Debye temperatures from elastic constant data.

Finally, I owe a very great debt of gratitude to my supervisor, Dr. L. A. K. Staveley, for his constant guidance, help and optimism during this work.

CONTENTS

I. INTRODUCTION 1

Object of this research. 8

II. DESIGN AND CONSTRUCTION OF THE CALORIMETER

1) The word 'Calorimeter' 16

2) General description 16

a) The sample container 21

b) The adiabatic shield 24

c) The cryostat 27

d) The helium economiser 29

e) The pumping system 30

f) The platinum thermometer 31

g) The measuring circuits 32

3) Temperature range and measurement 39

4) Automatic control 44

III. EXPERIMENTAL PROCEDURE

1) Filling the sample container 49

2) Handling the refrigerants 54

a) A hydrogen run 54

b) A helium run 55

c) A nitrogen run 56

3) Calculation of results 57

a) Preamble 57

Lengths of heating period 59

b) Corrections 60

c) A typical point 62

d) Presentation of results, and smoothing procedures 68

4) Leaks and minor setbacks 70

IV. EMPTY SAMPLE CONTAINER CALIBRATION

1) Heater resistances 75

2) The heat capacity of the empty sample container 76

3) The heat capacity of a standard substance-Benzoic Acid. 81

V. CALCITE AND ARAGONITE

1) Preparation and Analysis 87

2) Results 89

Aragonite 89

calcite 94

3) Discussion 99

Lattice vibrations 103

Calculation of Cp for calcite 106

Discussion of Cp calculated 109

Calculation of acoustic Debye Temperature 111

Conclusion 112

Early measurements - Summary 112

VI. DIAMMINO MERCURIC CHLORIDE

1) Preparation and Analysis 115

2) Results 117

3) Calculation of standard entropy of $Hg(NH_3)_2Cl_2$ 124

Interpretation of the standard entropy 132

Residual entropy in $Hg(NH_3)_2Cl_2$, and the dimer problem 135

Substances for further study 138

VII. ANHYDROUS SODIUM CARBONATE

1) Preparation and Analysis 140

2) Results 142

3) Discussion 148

Residual entropy in the hydrates of sodium carbonates 148

Interpretation of residual entropy in $Na_2CO_3 \cdot 10H_2O$ 152

Lack of disorder in $Na_2CO_3 \cdot H_2O$ 155

Residual entropy in hydrates - summary 156

APPENDIX 158

REFERENCES 159

ABSTRACT 165

List of Diagrams

		Facing Page
1.	Structures of, and environment of CO_3^{2-} in, calcite and aragonite	10
2.	The Calorimeter Console (photograph)	16
3.	The sample container	21
4.	The adiabatic shield	24
5.	The cryostat	27
6.	The Helium economiser	29
7.	Thermometer, and sample container heater circuit	36
8.	Shield heater (automatic control) circuit	39
9.	Thermometer calibration in the region of 90°K	43
10.	Fore and after drifts.	57
11.	A typical chart trace	60
12.	Deviations from a Smoothed curve, of the experimental points of a) an early run, benzoic acid, and b) a late run, Na_2CO_3.	83
13.	Comparison of smoothed molar heat capacities of benzoic acid	85
14.	Heat capacity plot of Cp vs T for calciteand aragonite	97
15.	Entropy plot of C_p/T vs T for calcite and Aragonite	98
16.	$C_p - C_v$ and C_v (internal modes) for calcite and aragonite	103

17. Optical modes of lattice vibrations for calcite. 104

18. C_p expt vs. C_p calc for calcite (Table) 106

19. Heat capacity plot of Cp vs. T for $Hg(NH_3)_2Cl_2$ 122

20. Heat capacity plot of Cp vs. T for anhydrous sodium carbonate 146

CHAPTER I

INTRODUCTION

INTRODUCTION

This thesis is concerned with the study of disorder in crystals. A low temperature, adiabatic calorimeter capable of making heat capacity measurements from a little above the boiling point of liquid helium to room temperature was constructed, the heat capacity of the empty sample container measured, and measurements of the heat capacity of benzoic acid carried out. These agreed well with the results of other workers.

Three rather diverse systems were chosen for study, but each is concerned with the problem of disorder in different ways. Two forms of calcium carbonate, calcite and aragonite, were studied because, although no configurational entropy term arises in either compound, early work reported a large discrepancy in the standard entropy. This discrepancy is a measure of the entropy that can arise solely from the effect of a different crystal lattice on a compound. Diammino mercuric chloride was chosen as it has a structure analagous to the random arrangement of 'rods' on a three-dimensional lattice; the three dimensional dimer problem is one that has interested scientists for many years. Anhydrous sodium carbonate completed a study, largely carried out by Waterfield (ref /), to find out whether the hydrates of sodium carbonate possessed residual entropy.

Before we discuss the systems in greater detail, we will briefly consider the evaluation of entropies from heat capacity data.

Third Law.

In this thesis, all symbols used are those currently employed in English thermodynamic literature, and are set out in an appendix. The entropy S_T, at a temperature T, is given by

$$S_T - S_o = \int_o^T (Cp/T)dT = \int_o^T Cp\ d(\ln T)$$

The third law states that S_o tends to zero as T approaches zero. It applies to a perfect crystal, i.e. a system in which each aspect is in internal thermodynamic equilibrium. An aspect is a mode that can involve a change in S, e.g. rotation, vibration, mixing. (Although perfect crystals have the lowest possible entropies at 0^oK, to assign the value zero to S_o is merely a convention).

Hence, if the third law is obeyed

$$S^o_{3rd\ law} = \int_o^{298.15} (Cp/T)dT$$

If phase transitions take place between 0 and 298.15^oK the sum of the entropies of transitions, $\Sigma \Delta S_{trans}$, must be added to $\int_o^{298.15} (Cp/T)dT$. ΔS_{trans} is given, from the second law, as $(\Delta H_{trans}/T)$.

Extrapolation to 0^oK

Measurements of Cp cannot be carried out either a) to 0^oK, (for theoretical reasons) or b) below about 8^oK in this calorimeter (for practical reasons). Hence, one must extrapolate from $\sim 8^oK$ to 0^oK.

At low temperatures,

$$Cv = aT^3$$

except for metals where an electronic contribution, varying linearily with T, must be added to the lattice contribution. Also as T approaches O, Cp - Cv approaches zero, and hence

$$Cp = aT^3$$

This is predicted from the Debye (continuum) theory of specific heats for temperatures less than $\sim \Theta_D/50$, where Θ_D is the Debye temperature. It hasbeen confirmed many times by experiment.

Hence, at lowest temperatures ($T \leq 8^\circ K$)

$$\int_o^T (Cp/T)dT = \int_o^T (aT^3/T)dt = aT^3/3 = (Cp)_T/3$$

This approximation has been used in this thesis.

Second Law Entropies.

If ΔG° and ΔH° are known from an isothermal, equilibrium study of a reaction the 'second law' standard entropy difference $\Delta S^\circ_{2nd\ law}$ may be obtained from

$$\Delta G^\circ = \Delta H^\circ - T\Delta S^\circ_{2nd\ law}$$

so that S° for one participating substance may be found if S° for all the other substances are known. Thus, the second law entropy for, say, a hydrate or ammoniate, e.g. $Na_2Co_3.H_2O$ can be obtained from heats of solution and equilibrium dissociation pressures, knowing

i) ΔH° for the reaction

$$Na_2CO_3\ (S) + H_2O\ (g) \longrightarrow Na_2CO_3.H_2O(S)$$

This can be found from a) ΔH°_A for $Na_2CO_3(S) + aq \longrightarrow Na_2CO_3(soln)$

b) ΔH°_{B} for $Na_2CO_3.H_2O(S) + aq \longrightarrow Na_2CO_3.H_2O$ (soln) C) ΔH°_{W} for H_2O (l) $\longrightarrow$ H_2O (g); whence $\Delta H^{\circ} = \Delta H^{\circ}_{A} - \Delta H^{\circ}_{B} - \Delta H^{\circ}_{W}$.

ii) ΔG° for the same reaction. Since $\Delta G^{\circ} = -RT \ln Kp$, and $Kp = {}^{1}/_{P_{H_2O}}$, $\Delta G^{\circ} = +RT \ln P_{H_2O}$ where P_{H_2O} is the water vapour dissociation pressure of the system.

An alternative approach, which in fact is being used by a co-worker to obtain $S^{\circ}_{2nd\ law}$ for diammino mercuric chloride $Hg(NH_3)_2.Cl_2$, is to measure the e.m.f. of a suitable cell. This measurement at one temperature, together with ΔH for that reaction at the same temperature gives ΔS. Alternatively ΔS may be found directly from the temperature coefficient of the e.m.f. In the cell

$$\ominus \quad Hg(l) \;\Big|\; [Hg(NH_3)_2]^{2+}_{(S)} \quad {}^{NH_4Cl}_{NH_3(aq)} \quad AgCl(S) \;\Big|\; Ag(S) \quad \oplus$$

the reaction is

$$Hg(l) + 2NH_3\,(aq) + 2AgCl_{(S)} \longrightarrow Hg(NH_3)_2Cl_2(S) + 2Ag_{(S)}$$

Now $\Delta S^{\circ} = \Sigma S^{\circ}_{products} - \Sigma S^{\circ}_{reactants}$

$$\therefore \quad S^{\circ}_{Hg(NH_3)_2Cl_2} = \Delta S^{\circ} + S^{\circ}_{Hg(l)} + 2S^{\circ}_{NH_3(aq)} + 2S^{\circ}_{AgCl(S)} - 2S^{\circ}_{Ag(S)}$$

Also, from the Gibbs-Helmholtz equation

$$\Delta G - \Delta H = T\left(\partial(\Delta G)/\partial T\right)_P,$$

Since $\Delta G = -2FE$

$$\therefore \quad \Delta S^{\circ} = -2F\left(\partial E/\partial T\right)_{P,\ T=25^{\circ}C}$$

iv) Deviations from the Third Law.

Since $S^{o}_{3rd\ law}$ is obtained by assuming $S_o = 0$, if

$$S^{o}_{3rd\ law} = S^{o}_{2nd\ law},$$

then the 3rd law is obeyed. If $S_o \neq 0$

$$S^{o}_{3rd\ law} < S^{o}_{2nd\ law}$$

Several substances have been found not to obey the third law, i.e. to have a positive 'zero-point' or 'residual' entropy. In the case of hydrogen (ref 2) this is caused by the presence of both ortho and para forms, and by the nuclear degeneracy of the ortho state; for CO (ref 3) and N_2O (refs 4,5) it arises because different orientations of the molecules along certain fixed axes in the crystal have about the same energy (the molecules enter the lattice with no discrimination between their ends; NO is similar.); In general, if there are W configurations (arrangements of the molecule in the lattice) that have about the same energy at the absolute zero then S_o may be given by

$$S_o = R \ln W.$$

This arises because the molecule is free to choose between W equally probable distinguishable arrangements, even at the absolute zero. For a disordered substance (i.e. one which can adopt more than one configuration) on cooling, two things can happen. Either, at some particular temperature, or range of temperature, one of its positions can become energetically more favourable than the others, resulting in all the molecules adopting this configuration and thus becoming ordered, or it can stay disordered down to the absolute zero, in which case it will possess residual entropy.

Correlation between Entropy of Disorder and R ln W. - A further discussion

There is no doubt that experimental values of entropy of transition and residual entropy are often close to R ln W, where W is an integer or simple fraction. Newns and Staveley (ref 6) found this to be so for a number of transitions in nitrates. Residual entropies in CO and N_2O have values close to R ln 2; the residual entropy of CH_3D is R ln 4 (ref 7) as would be intuitively expected from the presence of four distinguishable configurations of almost equal energy. Water possesses a residual entropy of R ln $^3/_2$ (ref 8) and a residual entropy of R ln 2 was found for $Na_2SO_4 \cdot 10H_2O$ (ref 9).

Boltzmann put forward the hypothesis that the statistical analogue of the entropy is related to Ω, the number of accessible and distinguishable quantum states, or complexions by

$S'' = K \ln \Omega$, where K is Boltzmann's constant.

This is supported by the facts that S and Ω are both functions of state, determined by U, V and n_i and that the logarithmic form of the relationship is the only one that will reconcile the additive properties of S with the multiplicative properties of Ω.

For a system of fixed energy, each accessible and distinguishable quantum state is equally probable. The totality of quantum states is an ensemble, and when, as in the case of a system of W equally energetically favourable configurations, each state is of equal energy,

the ensemble is said to be micro-canonical.

For a micro-canonical ensemble, the qualities $S' = K\Sigma Pi \ln Pi$ (where Pi is probability of a particular state) and $S'' = K \ln \Omega$, are equal. S' can be shown to be identical to the entropy, S if $\beta = {}^{1}/_{KT}$ and hence for a micro-canonical ensemble, S'' is the entropy.

The difference in entropy, ΔS between two states, one of which has Ω_2 possible configurations, and the other Ω_1 possible configurations is

$$S = K \ln({}^{\Omega_2}/_{\Omega_1})$$

Where one state is disordered and the other ordered, Ω_1 is one, and Ω_2 is W^N, the number of configurations of equal energy,

$$\text{i.e. } S = K \ln W^N = R \ln W.$$

This, it must be stressed again, applies to a micro-canonical ensemble for an isolated system, i.e. fixed energy, volume and composition for the system, and equal energy for each state. No account is taken of the effect on the entropy of redistribution of energy of the system over changed energy levels, i.e. to new quantum states that are created by the thermal energy of the system.

The expression $S = R \ln W$ can also be derived for an isothermal (open) system where the configurations of the disordered phase have ~~that~~ the same energies as each other, but a different energy from that of the ordered state. (See K. Denbigh, Principles of Chemical Equilibrium (1955) p. 427).

Accuracy

In concluding this general discussion of the third law, it is worth noting that considerable accuracy is required of the experimental data if their interpretation is to be possible. Thus, in the case of say $Hg(NH_3)_2Cl_2$ where S° is about 57 e.u., if residual entropy is present it will probably be of the order of 1 - 3 e.u., i.e. 2 - 5% of the total. The cumulative errors of a large number of steps are present in any residual entropy, and if this quantity is not to be eliminated by the sum of the errors, accuracy of the order of 0.2 - 0.3% must be aimed at at all stages. This calorimeter was designed to produce entropy figures to an accuracy of 0.25%, and from the results on benzoic acid, it would appear to do this.

The Object of this Research.

In considering disorder in crystals, the major part of the entropy of transition from an ordered to a disordered form arises from a configurational, R ln W, term, as discussed earlier in the introduction. If there is an attendant change in the lattice parameters, then there will also be an entropy change, arising from a change in the frequency distribution of the lattice vibrations. This latter entropy change is a difficult quantity to measure accurately, as it usually accompanies a configurational term which may be much larger. It appears however that in certain transitions, the 'lattice frequency' term may be very large; Newns and Staveley (ref 6) discuss the phase II → phase III transition in KNO_3, in

which no configurational change appears possible, yet the entropy associated with the phase change is 1.44 e.u. They mention that one of the few examples studied of an entropy difference arising solely from a difference in the frequency distribution of thellattice vibrations, is that, reported from early work, of 0.7 e.u. between the polymorphs calcite and aragonite.

Early measurements of the heat capacities of calcite and aragonite by Nernst (ref 10) on calcite from 20 to 90°K, Günther (ref 11) on aragonite from 20 to 50°K, Simon and Swein (ref 12) on calcite from 15 to 80°K and Anderson (ref 13) on both polymorphs from 55 to 300°K, revealed an entropy difference of about 0.87 e.u. A careful study of solubilities of the polymorphs in acid, and also of their heats of solution by Bäckström (ref 14) showed that the second law entropy difference, obtained from equilibrium considerations, was 0.74 ± 0.2 e.u. Hence the entropy discrepancy does not arise from residual entropy, since $S_o = 0$. Also no transitions were reported in the heat capacity, and the entropy discrepancy must therefore arise from some difference caused by the different crystal structures of the polymorphs.

The reported calorimetric entropy difference seemed to be excessively large to be explained in this way. Since Anderson's entropy figures depended on an extrapolation, using Debye and Einstein frequencies, from 0 to 56.2°K, and the entropy involved in this

Structure of Calcite

(Rhombohedral unit cell shown in bold lines, cleavage rhombohedron in thin lines)

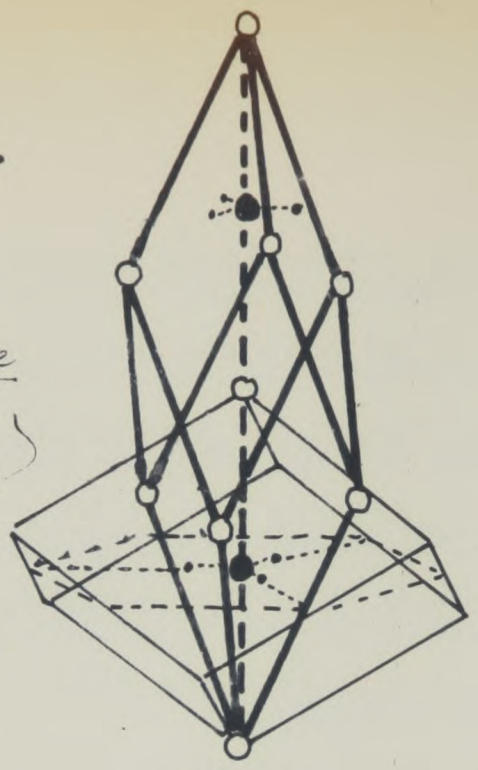

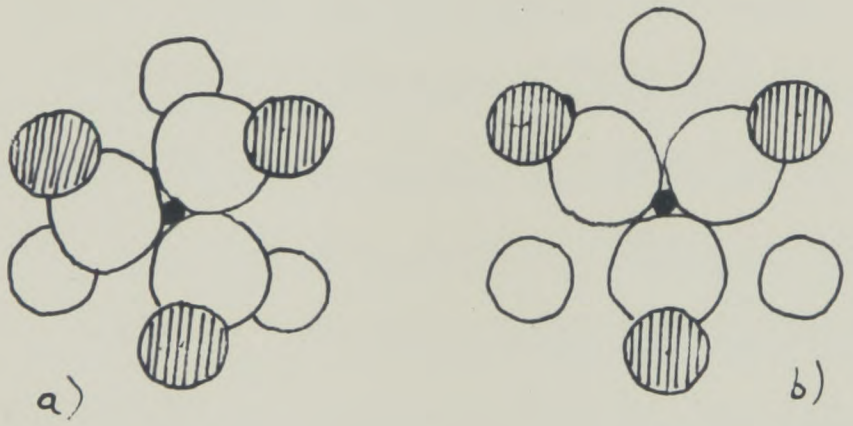

c-axis projection of environment of CO_3^{2-} ion in a) Calcite and b) Aragonite. ● = C; ◯ = O; ○, ◍ = Ca. The shaded cations lie in a plane above the unshaded ones.

Structure of Aragonite (showing pseudohexagonal arrangement)

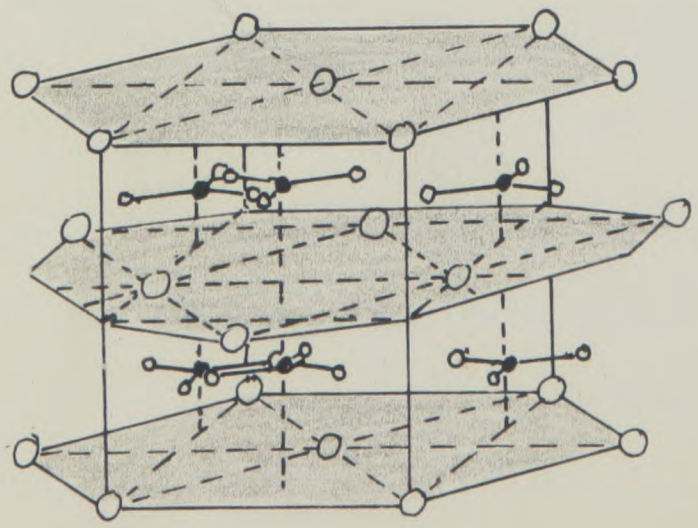

extrapolation was 2.42 e.u. for calcite and 1.51 e.u. for aragonite, it seemed that there was scope for careful heat capacity study over as large a temperature range as possible.

This was carried out over the range 10 - 300°K for calcite and 20 - 300°K for aragonite. The temperatures at the bottom of the range were in each case the temperatures where the contribution of the sample to the total heat capacity fell below the level where experimental accuracy exceeded the accuracy of a $C_p = aT^3$ extrapolation. The difference in crystal structure and in volume between the two polymorphs must imply a difference in the lattice vibrational frequency distribution, and later in this thesis calculations are presented which attempt to relate the frequency distribution in calcite to the experimental heat capacity. Too little is known about the optically active modes of vibration in aragonite to make a comparison between the frequency distributions of the polymorphs and the effect on the heat capacity.

The primitive cell for calcite is drawn on the facing page. The structure was determined by Bragg (ref 15) who found that the symmetry was trigonal, and that the structure could be conveniently referred to a bimolecular rhombohedral unit cell. The arrangement of ions may be visualized as being like that of NaCl, Na^+ being replaced by Ca^{2+} and Cl^- being replaced by CO_3^{2-} with some distortion caused by the incorporation of CO_3^{2-} discs into thelattice. Each calcium ion is surrounded by 6 carbonate oxygens. The structure of aragonite,

shown below, was found to be orthorhombic with four molecules per unit cell. Mimetic twinning results in the structure being pseudo-hexagonal, and the structure appears like that of nickel arsenide.

The environment of the carbonate ion is different, as shown in the ~~next~~ figure. In calcite, the carbonate oxygens have two nearest neighbours, as the CO_3^{2-} ion is aligned in such a way that the oxygen is not directly over or under a cation. In aragonite, the carbonate ion is rotated through 30° and the oxygens lie directly under cations in one layer, and at equal distances from two cations in the underneath layer. Here, therefore, the oxygens have three Ca^{2+} nearest neighbours, and also each Ca^{2+} is surrounded by nine oxygen atoms.

In calcite, the carbon in CO_3^{2-} is at the mid point of the distorted octahedron, i.e. midway between two layers of calcium ions; in aragonite, since the oxygens of CO_3^{2-} are equidistant from one ion in a layer of Ca^{2+} on one side and two ions in a layer on the other side, it follows that the carbon of CO_3^{2-} is displaced along the C axis.

The difference in heat capacity between calcite and aragonite therefore arises at least in part from the effect of the different environments of the carbonate ion.

Fusible White Precipitate

Considerable interest has been shown in the problem of finding the number of ways that dimers can be arranged on a lattice. For a two-dimensional lattice, the problem may be visualized in terms of the number of ways dominoes can be arranged on an infinitely large chessboard. Rigorous mathematical solutions for a two dimensional lattice have been obtained by the random walk method (ref 16) and by topological algebra based on an Ising model (ref 17). In each case, the number of available configurations is found to be $(1.791623)^n$, where n is the number of dimers, and

$$\exp\left(\frac{2G}{\pi}\right) = 1.791623, \text{ where } G = \frac{1}{1^2} - \frac{1}{3^2} + \frac{1}{5^2} \ldots\ldots$$

where G is Catalan's constant.

Fowler and Rushbrooke (ref 18), by considering the arrangement of dimers on a long plane strip up to six units wide, found that the number of configurations tended to a maximum of 1.80^n as the length of the strip was increased; eliminating boundary conditions by curling the strip round to form a long cylinder they found the number of configurations tended to a minimum of 1.80^n as the length of the cylinder was increased. They also arrived at some very approximate answers for the three dimensional case, by considering strips of lattice points one above the other. They found that the number of configurations seemed to approach 2.15^n for a simple cubic arrangement and some higher value, possibly 2.38^n for a b.c.c. arrangement.

Great interest has been shown in the solution of the three-dimensional case, because of among other things its bearing on the theory of solutions. To take a simple case, a quasi-crystalline theory of liquids applied to the benzene-diphenyl system, would have to take into account the number of ways of arranging diphenyl 'dimers' on a three dimensional benzene lattice.

The number of configurations, W, is a quantity that can be found from residual entropy or entropy of transition, using the R ln W relationship. Thus if the substance, whose residual entropy or entropy of transition could be found with some accuracy, had a structure analogous to the arrangement of dimers on a three-dimensional lattice, an experimental measure of the number of configurations would be obtained.

Diammino mercuric chloride (and also the bromide) is such a substance. It has a structure (ref 19) where ammonia units are in the body centres of a cubic lattice of chloride ions, and mercuric ions are randomly distributed in one-sixth of the face centres. This structure may equally well be visualised as NH_3-Hg-NH_3 'rods' (corresponding to the dimers of the theoretical problem) randomly arranged parallel to the three mutually perpendicular axes of the three-dimensional lattice. If a disordered structure of this type is cooled, there are two a priori possibilities, a transition to an ordered form, accompanied by measurable entropy of transition ~~to an ordered form, accompanied by measurable entropy of transition or~~ or resistance of disorder to the absolute zero, giving a residual entropy.

Theory (ref 20) predicted the latter, and measurements were carried out in this work on the heat capacity from 3 to 300°K to investigate this. The measurements from 3 to 12°K were carried out in the calorimeter built by Dr. R. M. Clay, ~~which is briefly described in the appendix.~~ (ref 21) Concurrent with this study, e.m.f. measurements on the cell already described were carried out by another worker, to find the 'second law' entropy, but these are not complete.

It is worth mentioning that although several studies comparing the second and third law entropies of hydrate systems have been carried out (see the next section), this is believed to be the first study of this type on an ammoniate. In fact, very few measurements even of the heat capacities of ammoniates have been performed, those of Dufy (ref 22) Ukei and Kado (ref 23) and Long and Toettcher (ref 24) on $Ni(NH_3)_6X_2$, where X = Cl, Br, I or NO_3, that of Zeigler (ref 25) on cobaltammine halides and the high temperature work on $Pt(NH_3)_2Cl_2$ (ref 26) being among the only examples.

C) Anhydrous Sodium Carbonate.

Measurements of the heat capacities of sodium carbonate and its stable hydrates ($Na_2CO_3.H_2O$ and $Na_2CO_3.10H_2O$) had been carried out in this laboratory by Goalby in 1950 (ref 27) and Bates in 1958 (ref 28) The measurement of the heat capacities of the hydrates, and also of their second law entropies, was repeated with much greater precision by Waterfield (ref 1). From his data it appeared that either the

earlier measurements of Cp of the anhydrous salt were wrong, or else the curious situation of the monohydrate being ordered, while the anhydrous salt possessed a residual entropy of about 0.6 e.u., prevailed. The heat capacity of the anhydrous salt was therefore redetermined.

CHAPTER II

DESIGN AND CONSTRUCTION

THE CALORIMETER CONSOLE.

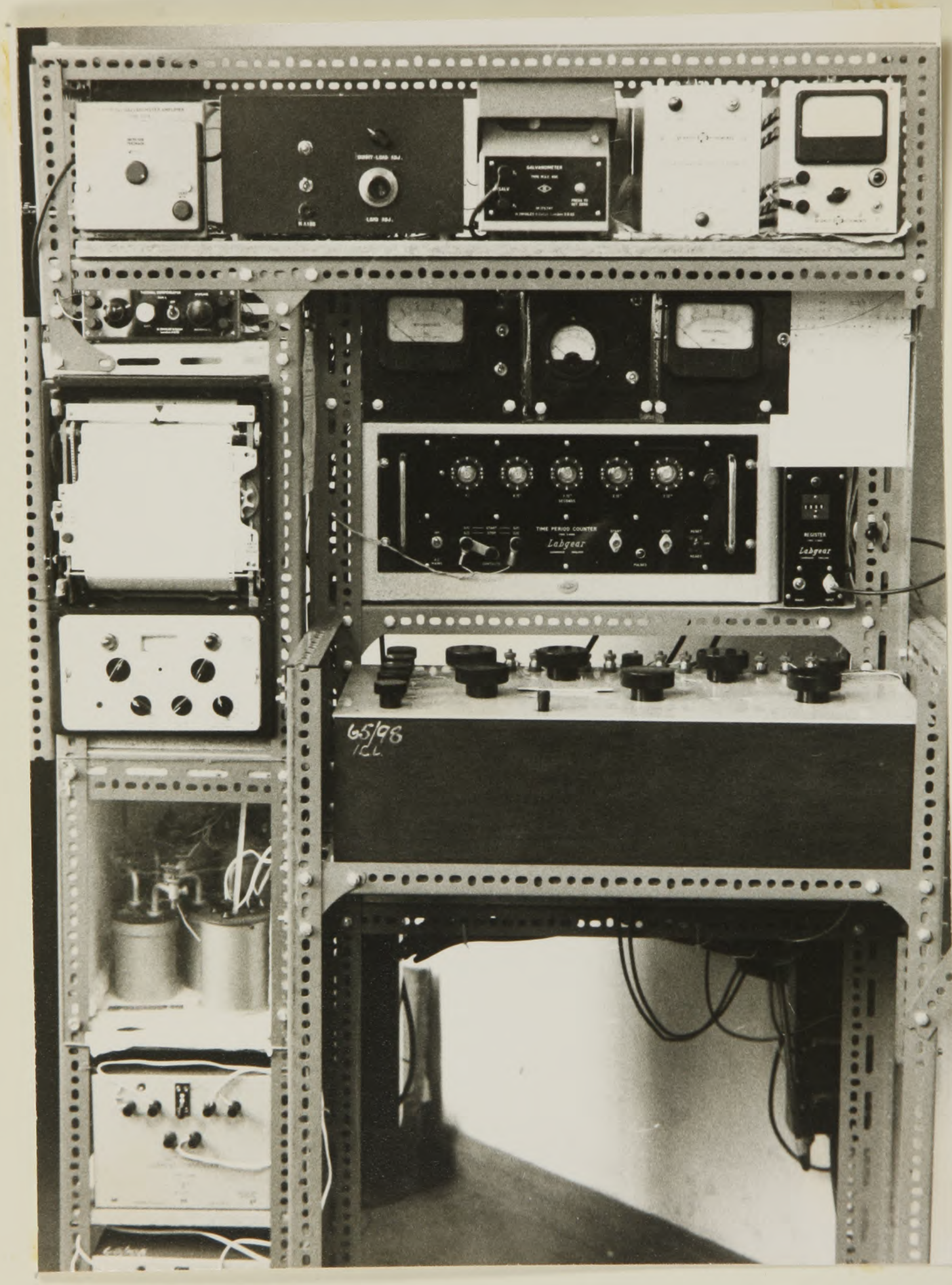

DESIGN AND CONSTRUCTION OF THE APPARATUS

1) The Word Calorimeter

When describing a calorimeter, there can be some confusion as to whether the vessel that holds the sample, or the whole apparatus that is used to measure the heat capacity, is meant by the word 'calorimeter'. It is hoped that in this thesis, the vessel that holds the sample has been consistently referred to as the sample container, and that the word 'calorimeter' has been used to mean the whole apparatus, or some large part of it.

2) General Description

Many low temperature calorimeters have been built in this country and abroad, but no commercial version is as yet available. It is therefore necessary to design and build such a calorimeter oneself. When a new calorimeter is built, it is desirable to introduce improvements suggested by earlier experience, and to adjust such factors as the size of the calorimeter and the temperature range covered to suit particular needs. In a small research group, it is undesirable to build a calorimeter that requires more than one man to operate it and this feature has been borne in mind in designing the calorimeter.

The apparatus is a low-temperature adiabatic calorimeter, capable of working from room temperature to the boiling point of liquid helium. No facilities are provided for pumping on the

refrigerants, and the temperature range is covered with three refrigerants, liquid helium (4.2 - 20°K), liquid hydrogen (20 - 77°K) and liquid nitrogen (77 - 300°K). Liquid helium is an expensive refrigerant and a device that precools the leads, thus economising in refrigerant, is incorporated.

Adiabatic conditions are maintained round the sample container by a shield which is heated when the temperature of the calorimeter rises above that of its environment. The temperature difference between the sample container and its surroundings is monitored by a pair of thermocouples, one on the calorimeter and one on the shield. The difference signal is fed to a microvoltmeter-amplifier, and then to a pen-recorder containing an automatic electronic device which adjusts the shield heater current so as to reduce the difference signal to zero.

On earlier calorimeters, the difference signal was fed to a galvanometer and monitored manually. This system has several disadvantages. Either a separate operator is needed to monitor the shield temperature, or the operator has not only to make several voltage and current measurements in the course of a heating period, but also to monitor the shield. This leads to operator fatigue and consequently to inexact control. In an automatic system such as that used here, operator fatigue is removed, and if for any reason the temperature of the environment should depart from that of the calorimeter, the pen recorder provides a record of this and corrections can be applied.

The experience gained from another calorimeter in the same laboratory showed that automatic control works most satisfactorily if the shield is of low mass. The leads for the platinum thermometer and sample container heater have to be brought into thermal contact with the shield in order that they should not carry heat to or from the sample container. Previously this was done by carrying them in grooves cut in the shield, and this necessitated a shield of some 0.050" wall thickness, and consequently of rather high mass. This problem has been solved by the use of pyrotenax cables*, consisting of mica insulated copper leads, packed in alumina inside narrow copper tubes. These tubes are soldered to the inside of the shield and are in good thermal contact with it. This has enabled a shield with a wall thickness of only 0.020" to be employed.

The sample container is platinum, rather than copper. This enables solids that corrode copper (e.g. ammines or cupric salts) to be examined. Alternative metals would have been tantalum, which is difficult to work, or gold, which is softer and less resistant to attack than platinum.

The measuring equipment is of as high a precision as possible. A potentiometer, capable of measuring to 0.1 μv, is used in conjunction with a highly accurate photocell amplifier and secondary mirror galvanometer to measure both the resistance of the platinum resistance thermometer and the heat imput to the sample container heater. Thermal e.m.f.'s across terminals are minimised by a

* Pyrotenax Ltd., Hebburn-on-Tyne, Co. Durham.

compensating device rather than by a system of reversing switches. Stabilised power packs are used to supply current to the calorimeter and shield heaters. That for the sample container heater incorporates a variable shunt which keeps the load taken from the diodes at a constant value, thus promoting stability. The heating time is measured on an electronic Labgear timer, capable of measuring to 10^{-4} sec. Although all the instruments are mounted on a compact portable console which only occupies 2' x 3' 6" of floor space, there was insufficient space to house this in the same room as the rest of the calorimetric assembly. In consequence, the instruments are located in another room and the leads carried through a conduit.

A highly efficient pumping system using a metal vacuum line and an oil diffusion pump, provides a vacuum of better than 10^{-6} torr, which minimises heat losses by conduction. Heat losses by radiation have been minimised by painting the sample container with a reflecting aluminium varnish. Copper leads are used to connect the sample container to the shield. Manganin leads would have considerably reduced heat conduction along the leads at very low temperatures but, because of their high resistance, would have resulted in imprecise measurement of the heat imput. As conduction along the leads proved only to be a problem below about $10^{\circ}K$, a region in which the platinum resistance thermometer is of low sensitivity, copper leads were preferred.

At the end of the author's part II year the position that had been reached in the construction of the calorimeter was as follows:

i) Investigation of copper corrosion showed that some less easily attacked metal would have to be used for the sample container and platinum was selected for reasons already given. It was found that labile ammines e.g. $HgI_2.2NH_3$ corroded copper within 24 hours and protection by gold plating, laquering, or both was shown to be ineffective in stopping corrosion. Cupric compounds also attack copper.

ii) An adiabatic shield weighing 500 grams, with the lead wires carried in grooves was prepared. A 500 ohm heating coil was wound on this and insulated in the manner described later. This shield was not used, because, as already mentioned, such a massive shield gave poor responses with automatic control.

iii) The helium economiser was wound and assembled; the lower copper block was insulated with paper and leads were wound on this, varnished and baked. The leads were strapped and varnished onto eggshell glass tubing passing inside the vacuum tube, and connected to the helium economiser. A similar glass tube carried the leads from the helium economiser to the plastic disc at the top of the vacuum tube.

Except for the minor stages outlined above the calorimeter was built in the first year of this research. This was a lengthy operation which involved:

i) Insulating and winding the heater coil on the sample container, fitting a thermocouple, fitting the platinum thermometer and completing the wiring inside the top hat. That this alone was

The Sample Container of The Calorimeter

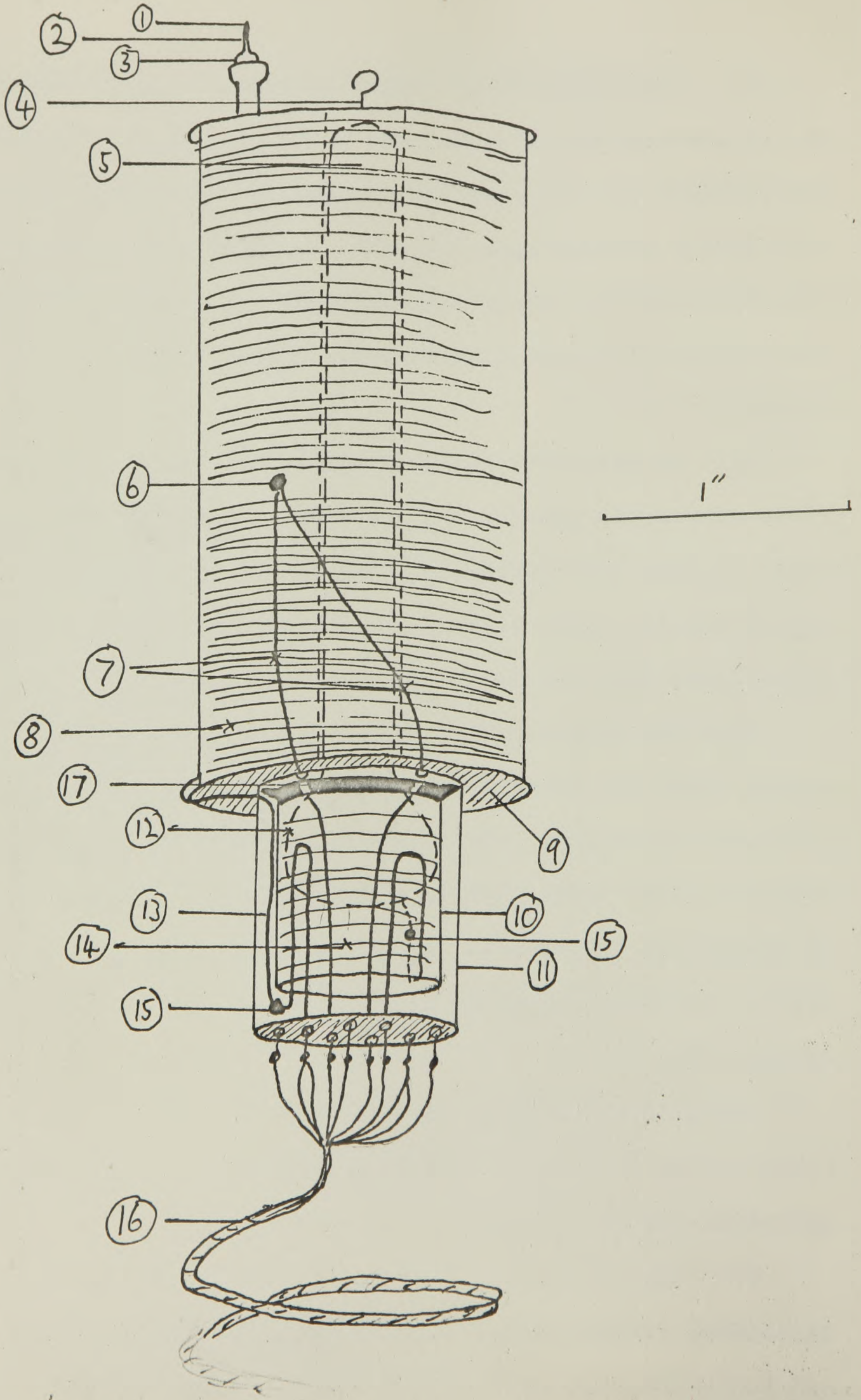

a lengthy operation which took several days can be seen from fig. I.

ii) Preparing the pyrotenax cables for the new shield, winding a heating coil on the shield, and preparing the connection board at the bottom of the shield.

iii) Assembling the cryostat.

iv) Constructing the all-metal vacuum line.

v) Fitting all the measuring and control apparatus in a compact console.

vi) Installing a wiring conduit to connect the console to the calorimeter.

The apparatus will now be described in detail.

A) The Sample Container

This is of 10% Rhodium-Platinum, soldered with gold, and was constructed in the laboratory workshop. This platinum alloy is tougher than pure platinum. The container is cylindrical 7.2 cm long, 2.6 cm in diameter, and has a capacity of about 25 cm^3. This capacity was a compromise between a larger size, which would have given more accurate data, and a smaller size which would have had a low heat capacity and would have needed only a little sample to fill it. The dimensions of the cylinder give the maximum volume for a given surface area. A central cylindrical well holds the platinum thermometer(5; numbers refer to the figure on the facing page) which is greased in with apiezon N grease to assist attainment of thermal equilibrium. A small hole by the suspension hook (4) enables air to escape from the central tube when the thermometer is

inserted.

On the top is a filling tube, through which the sample is introduced into the container. It is fitted with a platinum cap (3). The sample container can be evacuated, and subsequently filled with helium exchange gas at 2 - 3 torr, through a silver tube (2). This is sealed off with a pinch seal, covered with electrical or indium solder (1).

The bottom of the container (9) has affixed to it an open bottomed cylinder (10), which protects the fragile glass head (12) of the thermometer, and provides a surface round which leads (13) to the thermometer, heater and thermocouples may be strapped by silk (14) to bring them to the temperature of the container. This cylinder is covered with a 'top-hat' (11), secured by a circular metal strap at its base which is fixed by a screw onto a copper ring (17) soldered to the base of the cylinder. Both the cylinder and the top hat are copper; the outside of the top hat is covered with aluminium varnish (fine aluminium powder in one part G.E.C. glyptal low-temperature varnish, type 7031 and three parts solvent: 400 pts toluene; 190 pts ethanol: 10 pts water: 1 pt benzene) to cut down heat loss by radiation.

The thin leads from the heater, thermocouples and thermometer are soldered to thicker wires using thermal-free solder (15) (70.44% Cd: 29.56% Sn, obtained from Leeds Northrup Co.), which emerge through the plastic-insulated holes in the top hat and are

soldered to the cable (16). These thick wires reduce the risk of fracture inside the top hat. As 14 soldered joints had to be fitted inside the top hat, it will be appreciated that completion of the lower end of the sample container took two complete days (the diagram is 1½ times the actual size).

The single thermocouple (6) is soldered directly to the body of the sample container. The thermocouple is made of a ,26 swg. double silk covered (dsc) copper wire, soldered to a 20 swg constantan wire, with a baked-on mica coating for insulation, taken out of a pyrotenax cable. Constantan sometimes varies in composition and this type is used in the shield thermocouple.

The remainder of the cylindrical wall of the container, and the outer surface of the projecting cylinder are covered with cigarette paper soaked in glyptal varnish which has been baked at 140°C for 2 hours. This provides an electrically insulated surface. The sample container heater (8) is wound over the papered surface of the container. It consists of 21 metres of 38 swg manganim wire, wound non-inductively at 43 turns to the centimetre. The windings are varnished with glyptal laquer and baked, and a final layer of aliminium varnish baked on to cut down heat losses by radiation. The two leads from the heater (13) and the two thermocouple wires (7) are led to the projecting cylinder through holes in the base of the top hat, and grooves in the copper ring.

THE ADIABATIC SHIELD

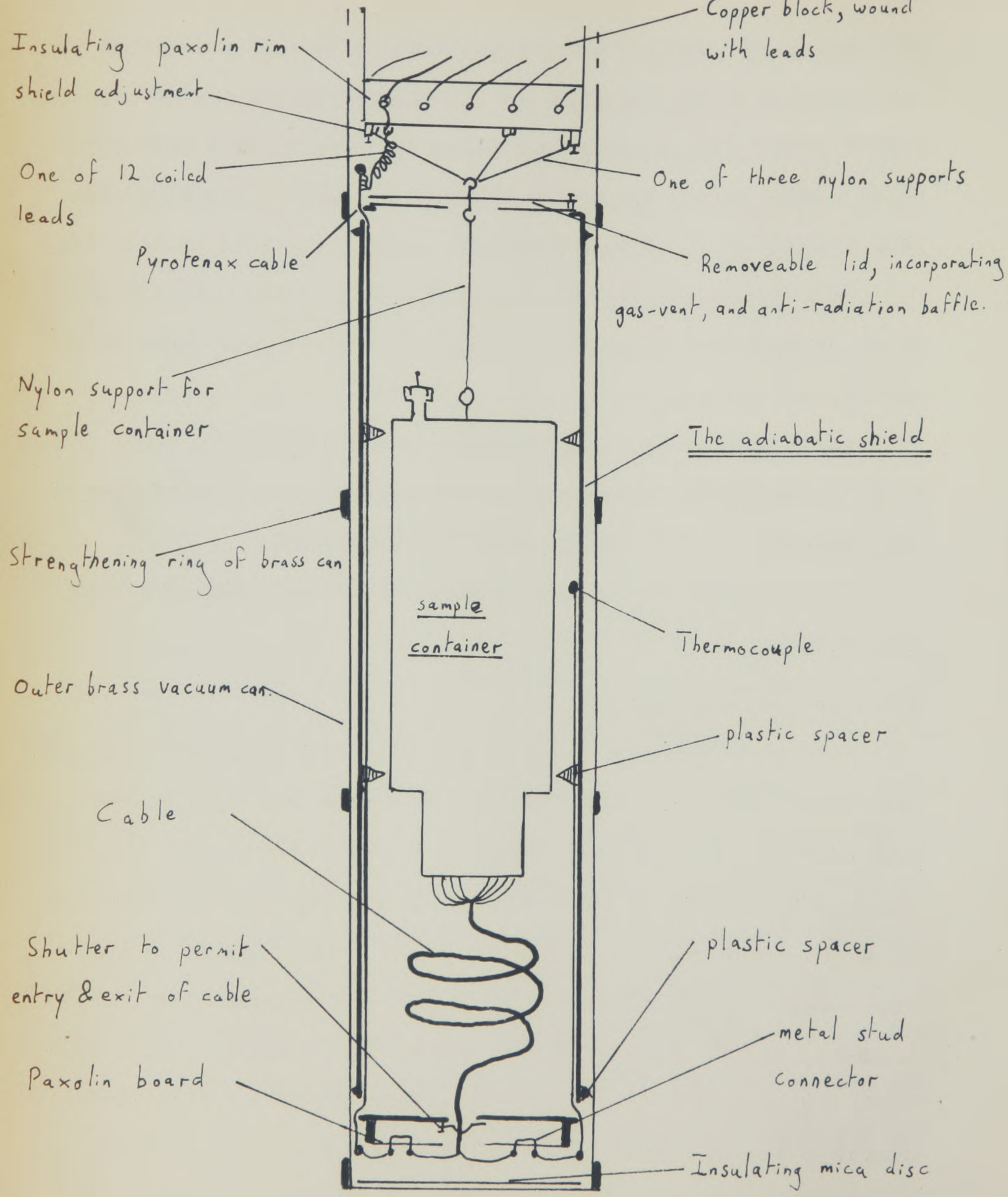

The cable consists of 10 wires, all of 40 swg, dsc copper except one of 43 swg, dsc copper and one of 'pyrotenax' constantan, both for the thermocouple. The wires are wrapped together with silk, formed into a spiral of 3 turns, varnished and baked. The bifurcations in the heater wires are made at the join between the cable and the container. This bifurcation provides one pair of wires to carry the current and one pair of wires with which to measure the voltage.

The container was leak tested, using a helium as a probe gas on a mass spectrometer detector, and found to be leak free both at room temperature and liquid nitrogen temperatures.

A similar container, made entirely of copper, has also been prepared.

B) <u>The Adiabatic Shield.</u>

This is a copper cylinder with a removable top. The walls are only 0.020" thick, to keep the mass as low as possible, as with automatic control, 'thermal lagging' is undesirable. The top consists of a circular plate with a central hole of 1 cm diameter, soldered to a disc, 4 mm above it, and having no central hole. (see dia.) This means that the inside of the shield can be evacuated, but that radiation cannot escape. The bottom of the shield is closed and a small hole is bored in the centre through which the cable emerges. This hole can be partly closed by an adjustable shutter. One centimetre below the base a circular paxolin board is attached,

containing metal contacts to which the cable leads are soldered. The other ends of the contacts are soldered to copper wires emerging from metal sheathed, alumina packed, pyrotenax cables sealed at the ends with araldite. The only disadvantage of these cables appears to be that it is necessary to seal the ends with araldite to prevent moisture affecting the insulating properties of the alumina, and this process, together with the heat used in soldering, makes the ends of the wire brittle and liable to snap off.

Although it was necessary for the cables to be outside the shield rim at the top, in order to be able to remove the lid without the leads getting in the way, they could not run down the outside surface of the shield as this would have provided an uneven surface on which to wind the shield heater and consequently this would not have been in good thermal contact with the shield.

The pyrotenax cables were soldered to the inside of the shield by the laboratory workshop, using the following technique. The cables were fitted in slots in the shield at top and bottom, and pressed against the inside walls of the shield by copper split rings. They were soldered in position by running solder all over the inner surface. The rings were then sawn out, with the exception of the rings at extreme top and bottom. That at the top was tapped to take the screws holding the lid, and the base of the shield was soldered to the one at the bottom.

At the top of the shield the pyrotenax copper wires are soldered to 38 swg, dsc coiled copper wires which are strapped to the projecting lengths of pyrotenax sheath at the top of the shield. These wires are then soldered to leads at thebaseof the copper block, from which the shield is hung. The shield, like the container, is suspended on nylon cord, breaking strain 3 pounds, tied with a special slip-free (half-blood) knot. Three cords run from a central hook on the shield to 3 adjustable hooks on the periphery of the copper block. With this system, the shield hangs vertically, and may be moved up and down, and in any lateral direction.

The outside of the shield is insulated with varnished cigarette paper, in the same manner as the container. A heater coil of 26 metres of 34 swg, dsc manganim wire is wound non-inductively on the outside, the windings being concentrated towards the ends of the shield to compensate for the extra mass of copper there. The shield temperature is monitored by one pyrotenax thermocouple, situated at the centre of theinside wall, and linked, constantan to constantan with the container thermocouple via the paxolin board at the base of the shield. Three spare shield thermocouples are also included. In the shield wall are inset pointed plastic spacers to prevent the container touching the shield, or the shield touching the brass can.

THE CRYOSTAT

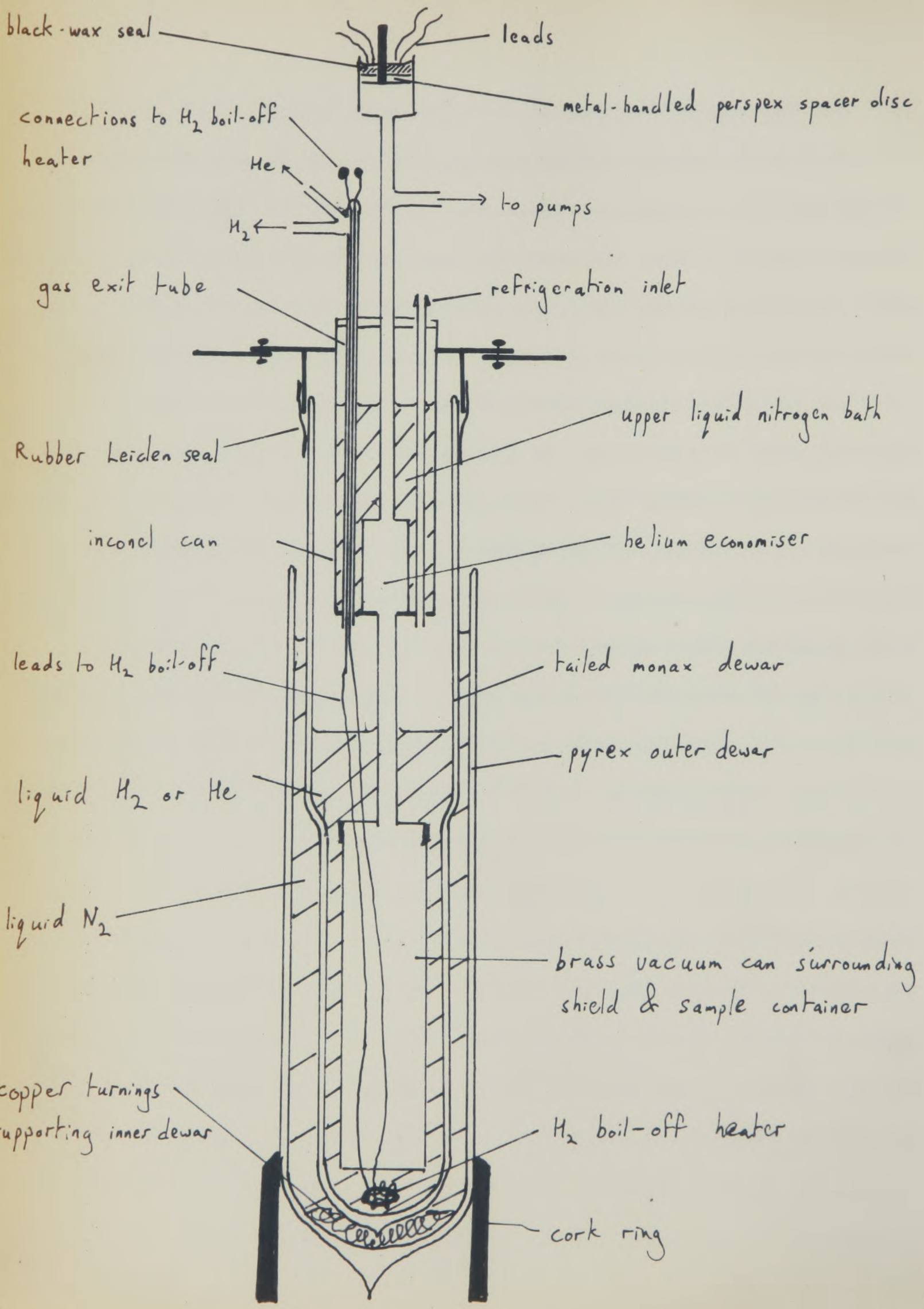

C) The Cryostat

To the rim at the top of the copper block is soldered a brass vacuum can which surrounds the shield. The solder used is low melting indium solder (Bi 49%; Sn 15%; Pb 18%; In 18%; m.p. 58°C).* The leads from the shield are soldered to stout copper wires attached to a paxolin ring which is riveted to the copper block. In previous calorimeters, trouble had been experienced when wires were carried from the base of the copper block to the shield. The wires tended to chafe and short on the edge of the block. With the present arrangement, if the wires chafe, they do so against an insulating surface and no short will result.

The 12 wires (10 from the sample container and 2 from the shield heater) are soldered to copper wires which are wound round the copper block, over a layer of varnished, baked paper. Six spare wires also start at this point. The purposeof the block is to bring the wires to the temperature of the refrigerant. The wires then pass inside a german silver tube. This metal is chosen to reduce heat conduction into the refrigerant. They are strapped and varnished to the surface of a length of 'eggshell' glass tubing, to minimise risk of shorts occuring. They then pass along the grooves of the helium economiser (see later), and along another length of german silver tubing, again bound and varnished to eggshell glass tubing. At the top of the cryostat they are soldered to stout copper wires, insulated by 8 layers of baked enamel, and pass through

* E. Catalino and J. W. Stout. J. Chem. Phys. 23 (1955) 1284.

holes in a perspex spacing disc, vacuum-sealed with black wax. Finally they are connected via a junction box to 12, 3.029 gauge copper wires which pass in a conduit along the corridor to another room where, for reasons of space, the measuring equipment is situated.

A side tube above the helium economiser leads to the pumping system. The refrigerant, liquid helium, hydrogen or nitrogen, is held in a tapered monax dewar which fits round the brass vacuum can, and extends up to the level of the helium economiser where it fits inside a brass flange. A wired-on rubber 'Leiden' seal between the top of the dewar and the outside of the flange, prevents escape of gas. When liquid hydrogen or helium are being used, an outer dewar containing liquid nitrogen surrounds the tapered monax dewar. Both dewars have transparent slits, to permit observation of the liquid level.

Refrigerants are siphoned in through a tube running through the helium economiser; evaporated gases escape through a similar tube which is connected via a glass T piece to an outlet outside the window for hydrogen, or to storage balloons in the case of helium.

For a helium run, the apparatus is pre-cooled by hydrogen. This is boiled off by means of a 5 ohm heater wound round a paxolin former, suspended below the brass vacuum can. The leads to this are of manganim to conserve refrigerant, and current is supplied at 18 volts.

THE HELIUM ECONOMISER

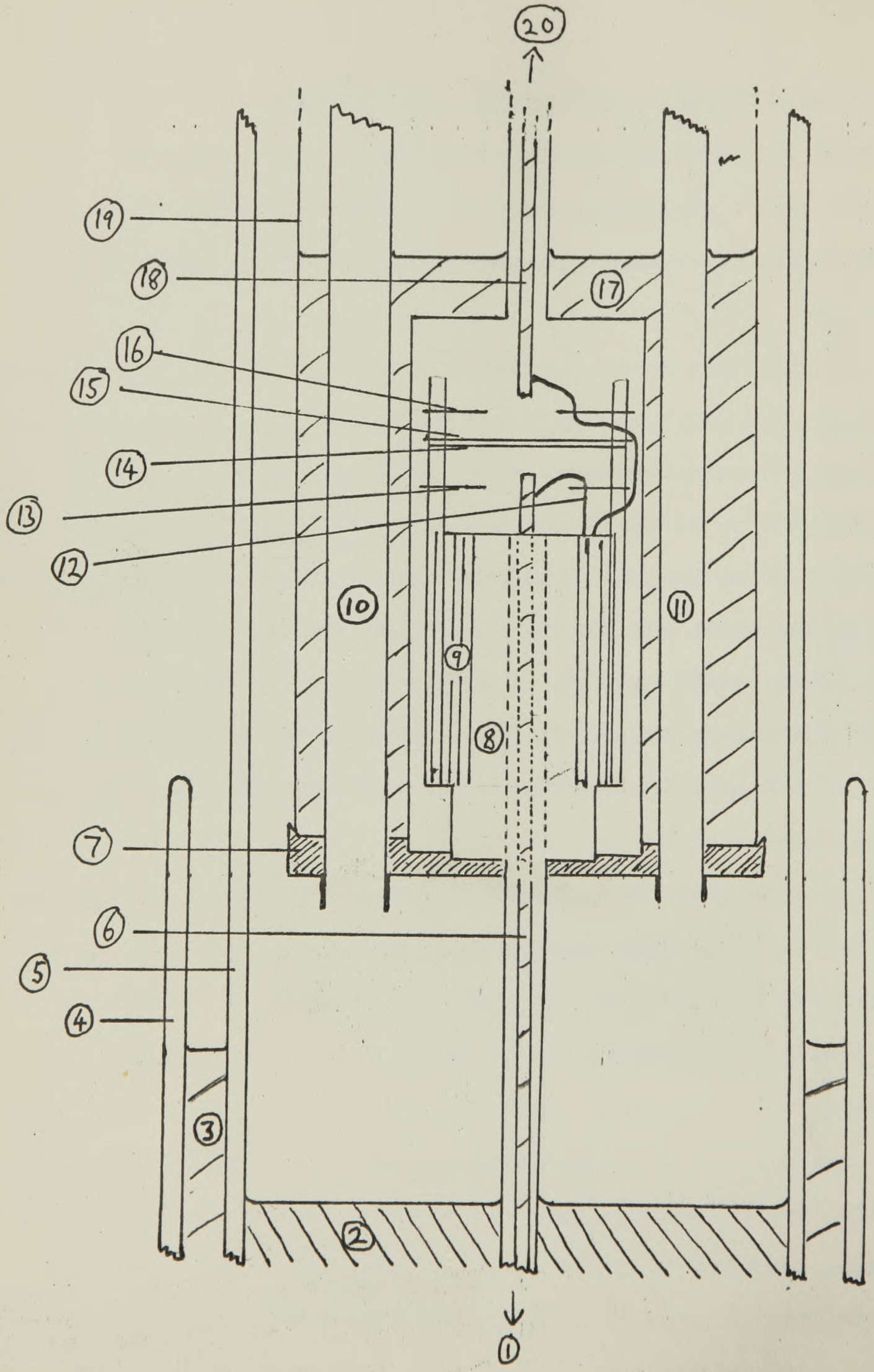

Figure 2. The Helium Economiser.

1. To calorimeter and shield.
2. Liquid hydrogen or helium.
3. Liquid nitrogen.
4. Outer dewar.
5. Inner, monax, dewar.
6. Lower cable of leads.
7. Brass base of economiser.
8. Copper block of economiser.
9. Grooves in block.
10. Entrant tube for liquid hydrogen or helium.
11. Exit tube for gaseous hydrogen or helium.
12. Path of one of the 15 wires.
13. Lower spacer.
14. Copper disc to prevent heat loss by radiation.
15. Plastic plate to prevent leads shorting on copper disc.
16. Upper spacer.
17. Liquid nitrogen.
18. Upper cable.
19. Inconel can.
20. To vacuum line and measuring instruments.

Half a litre of hydrogen may be boiled off in about 10 minutes. The leads to this are carried through the gas exit tube and leave the cryostat through an araldite seal in one limb of the glass T-piece.

D) The Helium Economiser

This is shown in the figure. A grooved copper block is soldered using cadmium solder (50% Sn; 32% Pb: 18% Cd, m.p. 145°C. White. Expt. Techniques in lower. temp. physics. 1st ed. p. 268), to the brass base of an inconel can which is filled with nitrogen. This restricts heat conductance down the leads and also provides a cold area at the top of the inner dewar.

E) The Pumping System.

If heat losses by conduction from the calorimeter are to be minimised, a good vacuum is essential. An all metal vacuum line, using $^{3}/_{4}$" yorkshire copper tubing, and rubber 'O' ring 'Genevac' seals is used. This system uses a rotary pump, provided with gas-ballasting facilities to maintain the cleanliness of the pump oil, and fitted with an automatic air-admittance valve to prevent suck-back of oil. This pump can lower the pressure, measured on a Pirani gauge, to 3×10^{-3} torr. An oil diffusion pump, using type 704 silicone oil, can then reduce the pressure to below 5×10^{-7} torr, as measured on a Penning gauge. For initial rough pumping, the diffusion pump may be bypassed. For all night working, the diffusion pump may be backed by a 6 litre metal fore-vacuum cylinder.

It is also found that when liquid helium is used as refrigerant, it is better to cut out the vibration caused by the rotary pump, by using the fore vacuum cylinder. This vibration is transmitted despite a rubber coupling between the rotary pump and the vacuum line. A glass line, linked to the pumping line through a Genevac connector permits the introduction of a measured pressure of helium exchange gas. The vacuum line is connected to the cryostat by a length of flexible metal tubing, designed to relieve strains.

F) <u>The Platinum Thermometer.</u>

This is a glass sheathed platinum thermometer, made by Tinsleys (No. 177698) and calibrated by the National Physical Laboratory from 10° K to 300°K. It was calibrated in this laboratory at 4.2°K which, in conjunction with the formula mentioned in the section on temperature measurement, extended the range to 4.2°K. The resistance at the triple point of water was checked, and found to differ slightly from the value found by the N.P.L.

G) The Measuring Circuits.

As already mentioned, the measuring equipment is in a different room from the cryostat, and the leads connecting them are stout, plastic sheathed cables, running in an earthed conduit to provide screening from outside interference. The equipment is housed on a compact mobile console.

Both the resistance of the platinum thermometer and the power input to the calorimeter are measured on a Tinsley type 43630-auto precision vernier potentiometer, which has four imput channels. Two ranges provide for measurement from +1.801010 volts to -15 microvolts in steps of 1 microvolt, and from +0.1801010 volts to -1.5 microvolts in steps of 0.1 microvolt.

The current to the potentiometer is supplied by a Tinsley type 5388 current controller. This consists of a high gain d.c. amplifier driving a d.c. current control system. The volt drop across a resistance (the feedback resistance) in the standardising circuit of the potentiometer is compared with the e.m.f. of a standard cell. The difference is fed into the d.c. amplifier which causes the current to change in the direction which reduces the error to below 1 part in 10^6. The actual current is supplied by an internal 'deac' accumulator. The lights to supply the beam for the photocells in the amplifier circuit were originally two 12 v. 12 w bulbs, supplied from a 12 v voltstat, constant voltage transformer.

As six of these bulbs failed in two months, the manufacturers advised modifying the arrangement of two lamps in parallel to one of two 6 v. 18 w lamps in series, and this modification was carried out.

The output from the transformer may be switched to an internal battery-charging circuit when the voltage of the accumulator drops to below 5.5. v. This state of affairs is shown by the failure of a light spot to appear on a small window in the front of the apparatus.

The standard cell used by the current controller for the potentiometer is one half of a Tinsley double Weston Standard cell, type 1149, the other half of which is connected to the standardizing circuit of the potentiometer. The makers advise that this set up produces greater precision than one in which two separate standard cells are used. The standard cell and the Tinsley type 3504 class S high precision standard resistors used in the measuring circuits, are kept in an enclosure insulated on five sides with 1" polystyrene foam and at the front with $^{3}/_{8}$" perspex sheet to permit the temperature to be read from an accurate mercury-in-glass thermometer in the enclosure.

The galvanometer used in conjunction with the potentiometer is a Tinsley type 5214 photocell galvanometer amplifier, the signal being passed to a secondary indicating galvanometer (Tinsley, type MS2.45E). The current to the 12 v. 36w. lamps in each of

these instruments is supplied by a 12 v. voltstat transformer. The signal from the potentiometer first passes through a Tinsley type 5214A thermal compensating unit. The parasitic e.m.f.'s are compensated for by setting the potentiometer to zero and disconnecting the supply to the circuit under test. The thermal compensator may then be adjusted to bring the galvanometer spot to zero. This unit has also a high precision set of series resistances to protect the galvanometer against too high an out-of-balance signal. This set of series resistances (10^7 ohm; 10^5 ohm; 10^3 ohm) is not in fact used as a similar more accessible set is fitted to the potentiometer.

Sufficient freedom from vibration is provided by the 1" chipboard shelves of the console on which the instrument rests, and by the rubber castors of the console. On the makers instructions all leads are of sheathed untinned copper wire to reduce parasitic e.m.f.'s. The sheaths are earthed, as are the cases of all instruments, to provide complete screening. The amplifier has an adjustable parallel feedback, and even with this in its least sensitive position, the sensitivity is sufficiently high for the deflection caused by 0.01 microvolts to be detected easily with the naked eye.

i) The Thermometer Circuit.

The current passing through the thermometer is supplied by a current controller, similar to the one used to supply the potentiometer. The feedback is supplied by a resistance, R_F, in series with the thermometer. The voltage across the thermometer, V_{Pt}, is compared with the voltage, V_{10}, across a standard 10 ohm resistance. The resistor temperature is read on the mercury-in-glass thermometer in the polystyrene enclosure, and from the makers calibration, the exact resistance, R_{10}, may be found. Then the resistance of the thermometer, R_{Pt} is given by

$$R_{Pt} = V_{Pt} \cdot R_{10}/V_{10}$$

The current used in an early trial experiment was 1 mA, as the N.P.L. calibrations were carried out using this current. In subsequent experiments a current of 3 mA was used, as this increased the potentiometer readings threefold. The error this gives to the temperature measurements is very slight, and will be discussed in the section on temperature measurement. The current (I) from the current controller is determined by the resistance of R_F, using the relations

$$I = V_{std.cell}/R_F$$

A system of reversing switches consisting of amalgamated copper rods dipping into mercury pools was constructed. Besides the network, A, that reversed current and feedback, and the network, B, that reversed the connections to the potentiometer, a further

THE MEASURING CIRCUITS

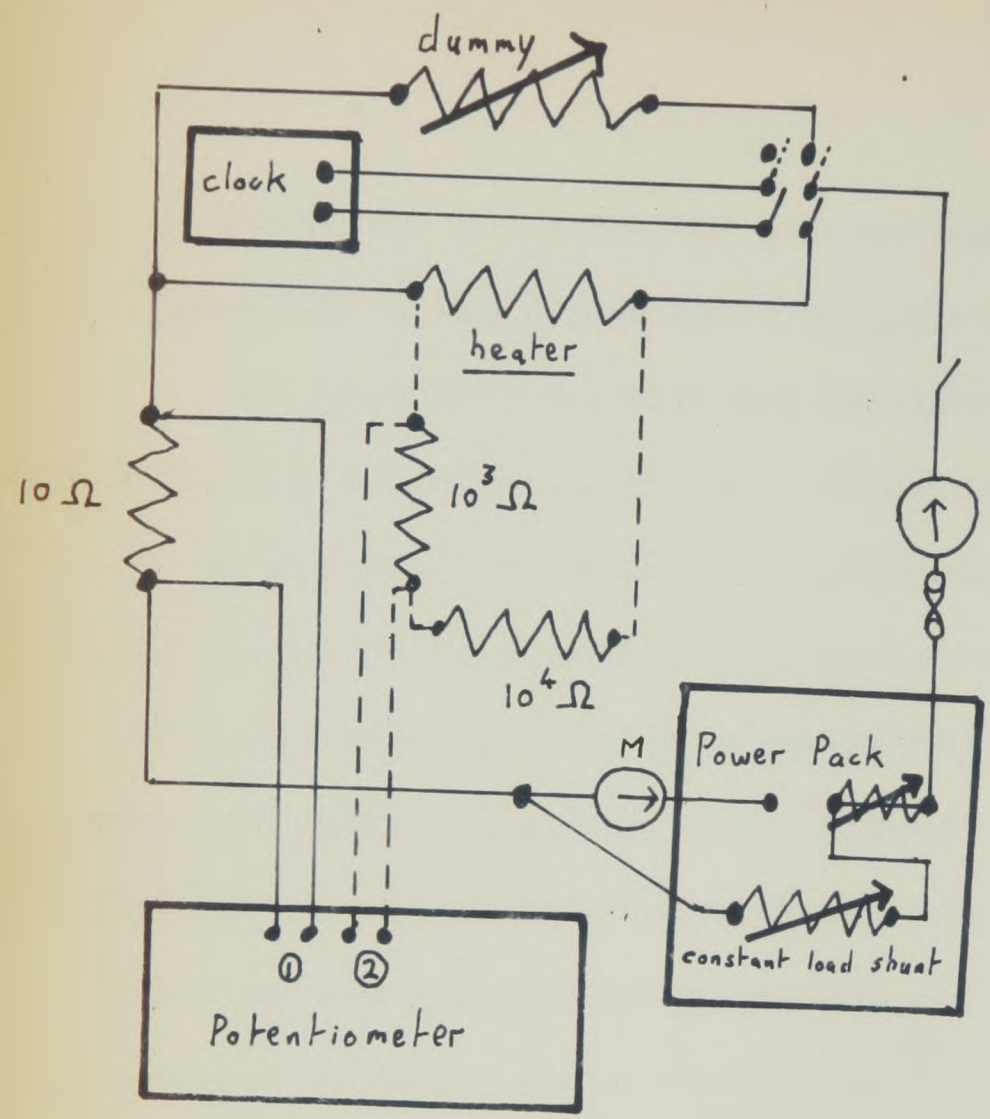

a) SAMPLE CONTAINER HEATER CIRCUIT

(dotted portion of circuit removed after heater resistance calibration.)

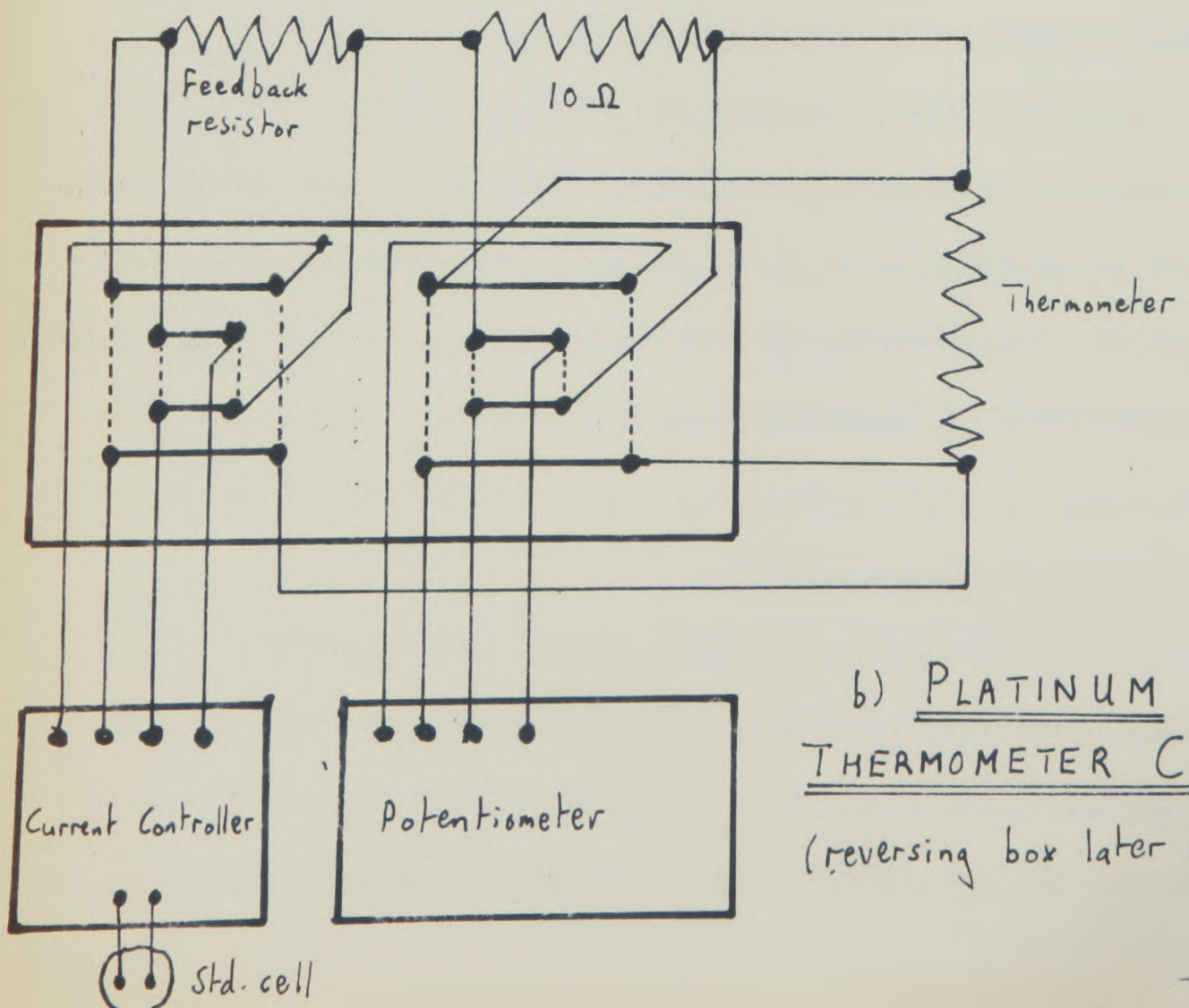

b) PLATINUM THERMOMETER CIRCUIT

(reversing box later removed)

network, C, not shown in the diagram, reversed the current through the potentiometer. In this way, by reversing A and B voltages could be measured with the thermometer current reversed, by reversing B and C, voltages, could be measured with the potentiometer current reversed, and by reversing A and C, voltages could be measured with both currents reversed. This reversing box was not used after the preliminary run as the current controllers had to be switched off before the circuits were reversed. They then took several minutes to settle down after being switched on again, and this prolonged the drifts, introducing greater inaccuracies than those that reversing was designed to eliminate. Thermal e.m.f.'s are therefore dealt with by the thermal compensator, which is reset about every fifth point during a run.

ii) The Sample Container Heater Circuit.

The current is supplied from a 27 v. stabilized power pack, fitted with a variable shunt, S, so that despite changesin the current required for theheater circuit, the output from the pack may be kept constant at 40 mA as shown on meter M. Three chains of diodes are used to smooth and step down the output of 55 v. taken from an internal transformer.

The current passes through a standard 10 ohm resistor calibrated by the makers, and then, by means of a two way switch, either through the calorimeter heater or through a variable decade box dummy whose resistance may be adjusted to the same value (within 0.1 ohm) as that

of the heater. This switch has another pole that starts a 'Labgear' electronic timer at the same time as the calorimeter heater is switched on. This decade timer, accentuated by a quartz oscillator measures the heating period to 10^{-4} sec.

The voltage across the sample container heater was measured, for the purpose of calibrating the heater resistance, via a potential divider. Although the resistance of the divider, made up of two precision Tinsley type 1104 resistors, one of 1000 ohms and one of 10,000 ohm, is large compared with the heater resistance of about 500 ohms, the current passing through the divider is not negligible. Let the total current in the circuit, as measured from the voltage across, and resistance of, the 10 ohm resistor be I. Let the current travelling through the heater be i_H.

$$I = V_{10}/R_{10}$$

$$I - i_H = V_{1000}/R_{1000}$$

$$\therefore \quad i_H = V_{10}/R_{10} - V_{1000}/R_{1000}$$

Now, the voltage drop across the heater equals that across the divider. Let the resistance of the leads from the heater to the divider be r.

$$V = (I - i_H)\ (R_{1000} + R_{10000} + r)$$

Let the power output of the calorimeter be ΔH.

$$H = i_H \cdot V \cdot t/J \text{ cals},$$

where t is the heating period and J(= 4.184) is Joule's equivalent

$$\therefore \quad H = (V_{10}/R_{10} - V_{1000}/R_{1000})(R_{1000} + R_{10000} + r).t.V_{1000}/R_{1000}.J$$

This is the expression used for the earliest runs, when values of the resistance of the calorimeter heater, R_H, were still being obtained. After values of R_H had been obtained from the expression

$$R_H = \frac{V_{1000}.(R_{1000} + R_{10000} + r).R_{10}}{V_{10}.R_{1000} - V_{1000}.R_{10}}$$

and had been smoothed graphically, and also fitted to a 5 term polynomial by a least squares programme, autocode 1000, on the KDF 9 computor, the simpler expression for ΔH shown below was used, ~~and~~ the potential divider being disconnected

$$H = \frac{V_{10}^2.R_H.t}{R_{10}^2.J}$$

iii) Shield Heater Circuit.

The purpose of the shield is to prevent the calorimeter either losing heat to, or gaining heat from, its surroundings. Consequently the temperature of the surroundings, which in effect is the temperature of the shield, must be kept the same as that of the calorimeter. The temperatures are monitored by copper/constantan thermocouples arranged in opposition so that when the temperatures are the same, no signal passes. When the calorimeter becomes hotter than the shield, a signal is passed to a Pye galvanometer modulator which indicates the size of the signal on a microvoltmeter. It

THERMOCOUPLE – SHIELD HEATER CIRCUIT

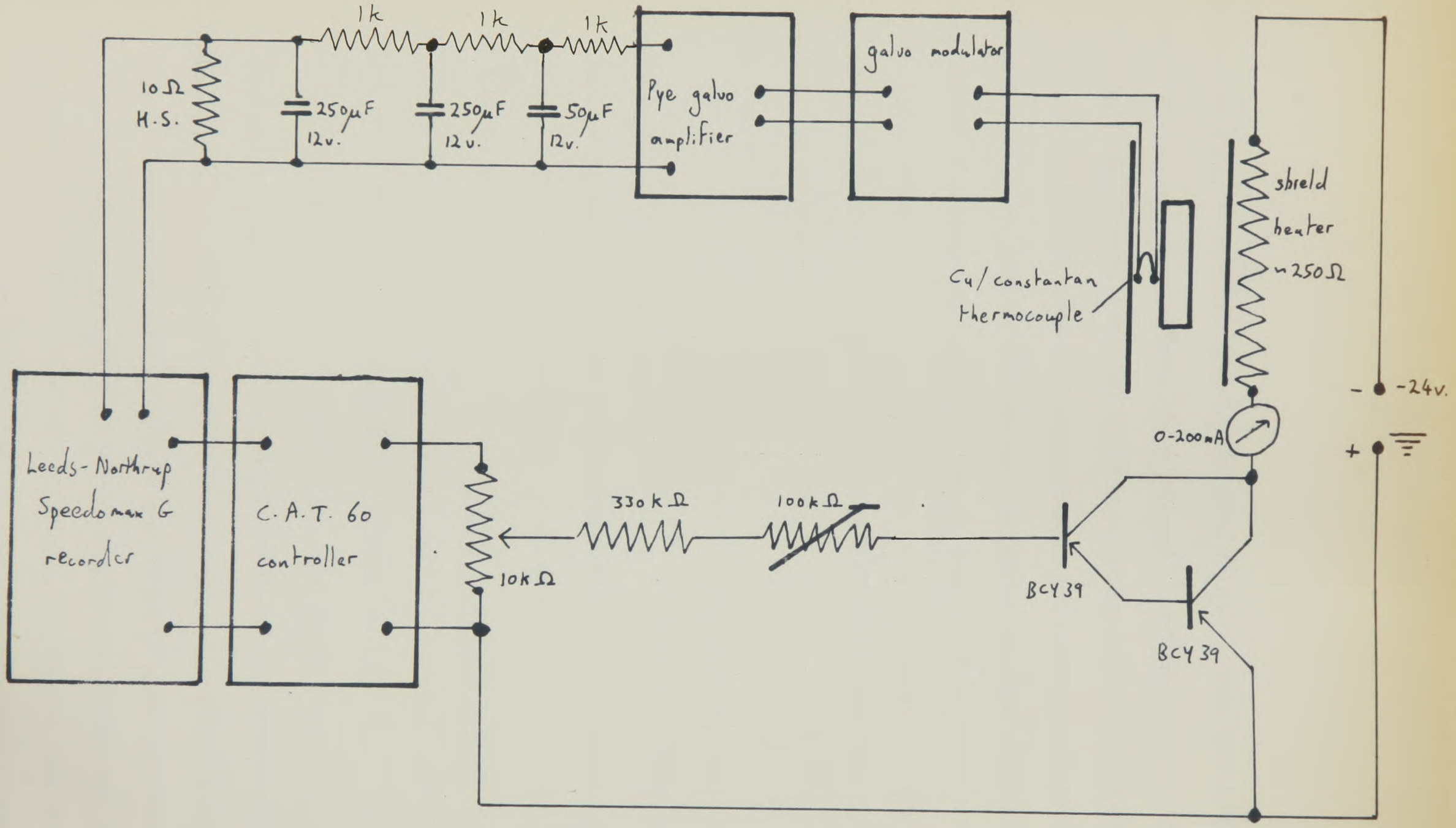

amplifies the signal which is passed through a linking circuit of capacitors and resistors to a Leeds-Northrup potentiometric chart recorder. This supplies a permanent record of the signal, and corrections can be applied from data obtained from the chart. An internal type C. A. T. 60 controller reacts to this signal in a way that will be described in the section on automatic control. The signal from the controller passes across a 10,000 ohm potential divider, and a part of the voltage developed is fed to theamplifier, which consists of two BCY39 transistors connected in tandem. The control voltage is applied to the base of the first transistor, and a shield current of up to 100 mA taken from the collector of the second which is at a negative voltage of not greater than 24 v. when on minimum load. The transistors are heat shunted by embedding them in an aliminium block using araldite, thus avoiding small leak currents. These can be a problem at thelower end of the range, where, because of the low heat capacity of the shield, currents of 5 mA or less are sufficient to maintain the temperature.

Temperature Range and Measurement

A platinum resistance thermometer is used for the whole range 4.2. - 300°K. Below about 35°K, a platinum thermometer is less sensitive than a doped germanium thermometer (ref 21) and the sensitivity drops sharply with fall in temperature.

Although temperature measurements using a platinum resistance thermometer are not very precise below about 15°K, the calorimeter was designed to operate down to the boiling point of liquid helium I for two reasons. The first is one of operational convenience; it enables temperatures below 20°K to be reached without recourse to pumping on liquid hydrogen. The advantages of this are twofold. The proceedure itself is inherently dangerous, and also the design of the cryostat is complicated, if means of pumping on the refrigerant have to be provided. The second reason is that magnetic transitions, in which this laboratory is also interested, frequently occur at temperatures below 20°K, and the versatility of the apparatus is increased if it is capable of observing these transitions.

The thermometer was calibrated at the National Physical Laboratory from 10°K to 300°K. As a check that the potentiometer and allied equipment was working adequately, the resistance, R_o, at the triple point of water was measured before the thermometer was insertedinto thesample container. A triple point cell described by Hall and Barber (ref 29) was used, and all the precautions they described were followed. A value of 24.6520 ± 0.0005 ohms was obtained as the mean of two determinations, giving a value at 273.15°K of 24.6510 ohms, compared with the N.P.L. value of 24.6500 ohms. The resistance of the thermometer at the triple point of water was then measured on a Smith's bridge, described in ref 1 , which was recalibrated for the purpose against an N.P.L.

calibrated 10 ohm resistance, and the same value for R_o, namely 24.6500 ohms, was obtained. This value, differing from the N.P.L. value by approximately 0.01°K at room temperature, was used in subsequent calculations.

a) Below 12°K.

The resistance of the thermometer was measured when the cryostat was filled with liquid helium, and helium exchange gas, at 0.5 torr pressure surrounded the inner container. The experience gained from another calorimeterin this laboratory showed that the sample container reached the helium boiling point within 15 minutes. This resistance, R_{He}, wastherefore taken to be the value at the boiling point of liquid helium, corrected for barometric pressure. It was used in conjunction with the resistance 12°K and the value of dR/dT at that temperature, taken from the N.P.L. calibration, to give the constants in the expression

$$R = a + bT^2 + cT^5$$

and from this expression, values of R and dR/dT were calculated at 0.1°K intervals. The term in T^5 apparently arises from considerations of lattice dynamics at low temperatures. Unfortunately, the value of R_{He} was not reproducible, varying by up to 15%.

As it was felt that sufficient time was given for the thermometer to reach 4.2°K, it was concluded that fluctuations in the thermal e.m.f.'s could be responsible for the observed variations or that alternatively the thermometer was not completely stable to

recycling at very low temperatures. In consequence, this expression was recalculated for each run, a value of R_{He} being determined at the beginning of the run. It is worth pointing out that the voltage across the platinum thermometer, using a current of 3 mA, is only about 36 microvolts, and that the instrument can only be read to 0.01 microvolts. Because of heat conduction along the copper cable a higher thermometer current wasnot used.

b) <u>$12^{\circ}K - 300^{\circ}K$</u>

The thermometer was calibrated by the N.P.L. against a standard platinum thermometer, and the calibration was presented in terms of deviations dW, from a standard table supplied of $W(= R_T/R_o)$ against temperature. Above $90^{\circ}K$, the N.P.L. measured the constants in the Callendar Van-Dusen equation

$$\xi T = \frac{R_t - R_o}{\alpha R_o} + \delta\left(\frac{t}{100} - 1\right)\frac{t}{100} + \beta\left(\frac{t}{100} - 1\right)\left(\frac{t}{100}\right)^3$$

and found $R_o = 24.6500$ ohms

(My value of $R_o = 24.6510$ ohms was used in subsequent calculation)

$\alpha = 0.00392628$

$\beta = 0$ ohm, t above $0^{\circ}C$

$\beta = 0.1101$ ohm, t below $0^{\circ}C$.

δ (estimated) $= 1.492$

Values of R and dR/dT for 0.1° increments of T were calculated on the KDF 9 computer using a programme kindly lent by C. G. Waterfield.

Comparison of dT/dR vs. T From the N.P.L. calibration and the Callendar Van-Dusen equation near 90°k.

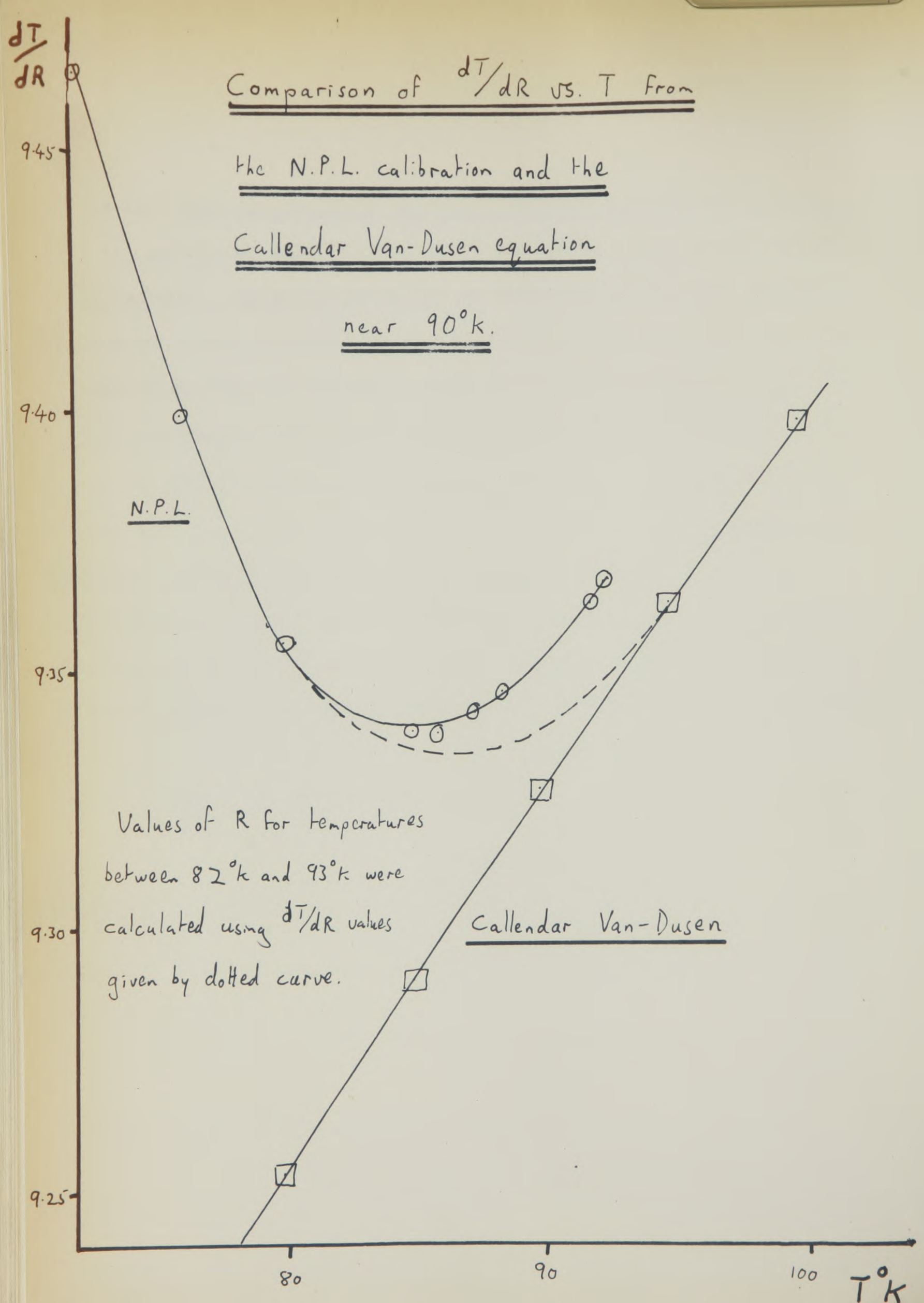

Values of R for temperatures between 82°k and 93°k were calculated using dT/dR values given by dotted curve.

A discontinuity between values of dR/dT calculated from the N.P.L. tables below 90°K, and from the Callendar Van Dusen equation above 90°K, is shown on the graph opposite. Values between 82° K and 93°K were therefore recalculated using values of dR/dT obtained from the dotted line. This removed the previous discrepancy between the two tables of the value of R_{90}.

AUTOMATIC CONTROL

If the temperature of the shield is automatically kept the same as the temperature of the sample container, then adiabatic conditions are maintained without the need for another worker to control the shield.

There are three main criteria that an automatic system must fulfill.

1) Control of the shield temperature must be as good as the best manual system, and be capable of dealing rapidly with a range of demand changes.

2) There must be an easy transition to manual control in case of need.

3) No disturbing interaction signals must be introduced into the calorimeter measuring circuits.

Early automatic control systems are reviewed by Waterfield (ref[ ) The system used here is the same as that used by Waterfield, and is based on that used by West and Ginnings, and Cooper et al.

A copper-constantan thermocouple with one junction soldered onto the sample container, and one junction sealed in an electrically insulated pyrotenax cable soldered to, and in good thermal contact with, the shield, supplies a signal of a few microvolts when the sample container temperature differs from the shield. (In Waterfield's apparatus, three junctions on the shield, at various heights of the wall and three junctions on the ~~calorimeter~~ sample container, again at varying heights, were used. The presence

of more junctions gave a bigger signal. However, the sample container used by Waterfield had a copper base and a platinum body, and there were junctions on both. Junctions were in thermal contact with both parts; there was a thermal gradient from the quickly heated copper to the less thermally conducting platinum; in consequence the signal generated was not proportional to the temperature difference of sample and surroundings and some imprecision was introduced.

In this calorimeter, only one junction was used on the shield, being situated half way up the shield, and only one on the sample container, half way up the platinum case. There is no junction on the copper cylinder affixed to the platinum case).

The signal from the thermocouple is fed to a Pye microvoltmeter-amplifier, type 11340/S, mounted on newspaper on a chipboard shelf of the console, to reduce vibration. The instrument is used clamped. The output from the jackplug at theback of the Pye is taken through a resistance-capacitor network to the recorder part of a Leeds and Northrup speedomax G recorder, which has a centre zero, and full scale deflection of $\pm$ 5 mV. The response time of the system is one second for full scale deflection. The chart produced gives a permanent record of the temperature difference between sample container and shield, and corrections can be applied. This is an advantage of the automatic over the manual system.

The bottom half of the recorder contains a current adjusting controller (C.A.T.60) and this operates on the out-of-balance signal from the control slidewire, which is on the same shaft as the pen-recorder slidewire.

The controller uses three, separately adjustable forms of control. Proportional control (expressed as a percentage of the ± 5 mV scale for full control current, e.g. 20% means that full control current is passed when the slidewire is 20% of the full scale away from the control point, i.e. 2 mV) gives an output current proportional to the deviation from the control point. The normal setting is in the region of 15 - 30% and is determined empirically. Reset control, expressed as resets for minute, works on the integral of the signal, and means that the longer the signal stays away from the control point, the more current will be put in to bring it back to the control point. The normal range used is 0.3 to 1.0 rsets/minute.

Rate control, expressed as repeats per minute, works on the differential of the signal. It depends on the rate at which the process deviates from the control point. It is really intended for processes that may suddenly deviate rapidly from the control point. In our system, when the biggest signal the recorder will get is at the beginning of a heating period of about $\frac{1}{2}^{\circ}$/min, rate control is a luxury and is used at a token 0.01 - 0.04 repeats/minute. Both rate and reset cut out on the high side of the control point (i.e. shield hot; the r.h.s. of the chart).

At the beginning and end of a heating period, especially when the shield and container are well above the refrigerant temperature, some manual intervention is helpful, and is achieved by turning the switch on the front of the recorder from auto to manual, and adjusting the rheostat knobs. If desired, manual operation can be used all the time, the controls being accessible to the hand from the operators seat.

The control current is passed through a 10,000 ohm potential divider, and part of the voltage developed is fedto the two-etage transistor amplifier. The divider is adjustable enabling all the current produced by the controller to be used when it is needed at high temperatures, but permitting smaller shield currents to be produced by the same controller current at lower temperatures.

The two BCY39 transistors in the amplifier are connected in tandem, the controller voltage being applied to thebase of the first transistor and a shield current of up to 100 mA taken from the collector of the second which is at a negative voltage of not greater than 24 volts when on minimum load. The power supply for the shield heaters is drawn from a variable voltage D.C. transformer. The transistors are heat shunted by embedding them in an aluminium block using araldite, thus avoiding small leak currents that can be troublesome at low shield currents (e.g. 5 mA).

Originally the thermocouple signal from the Pye was left on the most sensitive (X1) range and the Leeds Northrup on auto overnight,

resulting in the temperature the following morning being within 0.5^{o} of the temperature the previous night. After some trouble was encountered with the Leeds Northrup, requiring replacement of the amplifier, it was felt to be risky to leave the apparatus unattended for long periods while on auto, and instead, the Pye signal was shorted, and the current manually set at the value the instrument had arrived at automatically, for overnight periods.

CHAPTER III

EXPERIMENTAL PROCEDURE

EXPERIMENTAL PROCEDURE

1) Filling the Sample Container

Let us start with the sample container at the stage where it still contains the previous sample examined, and is still in the calorimeter. First, the outer can is removed using a large soldering iron (or if preferred, an electrical heating coil), taking care to release the vacuum in the calorimeter first. The twelve leads from the shield to the copper block are unsoldered, and the three nylon loops lifted off their adjustable hooks on the copper block. The shield/sample container assembly is then removed to the bench, where the ten connections from the cable to the shield are unsoldered. The six screws holding on the lid of the shield are unscrewed, the anti-radiation cover at the base of the shield is loosened and rotated out of the way, and the sample container, suspended from the lid, is lifted out. It is unhooked and weighed; this weight should be the same as the final weight of the sealed sample container, obtained just before it was put into the calorimeter. It will probably differ slightly ($\sim$ 0.001 gm) because i) moisture on the surface will have been pumped away after two weeks under high vacuum ii) the weight of solder on the ends of the cable that were attached to the shield may be slightly different.

In a quiet room, the silver tube is cut with a razor blade. A hiss should be heard when the tube is cut through, indicating that the pressure in the sample container is below atmospheric pressure. This shows that no leak had occurred, and also that in the original pumping, the silver tube was not blocked, so that the air was in fact evacuated.

The partial vacuum having been released, the cap is unsoldered, the silver tube and excess solder removed, and the cap weighed. Indium solder is removed from the groove in the sample container, and the sample shaken out. This, and the empty sample container are weighed to check i) that theweight of sample is correct ii) that all the sample has been removed.

The sample container is washedout and dried (usually water then distilled water x 3, then AR acetone x 2 then a compressed air stream to constant weight. (The sample container must not be heated in the oven under any conditions as the thermometer will loosen in its setting and some of the internal soldered joints may break.)) If necessary, it is stored in a dessicator. Except when replacement is needed, neither the cable nor the thermometer are normally removed from the sample container, and all weights are referred to a sample container with these components attached.

The container is then filled and the weight noted. A weighed length of silver tubing is soldered, using electrical solder, to the cap and the weight of cap plus tube noted, giving the weight of

electrical solder. The cap and tube are then indium soldered to the sample container, and the whole entity weighed, giving the weight of indium solder in the container/cap seal. A glass capillary joined to a B10 socket is then black waxed to the silver tube, and a piece of fine wire poked down the tube to test that it is not blocked. The whole is attached to a vacuum line and pumped out for several hours. (In the case of a substance with a significant dissociation pressure, e.g. a hydrate, or certain ammoniates, the sample container must be cooled to a temperature at which dissociation is negligible. This was not necessary for any of thecompounds studied in this thesis, as $Hg(NH_3)_2Cl_2$ was the only one that could dissociate, and its dissociation pressure was below 10^{-5} torr at room temperature).

The container is then left under vacuum, preferably overnight, to test for leaks. In the absence of leaks, helium gas under 3 torr pressureis passed into the sample container, thesilver tube is sealed about one cm. from the cap with a pinch vice, cut in the middle of the flattened portion with a pair of pliers, and a tiny blob of indium solder <u>immediately</u> applied to the cut edge. The silver tube must only be touched by the soldering iron for a <u>very short time</u> as otherwise the container/cap indium solder joint will melt and air will be admitted. The solder seal is inspected with a hand lens, and, if suitable, the entity is weighed. From this weight and also the weight of the silver tube residue and a buoyancy

correction (only applied when the container is sealed), the weight of indium solder used for theseal, and the weight of silver tube are found.

Corrections are now calculated for theheat capacities of the excess i) indium solder ii) electrical solder iii) silver tube relative to the weights used for the empty calorimeter run. A typical set of weighings is set out below.

Weighings of the Calcite run.

Wt. empty container = 59.4363 gm.

Wt. full of calcite = 89.6223 gm.

∴ Wt calcite = 30.1860 gm = 0.30159 Moles.

Hence $C_{Ptot} - C_{Pempty\ pot}$ - solder corrections = C_p raw, must be multiplied by a factor of 3.31577 to give C_{pmol}.

"t cleaned cap = 0.4381 gm.

Wt silver tube = 0.4460 gm.

Wt cap and tube = 0.9523 gm.

∴ Wt elect solder = 0.0682 gm (Std. wt = 0.0229 gm)

∴ XS elect. solder = +0.0453 gm.

Wt container + cap and tube = 90.9499 gm.

Wt. Indium solder I = 0.3753 gm.

Wt. residue tube = 0.3837 gm.

∴ Wt silver tube used = 0.0623 gm (std. wt = 0.0863 gm)

∴ XS silver tube = -0.0240 gm

Wt sealed container = 90.6138 gm. (gross)

Buoyancy correction = 0.0205 gm.

∴ net wt. sealed container = 90.6343 gm.

∴ Wt of Indium solder seal = 0.0455 gm.

∴ Total Wt of indium solder = 0.4208 gm (std wt = 0.3980 gm)

∴ XS indium solder = +0.0228 gm.

From the weights of excess solder and silver tube, a graph of heat capacity (corrections) against temperature is plotted, using the data in the appendix.

The sample container is now hung from the shield lid, inserted into the shield, the cable protruding through the hole in the bottom, and the lid screwed down. The anti-radiation cover at the bottom is fixed in position, and the cable is soldered to the shield. The resistances between each pair of wires and between each wire and the casing, are then measured with an Avo meter, to check for shorts and bad connections. The shield is then suspended by its nylon loops from the three hooks, the height of which are adjusted so that the shield hangs centrally (since all the loops stem from a central ring on the shield, it must hang vertically). Again the resistances are measured at the console junction box. The outer can is then soldered on.

EXPERIMENTAL PROCEDURE

2) The Refrigerants

a) A Hydrogen Run.

As explained in the later section, this is the first run to be carried out. The calorimeter is pumped out at room temperature for 48 hours, to remove moisture, air, and the after products of soldering. The two dewars are then put up, and filled with nitrogen. Exchange gas (~ 0.1 torr He) is put into the calorimeter to cool it to liquid nitrogen temperature, and then pumped out overnight.

The dewars are then rapidly lowered, liquid nitrogen poured from the inner to the outer, and the inner dewar, now empty, is immediately replaced and the Leiden seal wired on. (The inner dewar is not wiped to remove frosting; frosting disappears on replacing the outer dewar; wiping will result in irremoveable frosting). The outer dewar is replaced as quickly as possible. Before syphoning is started, a face mask is put on.

The hydrogen dewar is put into position (having turned on the warning light, opened the upper windows in the room and checked that the hydrogen outlet to the outside of the building is open and all other outlets shut) and the syphon attached. The syphon is started using a football bladder and the Leiden seal is watched. No bulging means that the syphon is blocked; excess bulging means a blocked

exit tube. While syphoning is in progress, but not before, the upper inconel can is filled with liquid nitrogen. (Early filling will block the syphon entry tube.). The outer dewar is topped up at this stage.

Pumping on the surroundings of the sample container, which has been proceeding during the syphoning is now discontinued and about 5×10^{-2} torr of helium exchange gas is admitted. When the syphoning is over, the hydrogen storage dewar is carried to the roof (wearing a facemask). When the sample container is at about $20.4^{\circ}K$, the exchange gas is pumped out; after two hours pumping or more the run may be started. The procedure involved in taking points is similar for runs at all three temperature ranges and will be discussed later.

ii) A Helium Run.

When the sample container is at about $20.4^{\circ}K$, the exchange gas is pumped out and the hydrogen boiled off until only a few cm^3 remain. The hydrogen outlet is closed, and the syphon, adjusted to a suitable length is inserted. Using all possible precautions, the syphon is pre-cooled by boiling the tiny amount of remaining hydrogen through it. No hydrogen must remain in the dewar as the heat required to solidify say 5 cm^3 of liquid hydrogen will use up nearly half a litre of liquid helium. The heater must be switched off immediately the last of the hydrogen is boiled off.

The helium dewar is connected to the syphon, the outlets to the balloons opened and the syphon is started with the bladder. As soon as liquid starts to syphon over, the ~~balloon~~ bladder is replaced by pressure from a helium cylinder. The liquid is sent over as quickly as possible, and syphoning must be stopped immediately the liquid level in the storage dewar reaches the bottom of the syphon. Exchange gas is let in, and pumped out as soon as the temperature of thesample container reaches the required value. When the pressure falls to below 10^{-6} torr, the valve to the rotary pump is closed off and the pump switched off to cut down vibrations. As all the wires used in the cryostat are copper, (with the exception of the manganin leads to the hydrogen boil-off) the longest that helium will remain in the dewar, even with the economiser in operation, is 5-6 hours.

iii) A Nitrogen Run.

Nitrogen is used to cover the whole of the range 77-300°K. CO_2-methanol is not used as a refrigerant. Nitrogen runs last many days, and a large dewar is used and topped up overnight.

Drifts for a Typical Point

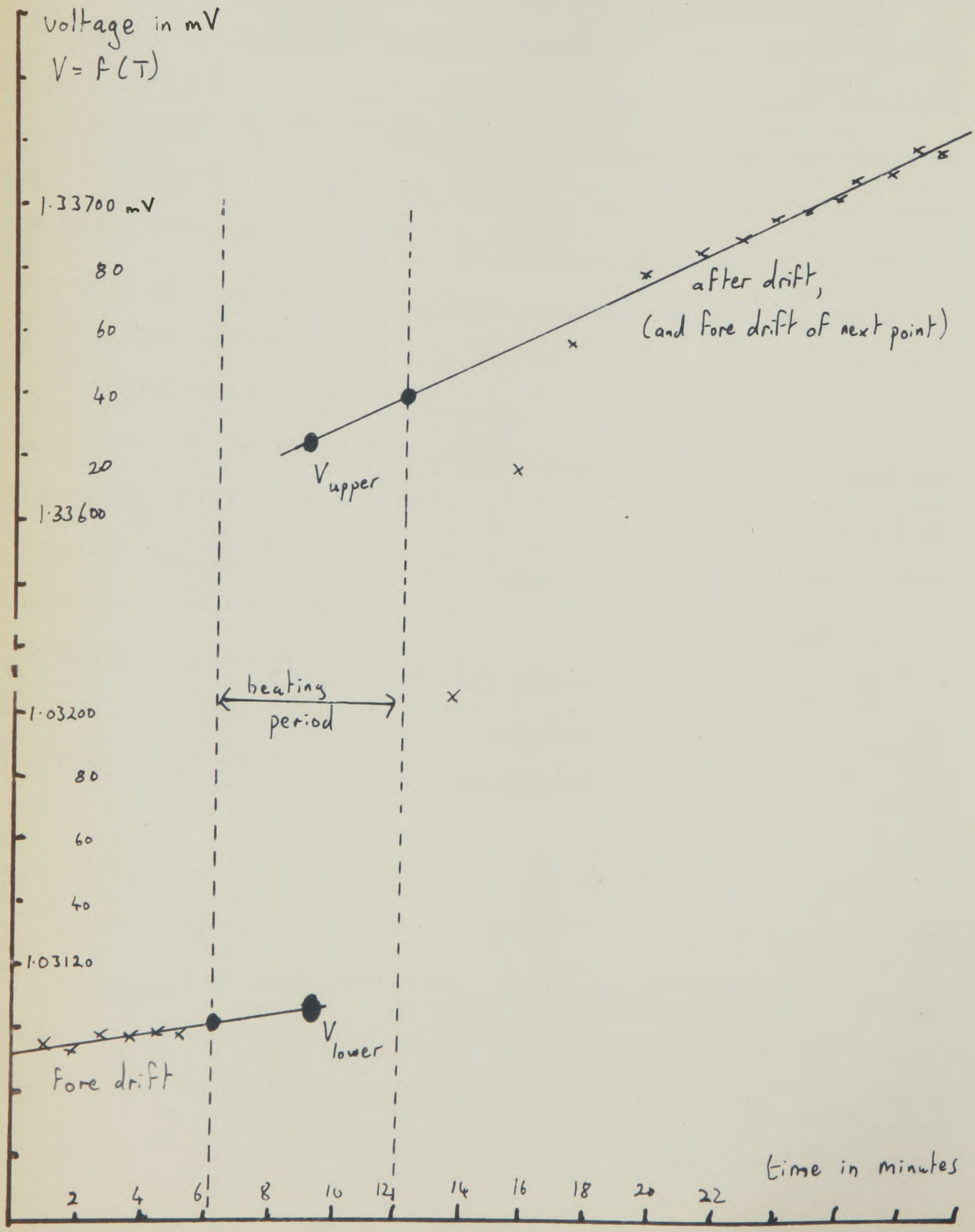

EXPERIMENTAL PROCEDURE

3) Calculation of Results

a) Preamble

Heat capacity points are worked out in the following way. Readings of voltage across the platinum resistance thermometer are taken at one minute intervals (half minute intervals for a helium run) for about 20 minutes, the current being measured (as the voltage across a standard 10 ohm resistance) at the beginning and end. This is the fore drift. The container heater, and simultaneously the clock, is switched on for theheating period. After the end of the heating period, measurements of voltage are taken irregularly until equilibrium (i.e. a steady drift) is reached. A drift is taken for about the same length of time as was needed to reach equilibrium. This serves as the afterdrift of the point, and the fore drift of the next point. A typical drift is between $0.0001^{\circ}K.\ min^{-1}$ and $0.001^{\circ}K.\ min^{-1}$ except at very low temperatures, where it may reach $0.01^{\circ}K.\ min^{-1}$.

The fore and after drifts are plotted as voltages against time, and extrapolated to the mid point of theheating period, giving V_{lower} and V_{upper} respectively. From these values, R_{upper} and R_{lower} are found, using the mean value for the fore drift current to find R_{lower}, and the mean value of the after drift current to find R_{upper}. Hence, T_{upper} and T_{lower} are found, and thus ΔT and T_{mid}

from

$$\Delta T = T_{upper} - T_{lower}; \quad T_{mid} = T_{fore} + \frac{T}{2}$$

Typical temperature intervals between points, and duration of heating periods are set out below. ΔH is calculated as explained in an earlier section, corrected for deviations of shield temperature as explained in the next section, and divided by ΔT to give $C_{p\ tot}$.

This is corrected if necessary for curvature, and the heat capacity of the empty container, $C_{p\ cal}$, and solder, $C_{p\ solder}$, subtracted. This gives $C_{p\ raw}$ which is multiplied by the mole factor (i.e. $^{1}/_{no.\ of\ moles\ of\ sample}$) to give $C_{p\ molar}$. Corrections are applied as follows.

i) Curvature. Only below $\backsim 15^{\circ}K$ or near a transition.

ii) Shield. Only above $\backsim 60^{\circ}K$ (thermocouples are rather insensitive at lower temperatures and produce too small a deflection for accurate correction).

iii) Solder. Over the entire range.

Temperature, $T^{\circ}K$	1st pt. $10^{\circ}K$	2nd pt. $10.5^{\circ}K$	$11-20^{\circ}K$	$20-50^{\circ}K$	$50-80^{\circ}K$	$80-200^{\circ}K$	$200-300^{\circ}K$
Length of heating period, T min	60 sec	90 sec	2 min	4-6 min	6-8 min	8-15 min	15-20 min
Temperature rise $T^{\circ}K$	$\frac{1}{2}^{\circ}K$	$\frac{3}{4}^{\circ}K$	$1-2^{\circ}K$	$2-4^{\circ}K$	$4-5^{\circ}K$	$5-8^{\circ}K$	$8-10^{\circ}K$
Refrigerant	liquid helium			liquid hydrogen		liquid nitrogen	

A Typical Chart Trace

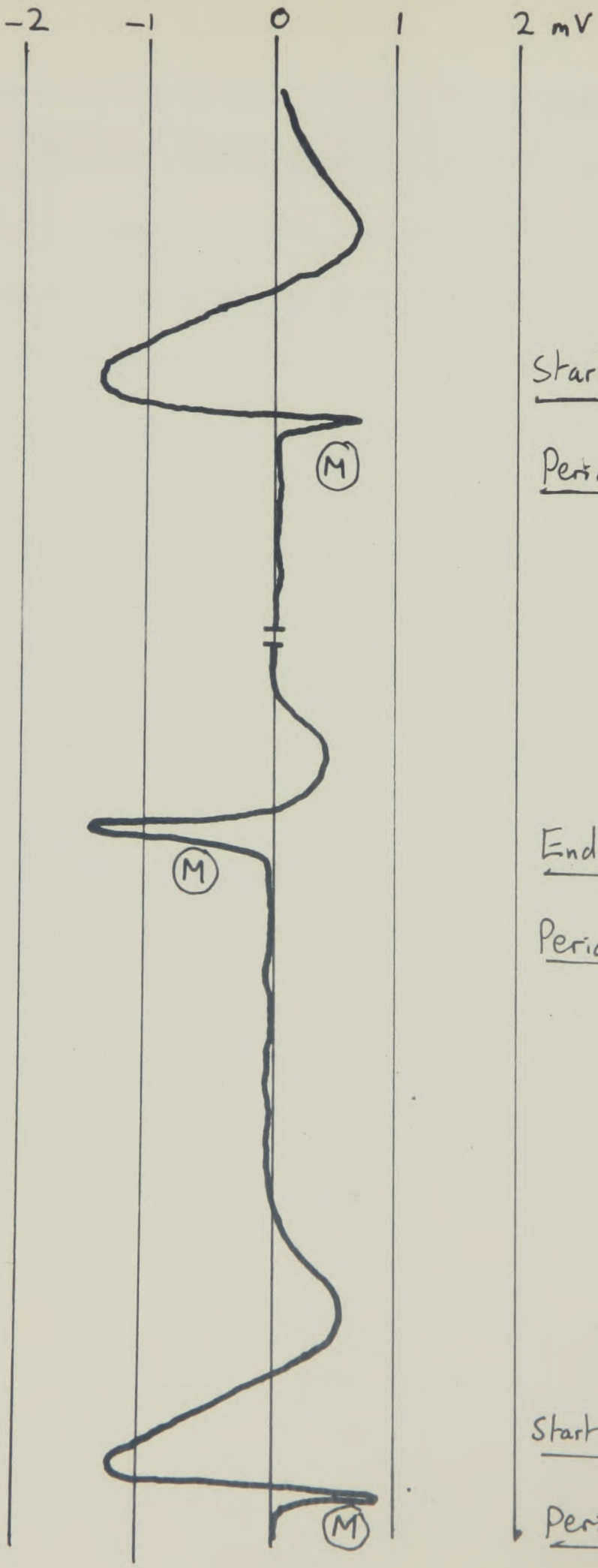

Point $Na/N_2/21$

Start of Heating Period

End of Heating Period

Point $Na/N_2/20$

Start of Heating Period

(M) indicates manual intervention

B) Corrections.

i) Corrections for shield temperature deviations.

The control chart record for each point is kept, and has the appearance shown on the page opposite. The control point is normally at 0, but once a day during a nitrogen run, the drift is taken with the control point at, say, + 1.0. This drift, which is used as the fore drift of one point and the after drift of a previous point, is a heating drift if the pointer is set to a plus value, and a cooling drift if set to a minus value. From the difference between the drifts at two control points, the drift per unit-point-deflection is calculated. Let this be

$$\phi = \text{ohms min}^{-1} \text{ (unit-point-deflection)}^{-1}$$

Now the total area of deflection on the chart is obtained by counting squares, area on the plus side (i.e. the 'shield-hot' side, being counted as positive and areas on the minus, 'cal-hot' side being minus). Let the area be A squares. Depending on the speed of the chart recorder, either one or two squares are traversed in two minutes. Let us take the caseof the chart recorder with a speed of half a square per minute. The area is then 2 x (number of minutes) x (no. of unit-pointer-deflections)

$$\therefore \quad \text{ohms} = \text{drift} \times \text{area} \times 2$$

$$\text{and} \quad \Delta H_S = C_p \cdot {}^{dT}/_{dR} \cdot \text{ohms} = 2 \cdot C_p \left({}^{dT}/_{dR} \right) \cdot \text{drift} \cdot \text{area}$$

c) A typical Point

This correction is added to the heat input, ΔH. Usually it is of the order of >0.1% of ΔH. In the example shown, it is slightly under 0.01%.

ii) Corrections for curvature.

At low temperatures, or near a transition, C_p varies considerably with T, and it is necessary to apply a curvature correction. This takes the form (ref 30)

$$Cp_{tot}\ (\text{corrected}) = Cp_{tot} - \left(\partial^2 Cp_{tot}/\partial T^2\right)_{T_{mid}} \cdot \frac{\Delta T}{24}$$

The correction, even when curvature is quite great, is usually small unless an abnormally large temperature interval has been used. Thus, in the run on $Hg(NH_3)_2Cl_2$, the following curvature corrections were applied. (The row marked % gives $\frac{\text{Correction x 100}}{Cp_{tot}}$

T_{mid} (°K)	8.437	8.816	9.725	11.070	12.243	13.436
Cp_{tot}	0.1649	0.2070	0.2597	0.2759	0.3751	0.4340
Curvature	-0.000014	negligible	-0.0003	-0.0003	-0.0003	-0.0003
%	0.008%	0	0.115%	0.109%	0.080%	0.069%

No corrections were applied to higher points.

c) A typical Point

Ambient temp = 23.5°C Tues 15th Aug '67; 12.46 p.m.

$Na/N_2/20$

V_{10} (circuit 3 range x 0.1)	time (mins)	$V_{thermometer}$ (circuit 4 range x 0.1)	Comments
30.11990 mV	39 40	58.07710 mV	Shield at 0
	41	14	
	42	17	Thermals
	43	20	③ = -0.73 micro V
	44	23	④ = -0.6 micro V
	45	23	
	46	30	Set to 4
Mean =	47	33	
30.12000 mV	48	38	Fore drift
	49	40	
	50	45	
	51	48	
	52	52	
30.12010	53½ 53	58	
V_{10} (circuit 1 range x 1)			
330.470 mV	2 ON 54	Heating Period	Shield off -35
442	4		
392	6	Mean = 330.352 mV	

V_{10} (Circuit 1, range x 1)			
350	$7\frac{1}{2}$		Heating Period
318	9		
262	11		
240	13 OFF 69	Time = 900.0489 secs	

I	t	V	Comments
30.07592 mV	35 36	60.78900 mV	Stopwatch restarted
	37	08	1.55 p.m. (i.e. 69 min
	38	16	on fore drift = 0 min on
	39	24	after drift)
	40	30	
Mean =	41	36	
30.07603 mV	42	42	
	43	50	After drift
	44	60	
	45	65	(Fore drift of
	46	72	$Na/N_2/21$)
	47	78	
	48	80	
	49	88	
	50	92	
	51	60.90002	
614	$54\frac{1}{2}$ 52	10	
	53	18	
	54	26	
			Heating Period of
			$Na/N_2/21$

C) A Typical Point

This is taken from the run on anhydrous sodium carbonate at about 220°K, using liquid nitrogen as refrigerant. The current through the thermometer is not reversed, but thermal e.m.f.'s are measured and compensated for. The last figure in the drift voltages is taken from the galvanometer. Circuit and range numbers refer to the potentiometer. The shield maintains adiabatic conditions the whole time. The trace is shown on an earlier page. It is under automatic control except a) near the boiling point of the refrigerant where cooling of the shield is slow, and it is switched off before the end of the heating period to prevent overheating (this has been done 35 ~~records~~ seconds before the end of this heating period) b) at temperatures about 200° above the b.p. of the refrigerant, shield current is turned to a maximum about 15 seconds before the beginning of the heating period.

From graphs of the fore and after drifts V_{Fore} = 58.07783 mV and V_{after} = 60.78600 mV. The fore and after resistances are then found by dividing by $V_{10\Omega,fore}$ and $V_{10\Omega,after}$ respectively. Two points must be noted here. i) This uses a value of 9.9997 ohms for the standard resistance. The resistance at 20°C from the N.P.L. calibration is 10.0000 ohms, and the temperature coefficient is -7×10^{-5} ohms deg^{-1}, giving the value quoted. In general, unless the ambient temperature is markedly different from 20°C, little

error is introduced into T_{Fore}, T_{after} or T_{mid} by taking $R_{10\Omega}$ as 10.0000Ω. Unless the ambient temperature changes by over half a degree from the fore to the after drift, negligible error is introduced in ΔT. ii) Normally, using the current controller, the current is independent of the resistance of the thermometer. A lot of difficulty was experienced with the current controllers at certain times, and in fact a 2 v. Exide type LCG.6 battery was used, in conjunction with a buffer resistance of about 650 ohms, for this run. R_{upper} = 20.21078 ohms; R_{lower} = 19.28215 ohms.

In this temperature range, the Callendar Van-Dusen equation was used. Values of R and $^{dT}/_{dT}$ at 0.1°K intervals had been printed on the KDF 9 lineprinter, and rather than calculating T_{fore} and T_{after}, the following simplification was used. R_{mean} was found as an average of R_{upper} and R_{lower}, and T_{mid} found from this value. Using $^{dT}/_{dR}$ at this value, Δ T was found from Δ R, i.e. 19.74646 ohms here T_{mid} = 223.60°K, T = 9.3061°K. introducing an error in ΔT of about 1 pt in 50,000.

The value of the resistance R' of the container heater was found from a large scale graph, to be 550.26 ohms at 223.60°K. From the mean value of voltage across 10Ω resistance I = 33.0352 mA, Δ H was found from the expression $\Delta H = I^2Rt/J$ using $J = 4.184$ cal. $joule^{-1}$ as a defined value, to be 129.1803 cals. For this point, the positive and negative chart corrections cancelled out, giving no correction to Δ H. Thus $Cp_{tot} = \Delta H / \Delta T$

was 13.881 cal/mole/deg. $C_{p\ cal}$ and Cp_{solder} at T_{mid} were 3.046 and 0.040 cal/mole/deg respectively; the mole factor was 2.19146 hence Cp_{mol} = 23.657 cal/deg/mole at 223.60°K.

The heat capacities were smoothed as explained in a later section. The point discussed above deviated from the smoothed value of the six term polynomial at that temperature by 0.071 cal/mole/deg, or -0.12%.

Presentation of Results, Smoothing Procedure and Calculation of Molar Properties

The results obtained in this work are set out in the following way. For each substance, the number of moles used, the excess weights of solder,* and the approximate percentage of the total heat capacity (i.e. container plus sample) that is contributed by the sample at 10, 20, 50, 100 and 300°K is listed. The experimental heat capacities follow. First, points obtained with liquid helium as a refrigerant are listed, then points using liquid hydrogen and finally points using liquid nitrogen. This results in points not being listed in order of rising temperature in the 'overlap' regions (20-25°K; 77-85°K).

For the empty container, smoothed Cp values at 10° intervals from 10-300°K are listed. For the substances, the smoothed functions entropy, $H-H^{\circ}_{o}$, $(H-H^{\circ}_{o})/T$, and $-(G-H^{\circ}_{o})/T$ are also given. Accompanying graphs show the salient features. Values for S(T), etc. From 0°K to the lowest measured temperatures were extrapolated, using a $Cp \propto T^3$ law.

Smoothing was carried out graphically below 50°K, and by the library programme 'autocode 1000' on the KDF9 computer from 50 - 300°K. This programme smooths the experimental results to a polynomial (5 or 6 term in the case of these results). The coefficients of the polynomial were used to obtain the smoothed functions, S, $H-H^{\circ}_{o}$,

* A + sign means contribution must be added to the empty container, i.e. subtracted from Cp_{TOT}

$(H-H^{\circ}_{o})/T$ and $-(G-H^{\circ}_{o})/T$, using the programme FAJBM123456 in appendix 1.

For all the substances, experimental heat capacities were calculated by subtracting the heat capacity of the empty container and the appropriate solder and/or curvature corrections from the total heat capacity at each point. The resulting molar heat capacities were then smoothed. This procedure differs from that of Waterfield (ref 1) and of Furukawa, Douglas and Ginnings (N.B.S. determination of Cp benzoic acid, ref 31) who smoothed their total results and then subtracted smoothed corrected heat capacities of the empty container.

The heat capacities of solder etc. at various temperatures, are listed in appendix 2.

Leaks and Minor Setbacks.

Out of the numerous possible setbacks in this branch of physical chemistry, only four occurred in this work. These were

1) a Leak
2) a Low-temperature leak
3) No exchange gas in sample container
4) Air left in sample container.

When the outer can has been soldered on, the normal procedure is to pump out the calorimeter on the rotary pump through the by-pass line until the pressure drops to about 8×10^{-2} torr. If the pressure takes longer than about two hours to drop below 1.5×10^{-1} torr, then a large leak may be the cause; this can be confirmed by closing off the pump and opening to the manometer. If there is not a large leak, atmospheric pressure will not be reached, although degassing will cause a considerable rise in pressure. If atmospheric pressure is reached within say 12 hours, there is a large leak. This is probably in the soldered rim of the outer can, although the tightness of the 'O' ring holders on the Genevac couplings should be tested. These should be hand tight. If the couplings seem alright, it is best to remove the can (release the vacuum first!) and run all the solder out of it, and to retin by heating gently direct in a bunsen flame, then running flux and a little additional solder round the rim. The flange of the copper block should be wiped clean, and any suspect patches sandpapered. The can may then be soldered

back on.

A low temperature leak is in one way more aggravating than an ordinary leak, in that the preliminary two days pumping has probably been finished and the dewar put up, but it is relatively easy to locate since it is in the portion of the calorimeter, under or near the surface of, the refrigerant. Almost invariably it is in the rim of the outer can and the only solution is to get rid of the refrigerant, drop the dewars, let the can warm up, and resolder. Although it is a good idea to test for a nitrogen temperature, low-temperature leak in the initial stages of pumping, by putting a dewar of nitrogen round the can, low-temperature leaks more usually open at liquid hydrogen temperatures.

Observations on a typical low-temperature leak were as follows. The vacuum under liquid nitrogen cooling was good (about 10^{-6} torr). When liquid hydrogen was siphoned in, the vacuum initially remained the same, and then, as the can cooled, deteriorated to about 10^{-3} torr with thepump still on. When the pumps were closed, the mercury level in the manometer took 5-10 minutes to fall one cm (low-temperature leaks are usually small). The pumps were opened and the pressure restored to 10^{-3} torr; the hydrogen was boiled off, the deward dropped, and the temperature noted. At $50^{\circ}K$, the heating rate of the sample container dropped considerably, indicating an improvement in vacuum, as also shown on the gauge.

Another, perhaps less typical, low-temperature leak was so large that the diffusion pump could not hold a pressure of 10 torr! The refrigerant was boiled off, whereupon the can warmed, the leak closed, the trapped gas in the can expanded and blew the mercury out of the manometer!

In the course of the work on aragonite, a hydrogen run was started and abandoned three times r nning, as in turn a low temperature leak, an exchange-gas-less calorimeter and an air filled calorimeter were encountered.

Lack of exchange gas can be diagnosed at any temperature. Instead of the sample container coming to equilibrium in a fairly typical time, the drift rate continues to change for three times as long as normal, and then a very uneven drift is obtained. Also, massive overheating may be observed, resulting in a cooling drift about 10 times as steep as normal initially. Always continue the run for a point or two in these circumstances as other phenomena e.g. transitions, and possibly some form of helium condensation on the surface of the sample, can give the same symptons. When the run on fusible white precipitate was being carried out, from 4.2°K upwards, on Dr. Clay's calorimeter, the first point overheated (partly because the heating current was twice as big as it should have been, resulting in a 25% increase in absolute temperature) and took 25

minutes or more to come to equilibrium. By 8°K, the equilibrium time was 18 minutes and by 10°K it was 3 minutes. It is felt that some form of adsorption or condensation of helium is involved, as the phenomenon is more pronounced for a powdered sample than for a lumpy sample.

No exchange gas usually means a leak in the sample container at either the end of the silver tube or at the cap, although in theory it could arise if the silver tube, having been clear enough to let the calorimeter be evacuated, then blocked and failed to let exchange gas in. If the soldering iron is left in contact too long when sealing the silver tube, the cap to calorimeter seal may soften and leak. In any case, the calorimeter has to be removed, re-evacuated and reinstalled, usually taking 1½ days followed by two days pumping.

If air is left in the sample container, the silver tube has usually been blocked either by solder to by sample for the whole of the pumping. This can and should be tested for by passing thin wire through the silver tube right into the sample container immediately before pumping out. 20 cm^3 of air at atmospheric pressure in place of 20 cm^3 of helium at 2 torr pressure will act equally well as an exchange gas above about 75°K, and will have a negligible effect on the heat capacity. Between about 55°K and 75°K it shows up on the Cp vs. T plot as a lump, maximum about 67°K, and falling off more rapidly than it rose. Its area is probably about 2-2.5 calories. In the case of the aragonite run, exchange gas in fact remained in

the sample container, and equilibrium was reached below, as well as above, 75°K, presumably because in sealing the silver tube, the iron was left on too long, the solder softened at the cap, air entered, but exchange gas, having to fight against an incoming current did not completely escape against incoming pressure of air and then the iron was removed and the solder set leak-free.

As in the case of the exchange-gas-less sample container, the sample container must be repumped. As air only shows up when it is liquid, i.e. 55-75°K effectively, since four-fifths is nitrogen, both the absence of air in the sample container and the absence of a low-temperature or other form of leak are shown in a hydrogen run, and for this reason the hydrogen run should always be done first.

CHAPTER IV

SAMPLE CONTAINER CALIBRATION

Resistance of the Sample Container Heater.

$T^{\circ}K$	R ohms	$T^{\circ}K$	R ohms	$T^{\circ}K$	R ohms
8.09	486.11	51.11	504.73	130.12	535.42
10.38	486.43	53.91	506.15	138.28	537.43
12.39	488.15	57.01	507.52	149.11	540.08
15.87	489.14	60.02	508.99	161.04	542.51
19.81	490.89	63.84	510.77	176.94	545.21
20.60	491.36	66.17	511.84	189.19	546.78
23.28	492.01	71.20	514.07	201.29	548.24
25.51	493.11	76.05	516.14	216.81	549.66
26.96	493.91	80.60	518.06	226.66	550.50
30.11	494.90	84.97	519.87	237.26	551.16
33.46	496.81	88.26	521.11	251.56	551.85
36.27	497.80	94.57	523.59	262.53	552.26
38.62	498.84	99.52	525.41	276.75	552.50
41.07	499.93	104.32	527.10	285.66	552.67
43.61	501.07	108.99	528.68	296.28	552.80
45.88	502.09	113.52	530.21	304.57	552.86
48.28	503.88	121.69	532.75		

The heater resistances have been fitted to a polynomial, using the above 50 points, and an additional 107 points not listed, giving

$$R = 4.831638 \times 10^{2} + 3.281919 \times 10^{-1} T + 3.194016 \times 10^{-3} T^{2} - 3.069221 \times 10^{-5} T^{3} + 9.296555 \times 10^{-8} T^{4} - 9.901555 \times 10^{-11} T^{5}$$

Empty Container

1) Wt Container + cable = 59.4363 gm.

(This weight applies to the benzoic acid, calcite, and aragonite runs only. For the $Mg(NH_3)_2Cl_2$ and Na_2CO_3 runs a minor modification was made to the cable, giving a weight of 59.4910 gm)

2) Wt cleaned cap = 0.4381 gm

3) Wt silver tubing used = 0.0863 gm

4) Wt elect. solder used = 0.0229 gm

5) Wt indium solder used = 0.3980 gm

6) *Buoyancy correction = 0.0205 gm

*applies only when container is sealed under reduced pressure.

Experimental Heat Capacities of the Empty Container

T°K	Cp (cal/°K)	T°K	Cp (cal/°K)
8.09	0.0098	050.36	1.058
8.50	0.013	53.95	1.172
10.38	0.030	57.85	1.292
12.39	0.048	62.15	1.412
15.87	0.094	66.82	1.541
17.57	0.123	71.70	1.654
18.57	0.138	76.64	1.764
19.40	0.146	82.17	1.892
19.81	0.157	85.97	1.972
20.29	0.158	90.67	2.061
21.60	0.194	95.15	2.136
21.95	0.201	99.50	2.183
23.26	0.225	104.15	2.245
23.28	0.224	109.07	2.312
25.17	0.272	113.84	2.372
27.33	0.329	118.46	2.435
29.75	0.394	122.98	2.488
32.61	0.482	127.04	2.531
35.87	0.584	131.44	2.558
39.43	0.702	135.78	2.597
43.25	0.822	140.06	2.600
46.84	0.943	143.91	2.665

Experimental Heat Capacities of the Empty Container (Cont/d)

T°K	Cp (cal/°K)	T°K	Cp (cal/°K)
144.27	2.654	208.92	3.003
150.68	2.721	218.01	3.044
157.39	2.755	227.00	3.057
163.95	2.795	235.95	3.079
170.35	2.832	244.87	3.105
176.71	2.862	253.74	3.125
182.99	2.893	262.53	3.154
188.95	2.923	271.28	3.173
189.04	2.913	279.93	3.187
195.14	2.962	288.42	3.219
201.29	2.973	298.18	3.234

Smoothed values of Cp of empty Container

T°K	Cp (cal/°k)	T°K	Cp (cal/°k)
10.0	0.025	110.0	2.331
20.0	0.159	120.0	2.447
30.0	0.405	130.0	2.546
40.0	0.720	140.0	2.631
50.0	1.045	150.0	2.706
60.0	1.352	160.0	2.771
70.0	1.613	170.0	2.829
80.0	1.844	180.0	2.880
90.0	2.036	190.0	2.926
100.0	2.196	200.0	2.968

Smoothed values of Heat capacity of the Empty Container (Cont/d)

$T^{o}K$	Cp	$T^{o}K$	Cp
210.0	3.005	260.0	3.144
220.0	3.038	270.0	3.167
230.0	3.069	280.0	3.190
240.0	3.096	290.0	3.215
250.0	3.121	300.0	3.244
		298.15	3.238

Benzoic Acid.

The sample used was that already used by R. M. Clay for checking the precision of his calorimeter, and the same sample was subsequently used by C. G. Waterfield in his calorimeter. It consisted of small tablets, obtained from B.D.H. as a thermochemical standard (calorific value 26435 ± 3 joules/gm). The batch number was 710726. The tablets were broken up into small lumps and kept in a dessicator over P_2O_5.

Benzoic Acid

$C_6H_5CO_2H$ M.W. = 122.072

Wt of sample = 27.3510 gm.

No. of Moles = 0.22406

Purity = 100% (assumed)

Corrections.

Silver tube	=	-0.0229 gm
Electrical Solder	=	-0.0741 gm
Indium Solder	=	-0.1942 gm

Contribution of Sample.

T^oK	%
10	81.1
20	78.5
50	67.2
100	70.0
300	71.0

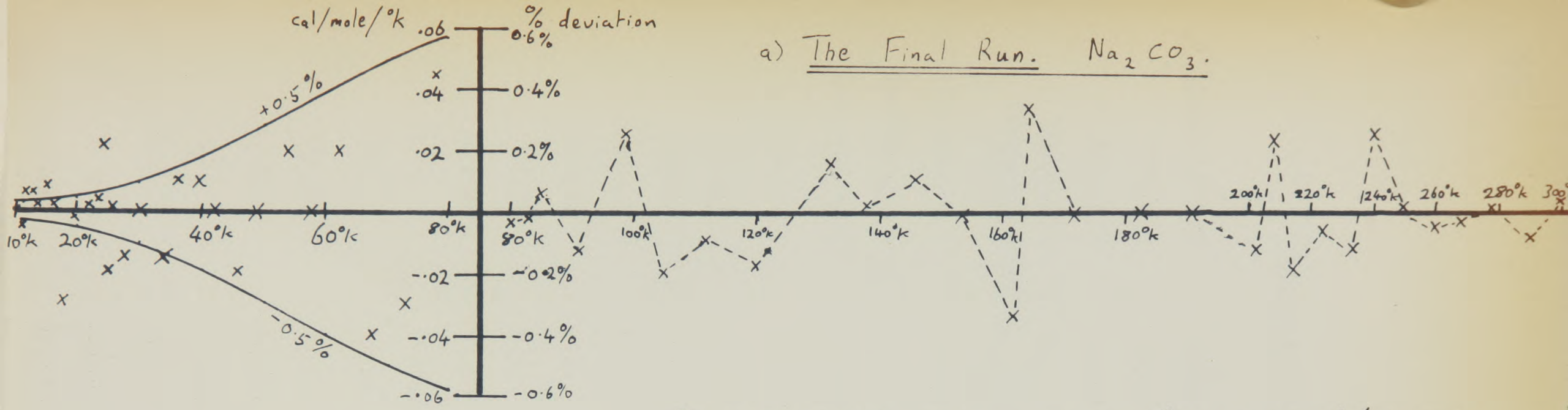

a) The Final Run. Na_2CO_3.

DEVIATIONS FROM THE SMOOTHED VALUES

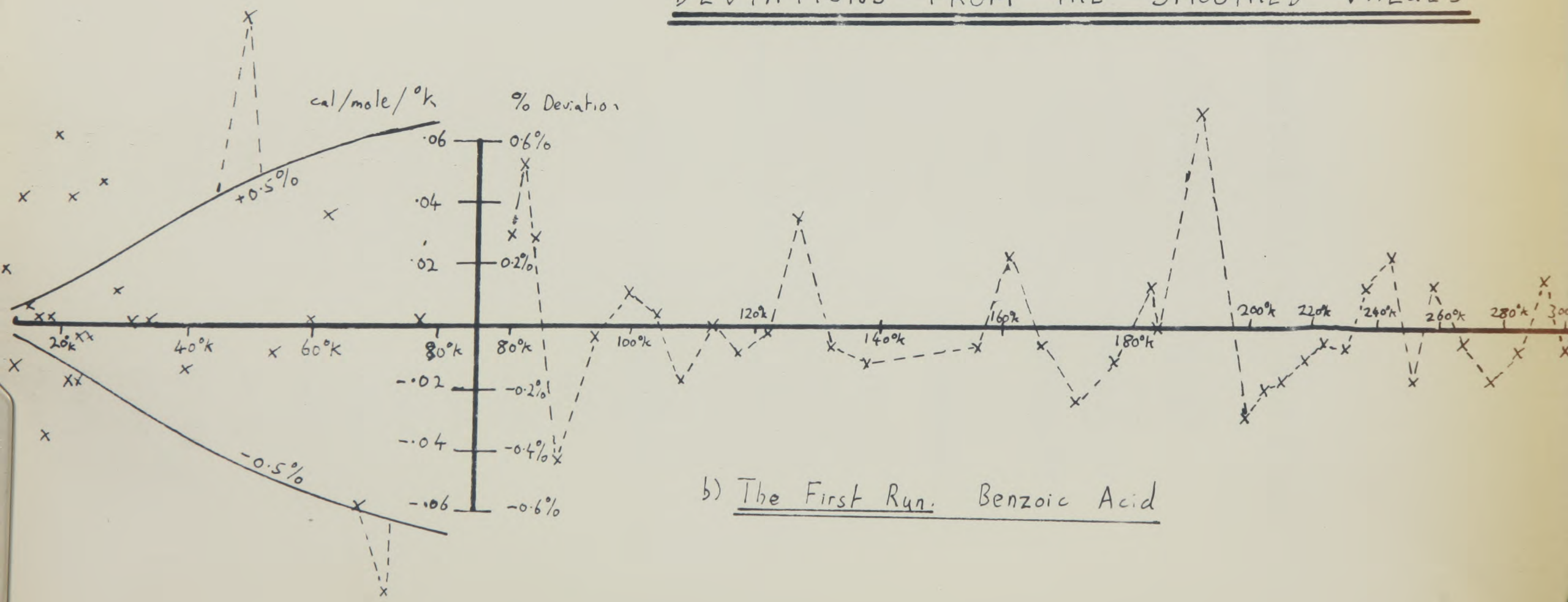

b) The First Run. Benzoic Acid

Experimental Molar Heat Capacities of Benzoic Acid

T°K	Cp (cal/mole/°K)	T°K	Cp (cal/mole/°K)
6.42	0.118	45.84	8.877
8.84	0.352	49.30	9.323
9.60	0.527	55.69	10.041
10.96	0.659	58.52	10.796
12.42	0.828	62.59	11.367
13.70	1.136	67.76	11.912
15.00	1.391	73.49	12.443
15.91	1.617	77.44	13.090
16.96	1.832	82.14	13.616
18.28	2.217	80.01	13.362
19.64	2.510	83.78	13.750
20.83	2.842	88.26	14.094
21.74	3.175	94.57	14.754
22.86	3.418	99.52	15.236
24.39	3.793	104.32	15.665
21.56	3.063	108.99	16.053
24.09	3.729	113.52	16.491
26.66	4.436	116.74	16.763
29 .06	5.034	121.69	17.218
31.66	5.677	126.61	17.727
34.62	6.368	132.05	18.142
40.13	7.556	138.28	18.695

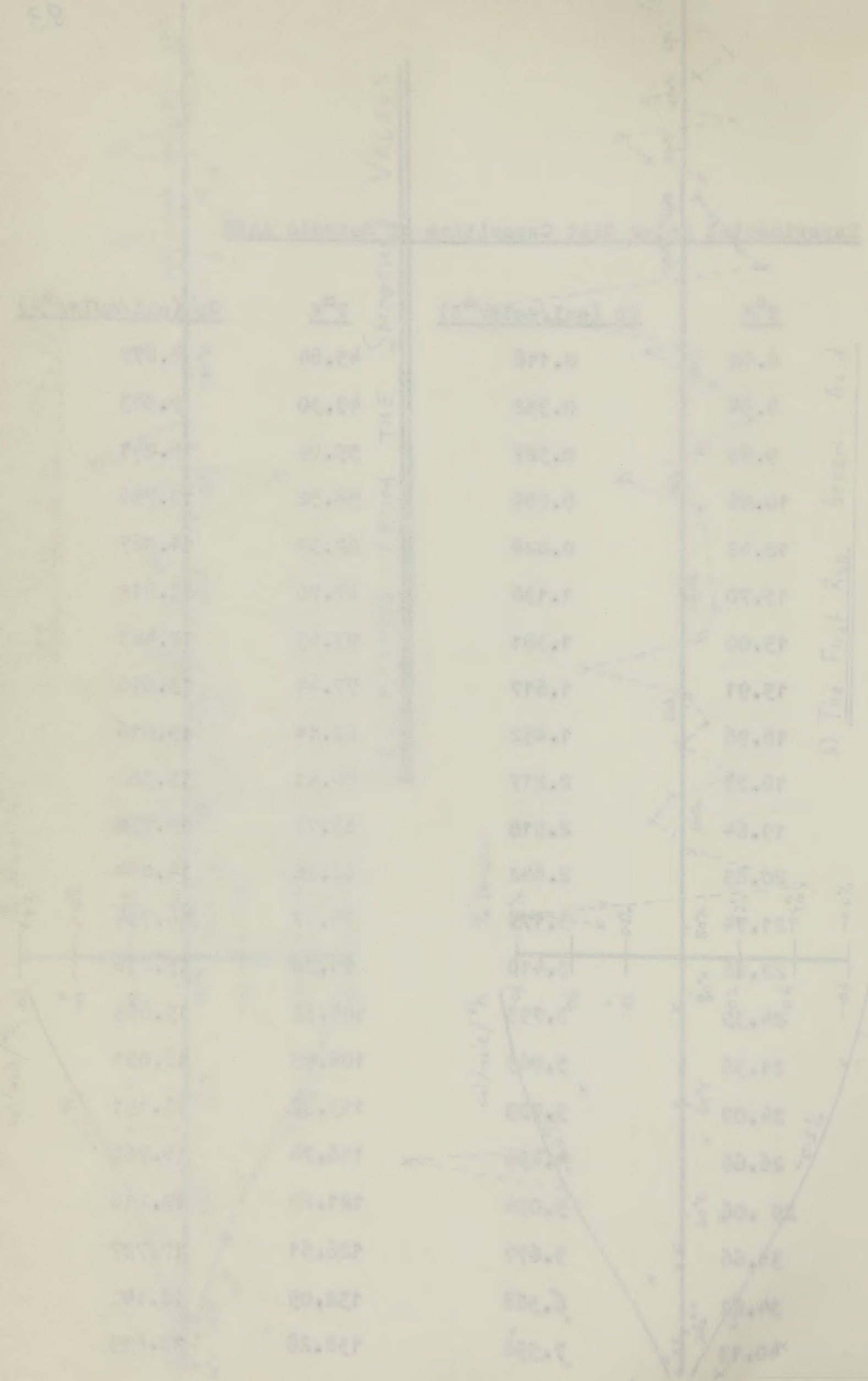

Experimental Molar Heat Capacities of Benzoic Acid (Cont/d)

$T^{\circ}K$	Cp (cal/mole/$^{\circ}K$)	$T^{\circ}K$	Cp (cal/mole/$^{\circ}K$)
156.01	20.342	223.23	26.961
161.43	20.914	230.09	27.671
166.67	21.351	237.26	28.487
172.43	21.859	245.02	29.349
178.34	22.458	251.90	29.978
184.18	23.083	258.99	30.857
184.84	23.114	267.57	31.754
193.39	24.123	276.75	32.754
198.99	24.439	285.66	33.781
204.45	25.006	293.66	34.749
210.48	25.622	300.66	35.423
216.81	26.283		

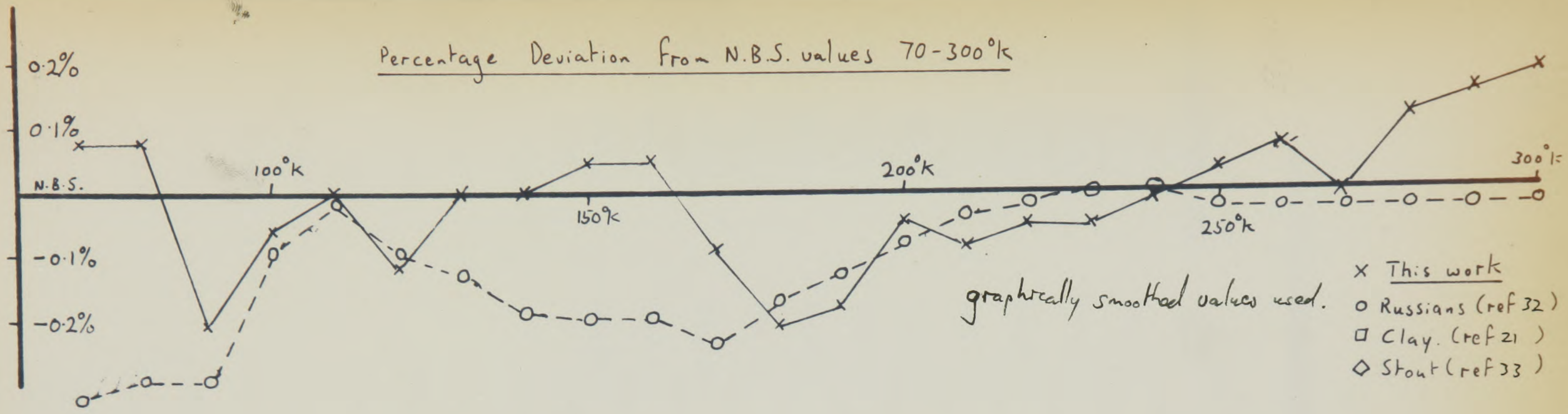

Comparison of Smoothed Molar Heat Capacities of Benzoic Acid.

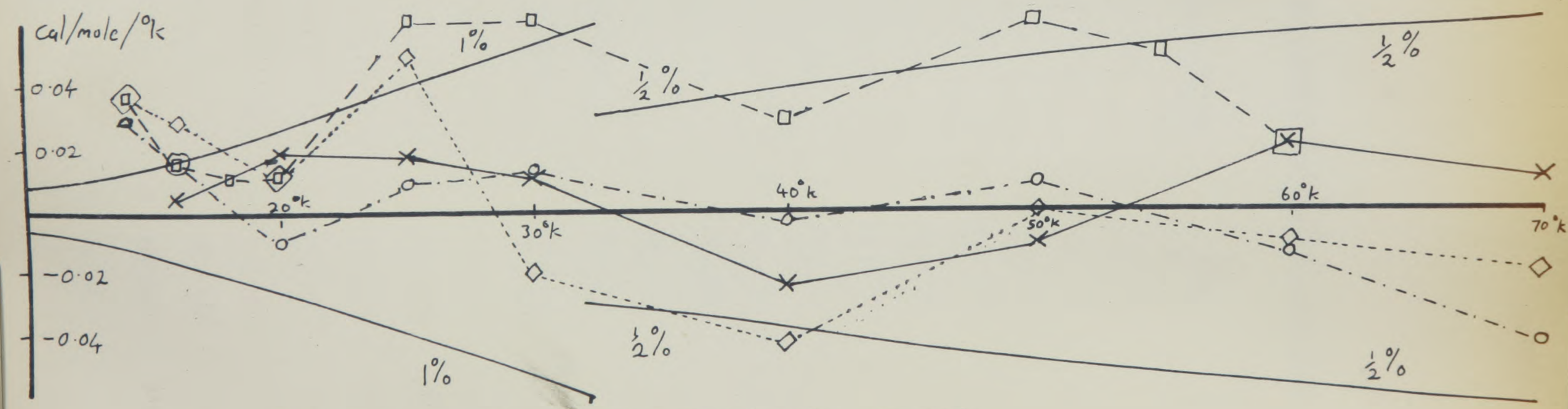

Deviation in cal/mole/°k From N.B.S. value 15-70°k

Molar Thermodynamics of Benzoic Acid

$T^\circ K$	Cp	$S^\circ(T)$	$(H-H^\circ_o)$	$(H-H^\circ_o)/T$	$-(G^\circ-H^\circ_o)/T$
10	(0.541)	0.166	1.725	0.17	0.01
20	2.648	1.092	16.18	0.81	0.28
30	5.248	2.648	55.47	1.85	0.80
40	7.547	4.479	119.57	2.99	1.49
50	9.463	6.375	204.7	4.09	2.28
60	10.954	8.236	307.0	5.12	3.12
70	12.217	10.022	423.0	6.04	3.98
80	13.322	11.727	550.8	6.88	4.84
90	14.324	13.355	689.1	7.66	5.70
100	15.265	14.913	837.1	8.37	6.54
110	16.174	16.411	994.3	9.04	7.37
120	17.071	17.856	1160.5	9.67	8.19
130	17.969	19.258	1335.7	10.27	8.98
140	18.876	20.623	1519.9	10.86	9.77
150	19.796	21.957	1713.3	11.42	10.53
160	20.731	23.264	1915.9	11.97	11.29
170	21.679	24.549	2127.9	12.52	12.03
180	22.642	25.816	2349.5	13.05	12.76
190	23.619	27.066	2580.8	13.58	13.48
200	24.610	28.302	2822.0	14.11	14.19

Benzoic Acid (Cont/d)

$T^{\circ}K$	Cp	S(T)	$(H-H^{\circ}_{o})$	$(H-H^{\circ}_{o})/T$	$-(G^{\circ}-H^{\circ}_{o})/T$
210	25.615	29.527	3073.1	14.63	14.89
220	26.637	30.743	3334.3	15.16	15.59
230	27.677	31.950	3605.9	15.68	16.27
240	28.738	33.150	3887.9	16.20	16.95
250	29.820	34.345	4180.7	16.72	17.62
260	30.922	35.536	4484.4	17.25	18.29
270	32.041	36.724	4799.2	17.77	18.95
280	33.167	37.909	5125.2	18.30	19.60
290	34.286	39.093	5462.5	18.84	20.26
300	35.374	40.274	5810.8	19.37	20.90
298.15	35.176	40.055	5745.6	19.27	20.78

CHAPTER V

CALCITE AND ARAGONITE

Preparation and Analysis of Materials.

) Calcite and Aragonite. (Both forms of $CaCO_3$).

Bohemian aragonite, and calcite of unspecified geographical origin but of high purity were kindly donated, as large lumps, by Dr. Kingsbury, the curator of the mineralogical collection in the University museum. These lumps were broken down, using a stainless steel morter, to a mixture of small lumps (desirable) and powder (less desirable). As most aragonite has a high strontium content (ref 34) the sample was analysed, using the X-ray fluorescence apparatus in the geology lab, under the guidance of Dr. Snelling of that department. The intensity of the Ka line of strontium in aragonite, using molybdenum radiation, was compared with that obtained from standard mixtures of AR $CaCO_3$ and AR $SrCl_2$.

Result. Molar % $Sr' = 0.13\%$

This percentage would have a negligible effect on the heat capcity of calcium carbonate. No analysis was carried out on calcite, as it was felt to be of a sufficient purity, but the carbonate content of aragonite was found, using the sample of calcite as a standard, in the following way.

A weighed amount of approximately molar HCl from a weight pipette was used to dissolve a weighed amount of calcite and the excess was titrated to a rough end point with std., approximately 0.5 molar sodium carbonate solution, from a weight pipette. An accurate end point was then reached using burettes containing

respectively HCl and sodium carbonate solutions, made by diluting 25 gm of each from a weight pipette to 250 cm^3.

The procedure was then repeated, using aragonite in place of calcite. The HCl was standardized against the sodium carbonate also using a weight pipette. Each determination was carried out in triplicate and the percentage of CO_3^{2-} in the aragonite found.

Result. % CO_3^{2-} in aragonite = 59.88% (Theor 59.95%)

Although the calcite was impeccably translucent, the aragonite had a yellowish tinge, thought to indicate silica impurity. From the above determination of carbonate content, the percentage of this impurity would be insufficient materially to affect the heat capacity results.

Aragonite.

$CaCO_3$. M.W. = 100.09.

Wt sample = 30.2892 gm

No of moles = 0.30262

Corrections

Silver tube = +0.0003 gm

Elect. solder = +0.0350 gm

Indium solder = +0.1930 gm

Analysis

CO_3^{2-} = 59.88%

(Theor 59.95%)

Sr^{2+} content = 0.137 %

Contribution of sample.

T	%
10	too low for accurate measurements
20	27.1
50	43.7
100	56.3
300	64.5

Experimental Molar Heat Capacities of $CaCO_3$-Aragonite

$T^\circ K$	C_p(cal/mole/$^\circ K$)	$T^\circ K$	C_p/cal/mole/$^\circ K$)
22.12	0.245	111.38	10.442
24.81	0.344	117.26	10.948
26.91	0.486	122.79	11.427
29.05	0.598	128.32	11.956
31.28	0.763	133.48	12.260
33.69	0.965	138.73	12.640
36.45	1.242	143.89	12.996
39.51	1.530	149.30	13.360
42.97	1.946	155.70	13.743
46.96	2.439	162.70	14.120
51.39	3.030	169.54	14.474
56.10	3.820	176.00	14.844
60.88	4.359	182.56	15.125
65.81	5.122	189.58	15.547
70.89	5.776	197.33	15.835
75.72	6.434	206.13	16.149
80.44	7.065	215.57	16.539
79.75	6.992	228.27	17.120
84.00	7.524	242.35	17.682
86.91	7.875	252.50	18.019
91.86	8.436	262.45	18.393
96.71	9.001	272.28	18.779

Experimental Molar Heat Capacities of $CaCO_3$-Aragonite (Cont/d)

$T^{\circ}K$	C_p(cal/mole/$^{\circ}K$)	$T^{\circ}K$	C_p(cal/mole/$^{\circ}K$)
101.25	9.464	281.92	19.275
106.01	9.933	291.04	19.394

Molar Thermodynamic Properties of $CaCO_3$ - Aragonite

$T^\circ K$	C_p	$S(T)$	$(H-H^\circ_o)$	$(H-H^\circ_o)/T$	$-(G^\circ-H^\circ_o)/T$
10	(0.023)	0.007	0.04	0.00	0.00
20	(0.180)	0.060	0.87	0.04	0.02
30	(0.660)	0.200	4.62	0.15	0.05
40	1.584	0.502	15.22	0.38	0.12
50	2.843	1.007	37.02	0.74	0.27
60	4.304	1.654	72.7	1.21	0.44
70	5.702	2.424	122.8	1.75	0.67
80	7.009	3.271	186.5	2.33	0.94
90	8.215	4.168	262.7	2.92	1.25
100	9.317	5.091	350.4	3.50	1.59
110	10.316	6.027	448.7	4.08	1.95
120	11.216	6.964	556.4	4.64	2.33
130	12.024	7.894	672.7	5.17	2.72
140	12.749	8.812	796.6	5.69	3.12
150	13.400	9.714	927.4	6.18	3.53
160	13.989	10.598	1064.4	6.65	3.95
170	14.525	11.463	1207.0	7.10	4.36
180	15.020	12.307	1354.8	7.53	4.78
190	15.483	13.132	1507.3	7.93	5.20
200	15.922	13.937	1664.4	8.32	5.62

$CaCO_3$ - Aragonite (Continued)

$T^\circ K$	Cp	S(T)	$(H-H^\circ_o)$	$(H-H^\circ_o)/T$	$-(G^\circ-H^\circ_o)/T$
210	16.345	14.724	1825.7	8.69	6.03
220	16.757	15.494	1991.2	9.05	6.44
230	17.162	16.248	2160.9	9.40	6.85
240	17.562	16.987	2334.5	9.73	7.26
250	17.957	17.712	2512.1	10.05	7.66
260	18.344	18.424	2693.6	10.36	8.06
270	18.721	19.123	2878.9	10.66	8.46
280	19.082	19.811	3068.0	10.96	8.85
290	19.420	20.486	3260.5	11.24	9.24
300	19.728	21.150	3456.3	11.52	9.63
298.15	19.674	21.028	3419.8	11.47	9.56

Calcite

$CaCO_3$ M.W. = 100.09

Wt Sample = 30.1860 gm.

No of moles = 0.30159.

Purity = 100% (Assumed)

Corrections

Silver tube = -0.0140 gm

Elect. Solder = +0.0453 gm

Indium Solder = 0.0228 gm.

Contribution of Sample.

T	%
10	34.7
20	45.0
50	51.2
100	56.3
300	65.1

Experimental Molar Heat Capacities of $CaCO_3$ - Calcite

$T^\circ K$	C_p(cal/mole/$^\circ K$)	$T^\circ K$	C_p(cal/mole/$^\circ K$)
10.88	0.057	38.42	2.188
12.17	0.076	41.98	2.623
13.72	0.098	46.22	3.140
15.20	0.135	51.26	3.793
16.16	0.155	56.77	4.499
17.20	0.204	62.21	5.239
18.24	0.268	67.57	5.852
19.30	0.321	73.12	6.506
20.41	0.403	78.69	7.155
21.59	0.475	84.21	7.775
22.76	0.577	80.61	7.361
23.91	0.664	87.00	8.110
25.04	0.753	94.54	8.830
26.22	0.879	102.44	9.526
21.65	0.514	112.41	10.524
24.78	0.720	118.59	11.002
27.53	1.005	125.03	11.542
29.27	1.157	131.91	11.993
32.02	1.442	139.97	12.537
35.22	1.814	149.27	13.190

Experimental Molar Heat Capacities of $CaCO_3$-Calcite (cont/d)

$T^\circ K$	C_p(cal/mole/$^\circ K$)	$T^\circ K$	C_p(cal/mole/$^\circ K$)
158.88	13.794	239.93	17.680
168.20	14.354	248.49	18.001
173.90	14.550	257.08	18.439
180.68	15.047	266.32	18.784
185.04	15.150	276.30	19.112
194.68	15.647	286.12	19.477
204.20	16.068	295.67	19.845
213.46	16.463	303.42	20.157
222.55	16.887		
231.48	17.295		

C_p mol

20

△ Calcite ——
□ Aragonite - - - -

15

10

5

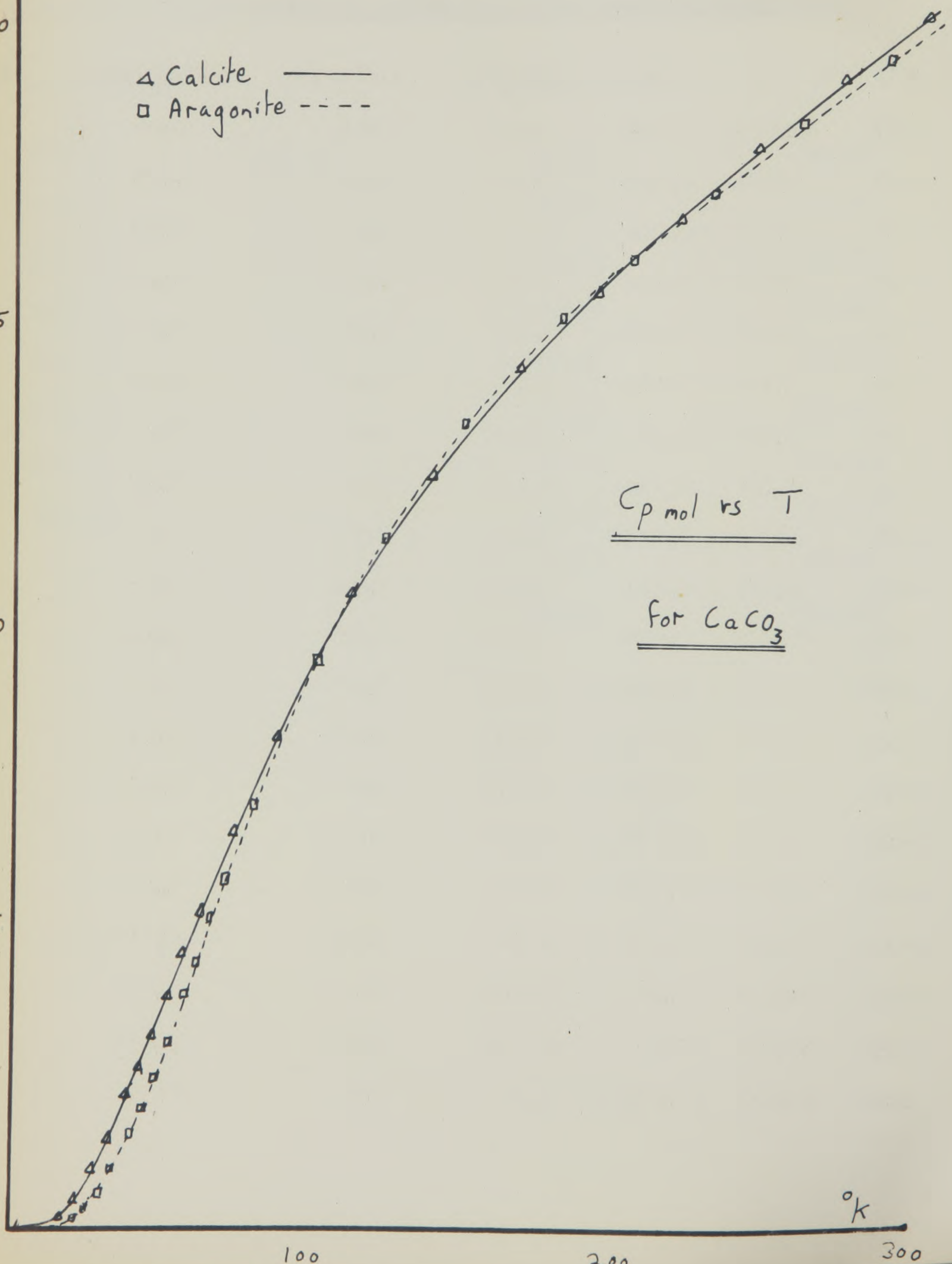

C_p mol vs T

for $CaCO_3$

Molar Thermodynamics of $CaCO_3$ - Calcite

$T^\circ K$	Cp	S(T)	$(H-H^\circ_o)$	$(H-H^\circ_o)/T$	$-(G^\circ-H^\circ_o)/T$
10	(0.049)	0.016	0.13	0.01	0.00
20	0.370	0.108	1.66	0.08	0.03
30	1.232	0.413	9.41	0.31	0.10
40	2.370	0.961	27.01	0.68	0.28
50	3.631	1.623	56.8	1.14	0.49
60	4.926	2.400	99.6	1.66	0.74
70	6.153	3.253	155.1	2.22	1.04
80	7.304	4.150	222.4	2.78	1.37
90	8.375	5.073	300.9	3.34	1.73
100	9.366	6.008	389.7	3.90	2.11
110	10.278	6.944	488.0	4.44	2.51
120	11.115	7.874	595.0	4.96	2.92
130	11.883	8.795	710.0	5.46	3.33
140	12.587	9.702	832.4	5.95	3.76
150	13.236	10.593	961.6	6.41	4.18
160	13.836	11.466	1097.0	6.86	4.61
170	14.396	12.322	1238.2	7.28	5.04
180	14.921	13.160	1384.8	7.69	5.47
190	15.419	13.980	1536.5	8.09	5.89
200	15.895	14.783	1693.1	8.47	6.32

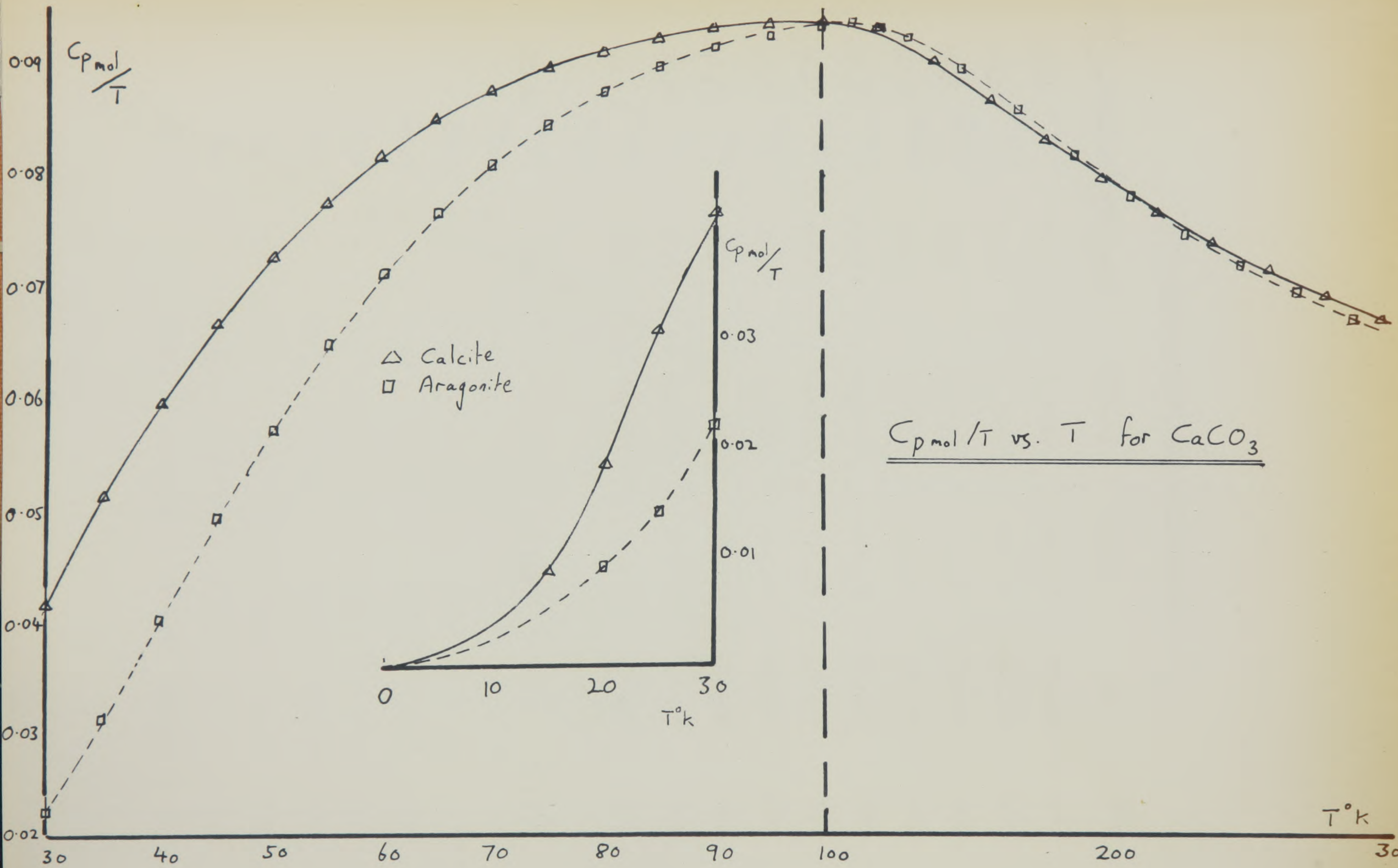

$C_{p\,mol}/T$ vs. T for $CaCO_3$

$CaCO_3$ - Calcite (continued)

$T^\circ K$	Cp	S(T)	$(H-H^\circ_0)$	$(H-H^\circ_0)/T$	$-(G^\circ-H^\circ_0)/T$
210	16.354	15.570	1854.4	8.83	6.74
220	16.800	16.341	2020.1	9.18	7.16
230	17.236	17.097	2190.3	9.52	7.57
240	17.663	17.840	2364.8	9.85	7.99
250	18.082	18.569	2543.6	10.17	8.40
260	18.493	19.287	2726.4	10.49	8.80
270	18.894	19.992	2913.4	10.79	9.20
280	19.282	20.686	3104.3	11.09	9.60
290	19.657	21.370	3299.0	11.38	9.99
300	20.014	22.042	3497.4	11.66	10.38
298.15	19.949	21.918	3460.4	11.61	10.31

Calcite and Aragonite. Discussion.

The standard entropies at 25°C are

S° Calcite = 21.92 e.u.

ΔS° = 0.89 e.u.

S° aragonite = 21.03 e.u.

These values were obtained by computer from the polynomials for the heat capacities, and were checked by measuring the area under the C_p/T vs. T curves, and by Simpsons rule using 10° temperature intervals. The above values may be compared with those of Anderson (ref 13) who found $S^\circ_{calcite}$ = 22.13 e.u.; $S^\circ_{aragonite}$ = 21.26 e.u.; ΔS° = 0.87 e.u.; his values involved extrapolation from 0°K to 56.2°K, using combinations of Debye and Einstein functions as discussed later.

The stable phase at room temperature and atmospheric pressure is calcite, but at higher pressures, aragonite becomes stable. The slope, (dP/dT) can be calculated for the pressure-temperature phase diagram of the calcite-aragonite system by using the value of ΔS found above, since $dP/dT = (dS/dV)_T \cong (\Delta S/\Delta V)_T$. Using the values of $\rho_{calcite}$ = 2.712 and $\rho_{aragonite}$ = 2.930, we find

(dP/dT) = 0.321 cal cm^{-3} deg^{-1} at 25°C.

for the slope of the calcite-aragonite interface at 25°C.

Much early work on the calcite-aragonite transition is invalidated as synthetic rather than natural aragonite was used and it has been shown by Korzhinskii (ref 34) that preparative

methods claimed to give aragonite yielded a product that behaved differently from natural aragonite.

Direct measurements on the aragonite/calcite I/calcite II phase diagram were carried out by Boettcher and Wyllie (ref 35) using natural calcite and aragonite, and from their diagram of the calcite I /aragonite interface

$$\frac{dP}{dT} = 0.33 \text{ cal cm}^{-3} \text{ deg}^{-1} \text{ at } 25^{\circ}C$$

which is in satisfactory agreement. The same authors found, incidentally, from dP/dT and Δ V for the calcite I/calcite II phase boundary, that $\Delta S_{\text{calcite I-calcite II}} = 1.26$ cal mole^{-1} deg^{-1}, which is close to R ln 2. Calcite II is a high temperature phase that cannot exist below the triple point of 480°C

As was mentioned in the introduction, the entropy discrepancy between the two polymorphs, calcite and aragonite does not arise because of residual entropy in one of them, nor does it arise because of a transition to a disordered form. Instead, it provides an example of what the magnitude of effects, arising from differences in crystal structures, on the entropy may be. Here, the difference in volume of the unit cell, resulting from different crystal structures, permits some modes of lattice vibration to be more easily excited in one polymorph than in the other. It is pertinent, therefore, to try and account for the difference in entropy by considering the available spectroscopic data. For calcite, very accurate data is available, and indeed one spectroscopist, Hexter (ref 36) has said

that 'Calcite is the touchstone in the application of modern theories of spectra of the solid state.'

In a unit cell of calcite, there are two formula units (ref 15) i.e. 2 Ca^{2+} ions and 2 CO_3^{2-} ions. Each ion has three translational degrees of freedom, and in addition each carbonate ion, being polyatomic, has three degrees of freedom of torsional oscillation. The tetraatomic carbonate ions also possess 6 degrees of internal freedom each (i.e. 3N-6, where N is the number of atoms in the ion). Therefore each formula unit possesses 15 degrees of freedom, and hence one mole of $CaCO_3$ possesses 15N degrees of freedom. To summarize,

Degrees of freedom for displacements of ion in lattice	=	6N
" " " " torsional oscillations of CO_3^{2-} ion	=	3N
" " " " lattice vibrations	=	9N
" " " " internal vibrations of CO_3^{2-} ion	=	6N
Total degrees of freedom for 1 mole of $CaCO_3$	=	15N

We may compare experimental values of Cp with values of Cv calculated from the spectroscopic data, since

$$C_p = (C_p - C_v) + C_{v_{int}} + C_v'$$

where $C_{v_{int}}$ is the contribution to the heat capacity of the internal modes of vibration of the carbonate ion, Cv' is the contribution of the lattice modes of vibration and (Cp - Cv) is given by the relation

$C_p - C_v = \frac{T \alpha^2 V}{\beta}$, where $\alpha = \frac{1}{V}\left(\frac{\partial V}{\partial T}\right)_p$; $\beta = -\frac{1}{V}\left(\frac{\partial V}{\partial P}\right)_T$

α being the coefficient of volume expansion and β the compressibility. Alternative approximate expressions, exist, e.g. that involving the Grüneisen constant, γ, where

$$\alpha = \frac{\gamma \beta C_v}{V}, \text{ where } \gamma = \frac{-d \ln \Theta_0}{d \ln V} = \frac{V}{C_v}\left(\frac{\partial P}{\partial T}\right)_V ; \therefore C_p - C_v = \frac{T \gamma^2 C_v^2 \beta}{V}$$

and also the Nernst-Lindemann approximation

$$C_p - C_v = A\, C_p^2 T, \text{ where } A \text{ is nearly constant.}$$

The first expression was used to calculate A, taking data for 300°K from Landolt-Bornstein and expressing the volume coefficient as the sum of the linear coefficient of expansion parallel to the unique axis and twice the linear coefficient perpendicular to the axis. $(C_p - C_v)$ at lower temperatures was calculated from $A\, C_p^2 T$. The quantity $\gamma = (C_p - C_v)$ is small, being only 0.268 cal mole^{-1} at 300°K for calcite (and 0.414 cal mole^{-1} for aragonite).

Calcite. Linear coeff. //axis = 2.621×10^{-5}
1axis = 0.540×10^{-5}
$\therefore \alpha = 3.701 \times 10^{-5}$ deg^{-1}
Compressibility = 1.31×10^{-9} cm^2 gm^{-1}
Density = 2.712 gm cm^3

$\therefore$ A = 0.2255×10^{-5} deg mole cal^{-1}

Aragonite. Linear coeff 1st axis = 3.460×10^{-5}
" " 2nd " = 1.719×10^{-5}
" " 3rd " = 1.016×10^{-5}
$\therefore \alpha = 6.195 \times 10^{-5}$ deg^{-1}
Compressibility = 2.2×10^{-9} cm^2 gm^{-1}
Density = 2.930 gm cm^3

A = 0.3549×10^{-5} deg mole cal^{-1}

cal/deg/mole

0·4

0·3

0·2

0·1

$C_p - C_v$

Aragonite

Calcite

100°k

200°k

300°k

cal/deg/mole

3·0

2·0

1·0

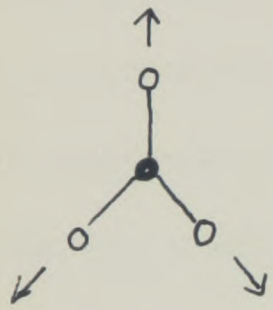

Calcite - Raman active
1087 cm^{-1}

Aragonite - Raman active
1084 cm^{-1}
(also i/r active 1080 cm^{-1})

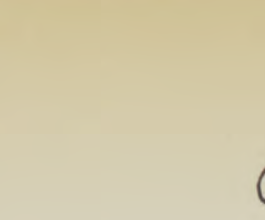

Calcite - i/r active 879 cm^{-1}

Aragonite - i/r active 866 cm^{-1}
(also Raman active 852 cm^{-1})

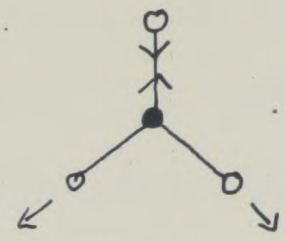

Calcite - Raman active 1432 cm^{-1}
(also i/r active 1429 cm^{-1})
DOUBLY DEGENERATE
Aragonite - i/r active 1492 cm^{-1} & 1504 cm^{-1}
(also Raman active, 1460 cm^{-1}; double deg.)



Calcite - i/r active 706 cm^{-1}
(also Raman active 714 cm^{-1})
DOUBLY DEGENERATE
Aragonite - i/r, 706 & 711 cm^{-1}
(also Raman active, 704 cm^{-1}; double deg)

C_v for the Internal Modes of Vibration of the CO_3^{2-} ion in Calcite and Aragonite

100°k

200°k

300°k

The contribution of the internal modes of vibration was calculated using Einstein functions; it is negligible below 80°K, but rises to about 2.67 cals mole^{-1} at 300°K. In calcite, there are 4 observed frequencies corresponding to the six modes of vibration; in aragonite the two degenerate modes are split, as the site symmetry is lower than the molecular symmetry of the CO_3^{2-} ion. The frequencies, taken from Nakamoto, I.R. Spectra of Inorganic and Co-ordination chemistry, ~~and~~ are shown opposite.

Smoothed values of (Cp - Cv) and Cv internal for calcite and aragonite are plotted on the facing page. We now discuss in detail the treatment of the lattice modes of vibration.

Lattice Vibrations

In the bi-molecular unit cell of calcite, there are eighteen modes of lattice vibration. Three of these modes behave rather like long wavelength acoustic waves in a continuum. The Debye theory of specific heats can be used to calculate the frequencies of elastic waves in a continuum from elastic constant data, and this is what has been done here. The contribution of the 3 acoustic modes per unit cell (i.e. $^3/_2$ modes per formula unit) to the heat capacity has been calculated from the macroscopic elastic constants. The calculation will be found in a later sub-section. As there are always 3 acoustic modes per lattice point, i.e. per unit cell, and aragonite has a tetraatomic unit cell, then in aragonite there are only $^3/_4$ acoustic modes per formula unit to contribute to the unit cell. The calculatio

Optical Modes of Lattice Vibration for Calcite

(15 modes per unit cell)

1) Rocking Frequencies of the CO_3^{2-} ions

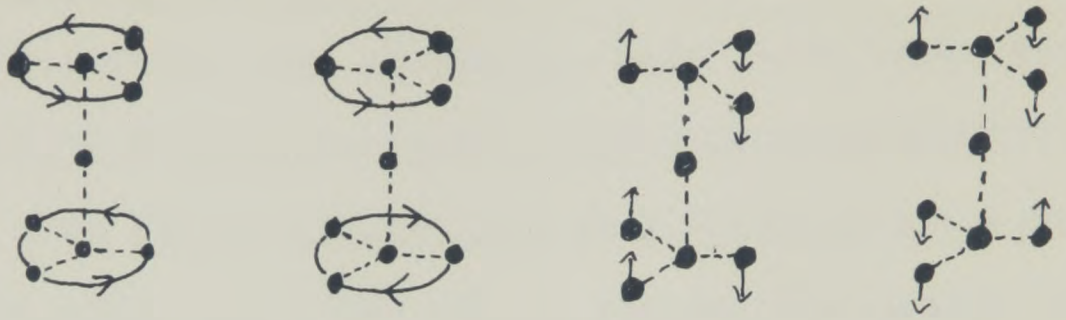

symmetry	$A_{2g}(1)$	$A_{2u}(1)$	$E_g(1)$	$E_u(1)$
degeneracy	1	1	2	2
active region	inactive	i/r	Raman	i/r
Frequency (in cm^{-1}) a) 100°k	? (99)	94	162	104
Frequency (in cm^{-1}) b) 300°k	? (99)	92	156·1	102

2) Vibrational Frequencies of the Ca^{2+} and CO_3^{2-} ions



symmetry	$A_{2g}(2)$	$E_g(2)$	A_{1u}	$E_u(2)$	$A_{2u}(2)$	$E_u(3)$
degeneracy	1	2	1	2	1	2
active region	inactive	Raman	inactive	i/r	i/r	i/r
Frequency (in cm^{-1}) a) at 100°k	? (269)	286·7	? (295)	228	316	302
Frequency (in cm^{-1}) b) at 300°k	?	281·8	?	224	306	296

of the contribution of these modes to the heat capacity of aragonite could again be calculated from a Debye function, but as explained later, this calculation was not performed.

To return to calcite, the remaining 15 lattice modes can in principle be excited by the electric field of a light wave, and are called the optical modes. Of these fifteen modes per unit cell, six are the 'rocking' modes of the carbonate ion (each of the two CO_3^{2-} ions in the unit cell having three degrees of freedom) and the remaining nine are the translational modes of the Ca^{2+} and CO_3^{2-} ions (see diagram opposite). In the diagram, the degeneracies quoted are those per unit cell; The frequencies for the Raman and i/r active vibrations are those found in unpublished work by Dr. G. R. Wilkinson of Kings College, London, who has kindly made them available to us. Three frequencies are not active, either in the Raman or the i/r, and the estimates shown in brackets, of Giulotto and Loinger (ref 37) for these frequencies were used. A value for the heat capacity per mole of calcite was calculated from all the modes of vibration, and compared with the experimental values at various temperatures.

The original intention was to carry out similar calculations on aragonite, but lack of data on the optical modes made this impossible. This made it rather pointless to calculate the contribution of the acoustic modes to the heat capacity of aragonite, and the original aim, to show that the differences in the heat capacities of calcite

and
)aragonite arose from differences in the lattice-vibrational spectrum, could not be carried out.

Nevertheless, we decided that it would be valuable to see whether the experimental heat capacity values of calcite agreed with calculated values. The contribution of the optical vibrational modes to the heat capacity was estimated by means of Einstein functions, on the advice of Dr. Wilkinson. Briefly, the reason for this is as follows. The energy in a lattice vibration or elastic wave is quantized, the quantum of energy being called a phonon (cf a photon for an electromagnetic wave quantum). A phonon of wavevector k has the momentum $hk/2\pi$, where h is Plank's constant. If k is plotted against ω, the wave frequency, then for a polyatomic lattice, according to the theory of Born and von Karman, the curve obtained has two branches, an optical branch and an acoustic branch. If there are p particles in the primitive unit cell of a lattice, then there are 3p curves on the k vs. ω graph, i.e. 3p branches to the phonon dispersion curve, of which 3 are acoustic and $(3p - 3)$ are optical. When the mass of one ion is much less than that of the other (which is admittedly only partly true for $CaCO_3$ where $Ca^{2+} = 40$ and $CO_3^{2-} = 60$), the frequency in each optical branch is approximately independent of the wavevector. The Einstein theory of specific heats is applicable to a series of oscillators vibrating with one fixed frequency (rather than a continuum of frequencies as in the Debye model), and can therefore be applied to the optical modes, the

CALCITE — C_p calc vs. C_p expt.

$T\,^\circ K$	C_v Inactive Modes	C_v Active modes	C_v Internal Modes of CO_3^{2-}	$C_p - C_v$	C_v acoustic modes $\Theta = 469^\circ K$	C_p Calc (using acoustic $\Theta = 469^\circ K$)	C_v acoustic modes $\Theta = 290.5^\circ K$	C_p calc (using acoustic $\Theta = 290.5^\circ K$)	C_p EXPT
15	0.006	0.018	/	/	0.007	0.031	0.030	0.054	0.127
20	0.041	0.118	/	/	0.018	0.177	0.072	0.231	0.370
30	0.197	0.625	/	/	0.061	0.883	0.287	1.109	1.232
40	0.388	1.355	/	0.001	0.143	1.887	0.503	2.247	2.370
50	0.567	2.154	/	0.002	0.270	2.993	0.818	3.541	3.631
100	1.480	5.953	0.017	0.021	1.213	8.684	2.000	9.471	9.366
150	2.039	8.397	0.241	0.062	1.913	12.652	2.575	13.214	13.236
200	2.379	9.705	0.824	0.119	2.299	15.326	2.650	15.677	15.895
250	2.570	10.426	1.709	0.186	2.515	17.413	2.784	17.682	18.082
300	2.684	10.854	2.673	0.268	2.646	19.125	2.845	19.324	20.014

the vibrational frequencies of which are relatively uninfluenced by the vibrations of neighbouring ions.

Two different values for the acoustic Debye temperature were used, that of Robie (ref 38), $\Theta_D = 469^\circ K$, also found by Anderson (ref 39), and that calculated by the author from a formula of Betts et al. (ref 40) for a trigonal lattice, giving $\Theta_D = 290.5^\circ K$ This calculation is given in a later sub-section.

Calculation of Cp Calcite.

On the facing page are presented calculated values of Cp at various temperatures. The calculated heat capacity, Cp calc, is the sum of the following contributions per mole.

i) The contribution of the following 15N/2 optical lattice vibrations, treated as EINSTEIN functions. (Inactive and active lattice mode contributions are listed separately).

These are listed on page 107.

Einstein Temperature in °K	Frequency in cm^{-1}	Degeneracy per unit cell	Degeneracy per formula unit	Degrees of Freedom of Einstein Function	Symmetry
386.9	269	1	1/2	N/2	$A_{2g}(2)$
142.4	99	1	1/2	N/2	$A_{2g}(2)$
424.3	295	1	1/2	N/2	A_{1u}
440.2*	306*	1	1/2	N/2	$A_{2u}(2)$
132.3*	92*	1	1/2	N/2	$A_{2u}(1)$
405.4*	281.8*	2	1	N	Eg(2)
224.6*	156.1*	2	1	N	Eg(1)
425.8*	196*	2	1	N	Eu(3)
322.2*	224*	2	1	N	Eu(2)
146.7*	102*	2	1	N	Eu(1)

The Einstein temperature, Θ_E is calculated from the optical frequencies by multiplying by 1.4386. The contribution to the heat capacity was calculated using the tables given in Journal of Industrial and Engineering Chemistry, 35, 640-1, which list values of Cv in cal $mole^{-1}$ deg^{-1} for various values of Θ_E/T, T being the absolute temperature. The frequencies listed with an asterisk in the table are the values at 300°K; values at lower temperatures were calculated from these values, and values for thesame mode at 100°K, by assuming the Grüneisen relation

$$\gamma = -d \ln \Theta / d \ln V$$

γ being a constant, V being the volume, calculated from data given in Landolt-Bornstein and Θ being the Debye temperature. No such correction was applied to the calculated frequencies of the inactive modes, as it was felt that they were not known sufficiently precisely to make such corrections worthwhile.

ii) The contribution of the 6N internal vibrations of the CO_3^{2-} ion, per mole, calculated as Einstein functions

iii) The Cp-Cv contribution discussed earlier.

iv) The contribution of the 3N/2 modes of acoustic vibration, treated as a DEBYE function. The first column of Cp calc lists values obtained taking a contribution of theacoustic modes based on a Debye temperature, $\Theta_D = 469^\circ K$, and the second column liste Cp calc, using $\Theta_D = 290.5^\circ K$.

Discussion of Cp Calc.

Neither set of calculated Cp values (i.e. those using $\Theta_D = 469^\circ K$ and those using $\Theta_D = 290.5^\circ K$) fit with the experimental Cp. Both calculated sets are low, but those using the author's value of the acoustic Debye temperature, i.e. $\Theta_D = 290.5^\circ K$, are in slightly better agreement with the experimental data. It will, however, be explained in the next section why Robie's value of $\Theta_D = 469^\circ K$ is likely to be correct. The error therefore must lie either in the frequencies from which the Cv contributions are calculated, or in the method by which the Cv contribution of a frequency is treated, or in Cp-Cv.

Dealing with the last point first, the data from which the $C_p - C_v$ contribution is calculated may be slightly imprecise, as may be the Nernst-Lindemann approximation used, but this contribution is a very small part of the whole.

The i/r and Raman frequencies are most unlikely to be greatly in error, as Dr. Wilkinson's values are similar to, but more precise than, earlier values obtained by Cabannes (ref 41) Hexler (ref 36) and many other workers. The inactive frequencies, calculated by Guilotto and Loinger may well be imprecise as they were calculated, using symmetry calculations, from the data of Cabannes. It is however less likely that the inaccuracy in Cp calc arises from inaccurate frequencies than from the function used to relate frequency to Cv, since at low temperature, the argument, Θ/T in the Einstein

function $C_v = f_E(\theta_E/T)$ is large, unless θ_E, the Einstein frequency, is small, and until the argument reaches a value below about 13, a one-dimensional Einstein function contribution can be completely neglected. Thus, at 15°K and 20°K, only frequencies for which θ_E is below about 200°K will make any real contribution, and the frequencies used in this work would have to be vastly in error to lift the calculated value say at 20°K from 0.177 cal/mole/deg to the experimental value of 0.370 cal/mole/deg. If on the other hand Debye functions were used, where an argument (i.e. θ/T) of about 20 will produce a small but significant contribution, then the effect of treating all the optical modes by Debye, rather than Einstein, functions would be to make Cp calc greatly exceed $C_{p\,expt}$ at low temperatures. When the argument, θ/T, is about 1.5 or below, the difference in the contribution to C_v of the two functions becomes slight, approaching the limiting value of R cal/mole/°K/degree of freedom when $\theta/T \rightarrow 0$, in both cases.

It seems likely, therefore, that the discrepancy between Cp calc, and Cp expt. arises not from any inaccuracy in the experimental data nor any gross mistake in the frequency assignment but in using an insufficiently sophisticated function to relate optical frequencies to C_v. More sophisticated treatments, such as the Born cut-off procedure and the theory of Blackman do exist, but the mathematics is less tractable than in the simple Debye and Einstein theories; in any case time did not permit any further improvements in the calculations to be made.

Since Einstein's theory of heat capacities assumes that vibrations in a lattice are simply harmonic, no account is taken of anharmonicity. According to Barron (ref 42) the effect of anharmonicity on the heat capacity is very small, but positive, for ionic crystals, and thus if anharmonicity was taken into account, the discrepancy at higher temperatures might be reduced.

Calculation of Acoustic Debye Temperature.

The Debye temperature for the acoustic modes was calculated from elastic constant data by the author from a formula of Bhatia et al (ref 40) applicable to a trigonal crystal, and found to be 290.5°K. This formula was designed to simplify the calculation of the average velocity of sound in the crystal, which involves an integral that is difficult to evaluate. According to Robie (ref 43), the formula leads to the average velocity $\bar{V}$, directly from

$$\bar{V} = \int \frac{(V_1 + V_2 + V_3)}{3} \cdot \frac{d\Omega}{4\pi}$$

whereas the mean sound velocity, V_m, that should be used in the Θ_D corrections is given by

$$V_m = \left[\frac{1}{3} \int \left(\frac{1}{V_1^3} + \frac{1}{V_2^3} + \frac{1}{V_3^3} \right) \frac{d\Omega}{4\pi} \right]^{-1/3}$$

and for a highly anisotropic solid, such as calcite, the two velocities can differ considerably. The Debye mean velocity, V_m weights the longitudinal velocity very much less than does the direct average $\bar{V}$. Robie (ref 38) finds a value of $\Theta_D = 469 \pm 1°K$, using the same elastic constant data (ref 44) as the author used in his calculation. Robie's value is confirmed by the value of 470°K

found by Anderson, (ref 39) using numerical integration over the $\Sigma 1/\nu_1^3$ surfaces, and in view of the explanation given by Robie as to why the formula is incorrect, there is little doubt that Robie's value is the correct one.

Lattice Frequencies of Calcite and Aragonite - Conclusion.

Dr. Wilkinson of Kings College, London hopes, in the near future, to complete the measurement and assignment of the lattice frequencies of aragonite.

Although the fit between calculated and experimental values of Cp for calcite is not perfect, and although the calculation of the heat capacity of aragonite could not be pursued for lack of experimental data, it is still felt that the discrepancy in heat capacity between the two polymorphs arises from differences in the lattice vibrational spectrum. It is felt that, in particular, the frequencies of torsional oscillation of the carbonate ions would be different in calcite and aragonite because of the difference of environment, as discussed in the introduction; consequently, it is thought that further spectroscopic work on aragonite will show higher frequencies for the $A_{2g}(1)$, $A_{2u}(1)$, $Eg(1)$ and $Eu(1)$ vibrations than are found for calcite.

Early Measurements on Calcite and Aragonite.

Günther in 1916 (ref 11) evaluated Cv aragonite, including the contribution of the internal carbonate modes, on the assumption that $CaCO_3$ molecules vibrate with respect to each other with a

Debye function and that Ca^{2+} and CO_3^{2-} ions will vibrate with respect to each other with an Einstein function, giving a three-dimensional Debye temperature of 317°K and a three-dimensional Einstein function of 280°K. Guinther's results are rather low and his theoretical approach is rather unsatisfactory. Jellinek (ref 45) using Guinther's data, but treating all vibrations as Debye functions, arrives at a six-dimensional Debye temperature of 375°K. He used only Debye functions because, as he states, the lattice contains only ions of almost the same mass. This is not very true for calcite where Ca^{2+} = 40 and CO_3^{2-} = 60.

Anderson in 1933 (ref 13) found that for aragonite, Cp was given by a 3-dimensional Debye temperature of 244°K, a 6-dimensional Einstein function of 342°K and a 6-dimensional ~~Debye~~ Einstein function of 1897°K. For calcite, he found a 3-dimensional Debye function of 180°K, a 6-dimensional Einstein function of 370°K and a 6-dimensional Einstein function of 1210°K. This approach, of treating the internal modes by one high temperature Einstein function, and the lattice modes by a combination of Einstein and Debye frequencies, was formerly much used.

Kalinkina (ref 46) found that calcite showed a $Cp \propto T^3$ relationship below 25°K, giving $Cp = 1.85 \times 10^{-4} T^3$. We found that $Cp \propto T^3$ only up to 16°K. He used a six-dimensional Debye function, Θ = 275°K, below 60°K, and from 60 to 100°K, the upper temperature

of his measurements, he uses the 6-dim. Debye function in conjunction with a 3-dim. Einstein function, $\Theta = 570^{\circ}K$. He also states that the extra growth of the heat capacity is caused by excitation of the rotational oscillations of the carbonate ion.

CHAPTER VI

DIAMMINO MERCURIC CHLORIDE

i) Preparation and Analysis.

The method of Glasson and Gregg (ref 62) was used. Two litres of a solution containing 500 ml of 0.880 ammonia and 300 gm of AR NH_4Cl was heated to 75°C and a solution of 50 g/l AR $HgCl_2$ was slowly added dropwise at this temperature, with constant magnetic stirring. When the white turbidity just did not clear (after the addition of about 200 ml $HgCl_2$ soln.), the flask was allowed to cool overnight in a polystyrene lagged container, the purpose of the slow cooling being to produce as large crystals as possible. Even so, the crystals were only about 0.2 mm long. The crystals were collected in a buchner funnel, washed with distilled water, and dried over P_2O_5. The yield was about 6 grams, and the process was repeated ten times.

Analysis for ammonia was carried out by back titrating excess HCl against sodium carbonate solution. The carbonate, which was used as a primary standard for theHCl, was anhydrous A.R.Na_2CO_3, which was heated for 30 minutes to 260 - 270°C with stirring, and allowed to cool over P_2O_5. All glassware used was calibrated.

Mercury was determined gravimetrically as the sulphide, and chloride as AgCl.

Results (mean of three determinations)

Hg	65.49%	(theor 65.61%)
NH_3	11.13%	(theor 11.19%)
Cl	22.99%	(theor 23.20%)

The sample was kept over P_2O_5 until used.

A co-worker, Pochon, took a powder photograph of the sample which tallied well with that used in the original structure determination by Bijvoet (ref 19).

Fusible White Precipitate

$Hg(NH_3)_2Cl_2$ M.W. = 305.74

Analysis

Hg = 65.49% (Theor 65.61%)

NH_3 = 11.13% (Theor 11.19%)

1) In R. M. Clay's Calorimeter

~~(See Appendix 3 for details of standard weights)~~

Wt Sample = 42.7756 gm

No. of moles = 0.13991

Corrections

Silver tube	=	+0.0344 gm
Elect. solder	=	-0.0017 gm
Indium solder	=	0.3184 gm
Grease, Apiezon T for insertion of thermometer	=	-0.0067 gm.

Contribution of Sample

T^oK	%
5	90.0
10	92.3
15	90.6
20	88.3

Experimental Molar Heat Capacities of $Hg(NH_3)_2Cl_2$ - Fusible White Precipitate.

i) In R. M. Clay's Calorimeter

$T^\circ K$	Cp(cal/mole/$^\circ K$)	$T^\circ K$	Cp(cal/mole/$^\circ K$)
3.08	0.0018	7.93	0.7198
3.57	0.0056	8.72	0.9385
3.82	0.0053	9.66	1.2122
4.06	0.0101	10.72	1.572
4.15	0.1713	11.84	2.008
4.50	0.1863	12.98	2.423
4.62	0.3009	14.23	2.816
5.10	0.3681	15.65	3.224
4.83	0.1737	17.21	3.860
5.50	0.3531	18.86	4.546
5.77	0.2766	20.63	5.125
6.24	0.3631	22.66	6.161
6.77	0.4660	25.32	6.883
7.30	0.5789		

Fusible White Precipitate.

$Hg(NH_3)_2Cl_2$. M.W. = 305.74

Analysis

Hg = 65.49% (Theor. 65.61%)

NH_3 = 11.13% (Theor. 11.19%)

2) In Main Calorimeter

Wt sample = 46.8054 gm

No of moles = 0.15309

Corrections

Silver tube = -0.0240 gm

Elect. Solder = +0.0422 gm

Indium solder = +0.1043 gm.

Contribution of Sample

T^oK	%
10	91.0
20	81.9
50	68.1
100	62.2
300	63.5

Experimental Molar Heat Capacities of $Hg(NH_3)_2Cl_2$ - Fusible White Precipitate (continued)

ii) In main calorimeter

$T^\circ K$	C_p(cal/mole/$^\circ K$)	$T^\circ K$	C_p(cal/mole/$^\circ K$)
8.44	0.986	21.29	5.405
8.82	1.244	23.02	5.799
9.72	1.544	25.13	6.650
11.07	1.578	27.67	7.597
12.24	2.146	30.35	8.485
13.44	2.440	32.96	9.387
14.88	2.979	35.81	10.399
16.39	3.495	39.05	11.464
17.97	4.092	42.60	12.653
19.51	4.622	46.66	13.829
20.86	5.142	51.20	15.187
22.09	5.597	60.75	17.624
23.50	6.050	65.36	18.682
25.24	6.728	69.93	19.485
26.98	7.329	74.80	20.459
21.69	5.390	80.14	21.288
23.61	6.091	85.64	22.190
25.44	6.532	81.79	21.608

Experimental Molar Heat Capacities of $Hg(NH_3)_2Cl_2$ - Fusible White Precipitate (continued)

T^oK	C_p(cal/mole/^oK)	T^oK	C_p(cal/mole/^oK)
88.36	22.490	175.90	30.100
92.62	22.980	184.45	30.590
98.15	23.699	193.54	31.184
103.95	24.247	202.49	31.674
110.77	30.845	211.33	32.190
119.12	25.763	220.06	32.765
127.82	26.625	229.11	33.144
137.93	27.428	237.42	33.660
147.67	28.180	246.69	34.117
156.46	28.872	258.94	34.836
108.87	24.829	268.79	35.247
114.49	25.377	278.65	35.774
120.39	25.933	288.46	36.227
167.65	29.545	298.14	36.861

Heat Capacity of $Hg(NH_3)_2Cl_2$

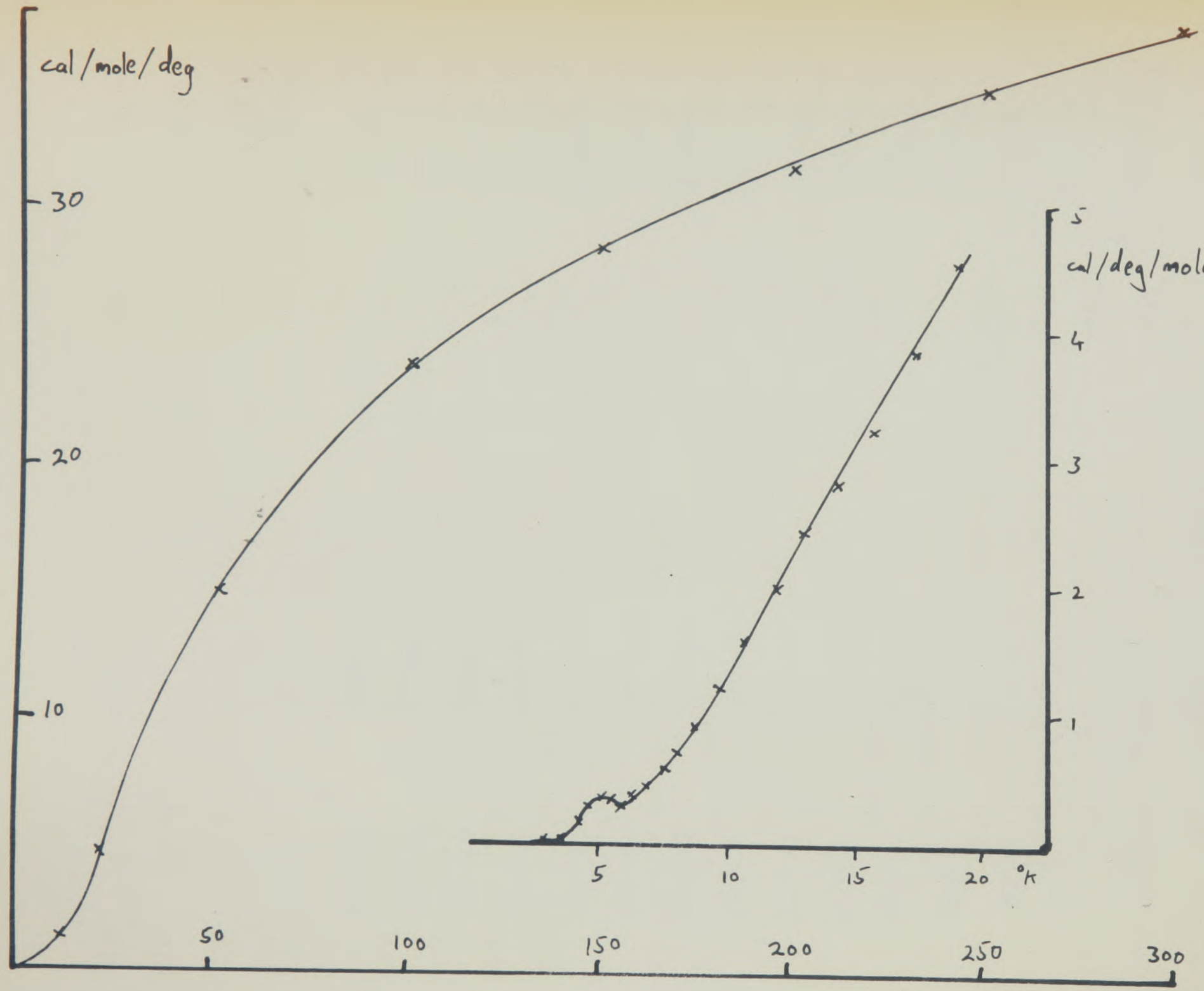

Molar Thermodynamics of Fusible White Precipitate, $Hg(NH_3)_2Cl_2$.

$T^\circ K$	C_p	$\sim(T)$	$(H-H^\circ_o)$	$(H-H^\circ_o)/T$	$-(G^\circ-H^\circ_o)/T$
10	1.324	0.467	3.60	0.36	0.11
20	4.805	2.440	33.90	1.70	0.73
30	8.408	5.073	99.55	3.32	1.74
40	11.790	7.960	175.25	4.38	3.55
50	14.793	10.927	348.7	6.97	3.95
60	17.490	13.873	510.7	8.51	5.36
70	19.589	16.733	696.5	9.95	6.78
80	21.276	19.463	901.1	11.26	8.20
90	22.678	22.052	1121.0	12.46	9.60
100	23.883	24.506	1354.0	13.54	10.97
110	24.946	26.833	1598.2	14.53	12.30
120	25.905	29.045	1852.6	15.44	13.61
130	26.782	31.154	2116.1	16.28	14.88
140	27.592	33.168	2388.0	17.06	16.11
150	28.345	35.098	2667.7	17.78	17.31
160	29.050	36.950	2954.7	18.47	18.48
170	29.715	38.731	3248.6	19.11	19.62
180	30.349	40.448	3548.9	19.72	20.73
190	30.958	42.105	3855.5	20.29	21.81
200	31.550	43.708	4168.0	20.84	22.87

Fusible White Precipitate, $Hg(NH_3)_2Cl_2$ (continued)

$T^\circ K$	C_p	$S(T)$	$(H-H^\circ_o)$	$(H-H^\circ_o)/T$	$-(G^\circ-H^\circ_o)/T$
210	32.128	45.262	4486.4	21.36	23.90
220	32.695	46.769	4810.5	21.87	24.90
230	33.251	48.235	5140.3	22.35	25.89
240	33.793	49.662	5475.5	22.81	26.85
250	34.318	51.052	5816.1	23.26	27.79
260	34.824	52.408	6161.8	23.70	28.71
270	35.317	53.731	6512.5	24.12	29.61
280	35.812	55.025	6868.2	24.53	30.50
290	36.343	56.290	7228.9	24.93	31.36
300	36.904	57.533	7595.4	25.32	32.21
298.15	36.846	57.304	7527.1	25.25	32.06

Calculation of the Standard Entropy of $Hg(NH_3)_2Cl_2$.

From the measurements of the heat capacity, the value for $S^\circ_{3rd\ law}$ obtained from the computer calculated polynomial is

$$S^\circ_{3rd\ law} = 57.30 \text{ e.u.}$$

As in the case of the other compounds studied in this work, this figure was confirmed by measuring the area under the Cp/T vs T graph, and by the use of Simpson's rule at 10° intervals. No significant transitions were found.

As was mentioned in the introduction, S° from equilibrium measurements for $Hg(NH_3)_2Cl_2$ was being measured by another worker (ref 63). He used the cell

$$\ominus\ Hg(l) \;\Big|\; Hg(NH_3)_2Cl_2(s),\ NH_4Cl\ (aq),\ NH_3\ (aq) \;\Big|\; AgCl(s) \;\Big|\; Ag(s)\ \oplus$$

the dotted line indicating a salt bridge. The reaction in this cell was found to be

$$2\ AgCl(c) + 2NH_3(aq) + Hg(l) \longrightarrow Hg(NH_3)_2Cl_2 + 2Ag$$

and hence the e.m.f. depends solely on the partial pressure of the ammonia above the solution.

There are several points of interest in connection with this cell. The first is that silver is the positive, i.e. oxidising electrode, although from the standard electrode potentials it would be expected that mercury would be the positive electrode. This is because of the great stability of the mercuric complex. The second point is

that a mercury/mercuric electrode is normally impossible because mercury and mercuric ions normally react to give the virtually insoluble mercurous salt. Here the concentration of free Hg^{2+} is very low, as most of it is complexed with ammonia, and consequently, if the ammonia concentration is high enough, the solubility product of mercurous chloride will not be exceeded. Pochon (ref 63) found, using Manalov's approximate data (ref 64) for the solubility product of the complex, that if the ammonia was $^{N}/_{10}$ or greater, Hg_2Cl_2 was not precipitated. The concentration of chloride ion does not affect the formation of mercurous chloride. This is because

$$[Hg_2^{2+}] / [Hg^{2+}] = 166 \quad \text{(ref 65)}$$

$$[Hg(NH_3)_2^{2+}] / [Hg^{2+}] [NH_3]^2 = 10^{17.4} \quad \text{(ref 66)}$$

$$\therefore [Hg_2^{2+}] = 10^{-21.2} / [NH_3]^2 [Cl^-]^2$$

$$\therefore [Hg_2^{2+}] [Cl^-]^2 = 10^{-21.2} / [NH_3]^2$$

The third point of interest is that an Ag/AgCl electrode cannot normally exist in the presence of ammonia solution as the silver chloride is dissolved. Here the presence of ammonium chloride means that in $^{N}/_{10}$ ammonia solution, only 1.3×10^{-4} moles litre^{-1} of silver chloride is dissolved, and it is feasible to reduce the amount of AgCl removed from the electrode by pre-saturating the solution with a little solid AgCl.

To obtain the accuracy of 0.1 e.u. in S^{o}, required on these measurements, Pochon found that the partial pressure of ammonia above the solution had to be known only to a precision of slightly better than 1 mm Hg.

S° was calculated in two ways.

i) Using the temperature coefficient of the e.m.f.

Here, for the reaction

$$2AgCl(c) + 2NH_3(aq) + Hg(l) \longrightarrow Hg(NH_3)_2Cl_2(c) + 2Ag(c)$$

$$S^{\circ}_{Hg(NH_3)_2Cl_2} = \Delta S - 2S^{\circ}_{Ag(S)} + 2S^{\circ}_{AgCl(S)} + 2S_{NH_3(aq)} + S^{\circ}_{Hg(l)}$$

ΔS is found from

$$\Delta S = 2F.\left(\frac{\partial E}{\partial T}\right)_p$$

$S_{NH_3(aq)}$ is found indirectly from the heat of solution, the standard entropy of the gas, and the pressure of gas over a solution of the normality involved. Thus, $\bar{S}_{NH_3(aq)} = \bar{S}_{NH_3(g)} - \frac{\Delta \bar{H}_{soln}}{T}$

~~Thus~~ and $\bar{S}_{NH_3(g)} = \bar{S}^{\circ}_{NH_3(g)} + R \ln \frac{1}{P}$, where P is in atmospheres

A provisional value of $(\partial E/\partial T)_p$ was obtained by Pochon using measurements of E at three temperatures only. He found that

$\left(\frac{\partial E}{\partial T}\right)_p$ = -0.0010 volts (allowance must be made for change in NH_3 dissoc. pressure.

$\therefore$ S = -46 e.u. (ref 63)

For $^{N}/_{10}$ NH_3; $\Delta H_{soln.}$ = 8.19 kcal/mole, (ref 49)

$S^{\circ}_{NH_3(g)}$ = 45.94 e.u. (ref 68)

P_{NH_3} = 25/760 atm. (ref 67)

$\therefore$ $S_{NH_3(aq)}$ = 25.45 e.u.

S°_{Hg} = 18.17 e.u.

S°_{Ag} = 10.20 e.u.

S°_{AgCl} = 23.00 e.u.

$$\therefore \quad S^{\circ}_{Hg(NH_3)_2Cl_2} = -46 - (10.20 \times 2) + (23.00 \times 2) + (25.45 \times 2) + 18.17$$

$$= \underline{48.67 \text{ e.u.}}$$

This value is lower than the third law value, which is impossible. Possible sources of error are

a) $(\partial E/\partial T)_p$. This is a provisional value and will be redetermined

b) Inaccuracy in values of S°.

c) Inaccuracy in the calculation of $S_{NH_3(aq)}$. The heat of solution taken here is for ammonia in water; the electrolyte of the cell is in fact an ammonium chloride solution and this may affect the ΔH. Also, ionization is assumed to be surpressed.

ii) Using standard enthalpies and one value of the e.m.f.

For the reaction

$$2AgCl(S) + 2NH_3(g) + Hg(l) \rightarrow Hg(NH_3)_2Cl_2(S) + 2Ag(S)$$

$$\Delta G^{\circ} = \Delta H^{\circ} - T\Delta S^{\circ} = -2FE^{\circ}$$

$$E^{\circ} = E - \frac{RT}{2F} \ln (P_{NH_3})^2$$

From Pochon's work, $E = 0.0789$ v at $25^{\circ}C$,

$$P_{NH_3} = {}^{25}/_{760} \text{ atmospheres}$$

$$\therefore \quad E^{\circ} = 0.1653 \text{ v.}$$

$$\therefore \quad G^{\circ} = -7,630 \text{ cal}$$

H° is found from the following data

$2NH_3(g) + HgCl_2 \longrightarrow Hg(NH_3)_2Cl_2 \quad \Delta H_1^\circ = -51.3$ kcal (ref 69)

$Hg + Cl_2 \longrightarrow HgCl_2 \quad \Delta H_2^\circ = -53.4$ kcal

$2\,AgCl \longrightarrow 2\,Ag + Cl_2 \quad \Delta H_3^\circ = 2 \times 30.4$ kcal

$\therefore \underline{\Delta H^\circ = -43.9 \text{ kcal.}}$

$\therefore \underline{\Delta S^\circ = -121.7 \text{ e.u.}}$

Now

$$S^\circ_{Hg(NH_3)_2Cl_2(c)} = S^\circ - 2S^\circ_{Ag(c)} + 2\,S^\circ_{AgCl(c)} + 2\,S^\circ_{NH_3(g)} + S^\circ_{Hg(l)}$$

$$= -121.7 - 20.4 + 46.0 + (2 \times 45.94) + 18.17$$

$$= 13.9 \text{ e.u.}$$

This answer is even lower than that obtained from the temperature coefficient of the e.m.f. and is of course absurd. The error is most likely to arise from an incorrect figure for ΔH° as errors in E or P_{NH_3} would have to be gigantic to explain the discrepancies, unless, of course, the cell reaction is different from that which we have taken it to be. Even if this is in fact so, the figure of -51.3 kcal, found by Biltz (ref 69) for the reaction

$$2NH_3(g) + HgCl_2 \longrightarrow Hg(NH_3)_2Cl_2$$

Seems rather surprising when one considers the values he found for the same reaction involving the bromide and iodide complexes, namely -32.4 and -24.6 kcal $mole^{-1}$ respectively. That is, he found that the discrepancy between bromide and chloride was greater than that between iodide and bromide. Since the chloride and bromide are isomorphous (ref 19) (although the iodide is not (ref 69)) one

can arrive at a measure of the heat of formation of the chloride complex with respect to the bromide complex from lattice energy considerations.

Let the lattice energies of $Hg(NH_3)_2Cl_2(c)$ and $Hg(NH_3)_2Br_2(c)$ be $L_{complex\ Cl}$ and $L_{complex\ Br}$, and let the lattice energies of $HgCl_2(c)$ and $HgBr_2(c)$ be L_{Cl} and L_{Br}. Then ΔH_X for the reaction

$$Hg(NH_3)_2X_2(c) \longrightarrow HgX_2(c) + 2NH_3(g)$$

where X = Cl or Br, can be found from the three steps

$Hg(NH_3)_2X_2(c) \longrightarrow Hg(NH_3)_2^{2+}(g) + 2X^-(g)$	$L_{complex}$
$Hg(NH_3)_2^{2+}(g) \longrightarrow Hg^{2+}(g) + 2NH_3(g)$	$\Delta H'$
$Hg^{2+}(g) + 2X^-(g) \longrightarrow HgX_2(c)$	$-L_{halide}$

Then $\Delta H_X = L_{complex} - L_{halide} + \Delta H'$

L_{halide} can be found from the Born-Haber cycle for

$Hg X_2(c) \longrightarrow Hg^{2+}(g) + 2Cl'(g)$	Heat absorbed, L_{halide}
$Hg^{2+} + 2e \longrightarrow Hg(g)$	$-I$
$2X^- - 2e \longrightarrow 2X(g)$	$+2E_{halide}$
$2X \longrightarrow X_2(g)$	$-D_{X_2}$
$Hg(g) \longrightarrow Hg(l)$	$-L_{sublimation}$
$Hg(l) + X_2(g) \longrightarrow HgCl_2(c)$	$+\Delta H_{formation}$

where L_{halide} is again the lattice energy of $Hg(halide)_2$; E_{halide} is the electron affinity of the halide ion, I is the ionization potential for mercury going to mercuric ion, D is the dissociation energy of a molecule of halogen, $L_{sublimation}$ is the latent heat of

sublimation of liquid mercury, and $\Delta H_{formation}$ is the heat of formation of Hg (halide)$_2$.

$$\therefore \quad 0 = L_{halide} - I + 2E_{halide} - D_{X_2} - L_{sublimation} + \Delta H_{formation}$$

Considering the difference between the chloride and the bromide, since I and $L_{sublimation}$ are the same in each case, we get

$$0 = (L_{Cl} - L_{Br}) + 2(E_{Cl} - E_{Br}) - (D_{Cl_2} - D_{Br_2}) + (\Delta H_{fCl} - \Delta H_{FBr})$$

$$= (L_{Cl} - L_{Br}) + 10 - (57.8 - 46.1) + (-55 + 40.5)$$

$$\therefore \quad \underline{L_{Cl} - L_{Br} = + 16.2 \text{ kcal/mole}}$$

Now, $\Delta H_{Cl} - \Delta H_{Br} = L_{complex\ Cl} - L_{Cl} + H' - L_{complex\ Br} + L_{Br} - \Delta H'$

$$= (L_{complex\ Cl} - L_{complex\ Br}) - 16.2$$

An estimate of the difference in the lattice energies of the complexes must now be made. The closer together the ions in a lattice are, the higher the lattice energy will be, as is borne out by the L.E. for $HgCl_2$ being greater than the L.E. for $HgBr_2$, the latter having the larger lattice dimensions. In the complexes, the ions are further apart than in the halides, and consequently $(L_{complex\ Cl} - L_{complex\ Br})$ will be less than $(L_{Cl} - L_{Br})$ but greater than 0. Taking an approximate value of 10 kcal, we find

$$\Delta H_{Cl} - \Delta H_{Br} = 10 - 16.2$$

$$\simeq -6 \text{ kcal mole}^{-1}$$

Hence, the heat of formation of the chloride complex should <u>exceed</u> the heat formation of the bromide complex by about 6 kcal mole^{-1}

as Δ H here is in fact the reverse of the quantity measured by Biltz. Now, taking ΔH_{Br} as Biltz's value, i.e. -32.4 kcal mole^{-1} we get

$$\Delta H_{Cl} = +6 - 32.4 \simeq 26 \text{ Kcal mole}^{-1}$$

A new experimental measure of this quantity is evidently needed.

To summarize, the position regarding '2nd' and '3rd' law standard entropies of $Hg(NH_3)_2Cl_2$ is:

S° (e.u.)	Means of measurement	Likely source of error.
57.31	from Cp, 3rd law.	-
48.67	from cell, using $(\partial E/\partial T)$. value of $(\partial E/\partial T)$	
13.9	From cell, and std. enthalpies.	ΔH_F for $Hg(NH_3)_2Cl_2$

Interpretation of the Standard Entropy of $Hg(NH_3)_2Cl_2$.

As mentioned in the introduction, diammino mercuric chloride (fusible white precipitate) has a disordered structure at room temperature, in which the mercuric ions occupy one-sixth of the face centres of the cubic lattice in a random manner. On cooling, there are two a priori possibilities, a transition to an ordered form, or persistance of disorder to the absolute zero.

No transition was observed down to 3°K (with the exception of a small anomaly between 3 and 5°K contributing only about 0.07 e.u.) and it therefore appears that disorder persists to the absolute zero. In principle therefore, there will be a residual entropy associated with the randomness of the mercury positions, and this can be measured by comparing the '2nd' and '3rd law' entropies. The relevance of this value of residual entropy to the dimer problem will be enlarged on later.

Other effects may arise in this substance, however, which will make the residual entropy a less easy quantity to determine. From low-temperature heat capacity studies on $Ni(NH_3)_6X_2$ where X = Cl, Br or I, Van Kempen, Huiskamp, Miedema and Duffy (ref 22) found that three distinct transitions occured. These were

i) a transition caused by a co-operative movement of NH_3 units in the lattice. This took place at higher temperatures than the other transitions

ii) An anti-ferromagnetic transition, caused by alignment of the nickel nuclear spins. This transition contributed R ln 3 e.u. and took place at a temperature between thoseof the other two transitions, except for the iodide where it was superimposed on the lowest transition

iii) A transition, taking place at temperatures below $\underline{0.3^{\circ}K}$, caused by Schottky effects arising from quantum mechanical tunneling through the barriers to hindered rotation of the ammonia units. This contributed $\underline{6\ R\ \ln\ 2\ e.u.}$

Considering now $Hg(NH_3)_2Cl_2$, firstly the anti-ferromagnetic transition cannot arise, as mercuric ions have no unpaired electrons, and secondly the co-operative transition cannot occur as the orientations of the ammonia molecules in the lattice are random, whereas in the nickel salts, neighbouring ammonia molecules are in some definite orientation relative to their neighbours.

The quantum mechanical tunneling transition in principle could occur in $Hg(NH_3)_2Cl_2$. In the nickel salt, the specific heat anomaly arises because tunneling through the potential energy barrier to rotation causes a splitting in the energy levels of the vibrational states. For the nickel ammines, the energy level of each vibrational state is split into two, and the energy difference, Δ E, between the two levels gives rise to a Schottky anomaly of R ln 2 for each NH_3 unit,

i.e. of 6 R ln 2 for the 6 NH_3 units in the molecule. For the deuteroammoniates (ref 71), the same anomaly is found.

Hence, in $Hg(NH_3)_2Cl_2$ it seems possible in principle that there could be a transition occuring at a very low temperature, and contributing 2 R ln 2 e.u. to the molar entropy.

Residual Entropy in $Hg(NH_3)_2Cl_2$ and the Dimer Problem.

The dimer problem is one that has long interested scientists, particularly mathematicians and physicists. In its two-dimensional form, it is essentially the problem of the number of ways in which a chess board can be covered with dominoes, each domino occupying two horizontally or vertically adjacent squares. As was explained in the introduction, the randomly orientated NH_3-Hg-NH_3 'rods' in the three dimensional cubic lattice of $Hg(NH_3)_2Cl_2$ make this compound an example of an arrangement of 'dimers' (here these are the NH_3-Hg-NH_3 'rods') on a three-dimensional lattice.

This bearing that the number of ways of arranging dimers on a three dimensional lattice has on physical chemical theories of for example, the arrangement of large molecules in a 'quasi-crystalline' liquid, the arrangement of polymer units on a regular lattice or the adsorption of gas dimers on a surface, is apparent. A rigorous mathematical solution of the three-dimensional dimer problem has not been found, although as mentioned in the introduction, Fowler and Rushbrooke (ref 18) predicted from an approximate method, that the entropy associated with the disorder would be

$$R \ln 2.38 = 1.72 \text{ e.u.}$$

Fowler and Rushbrooke's methods for the two-dimensional problem were discussed in some detail in the introduction, but it is pertinent to consider here the two exact solutions for the two dimensional case, as, although these have not yet been successfully applied to the

three-dimensional case, in the words of Green and Hurst (ref 20) 'it is difficult to see any essential way in which this differs from the two-dimensional problem already considered'.

i) The Ising Model Solution.

The Ising model was put forward in 1925 as an elementary model of a ferromagnet, in which each atom possessed spin, and therefore magnetic moment. In the Ising model, as in all model theories of this kind, the mean potential energy of a cell, or unit, is expressed as the sum of the energies of the configurations in individual cells, plus the interaction energy of the configurations in pairs of cells or units. The Ising model applies to the case when there are two distinct configurations in each cell, and takes account of nearest neighbour interactions only. It is discussed in detail by Domb (ref 72).

Fisher and Temperley (ref 17) applied operator techniques, the mathematics of which is very difficult, to a two-dimensional lattice, completely covered with dimers (unlike Fowler and Rushbrooke's lattice which was not completely covered). No interactions were considered other than the hard core infinite repulsive forces between the dimers, and the problem was essentially to arrange the dimers so that none overlapped. As previously mentioned, they arrived at the figure R ln (1.791623) for the number of available configurations. The closeness to this of Fowler and Rushbrooke's value of R ln (1.80) for a two-dimensional lattice,

enhances the value of the latter's estimate for a three-dimensional lattice, arrived at by approximate means.

2) The Random Walk Solution

This was put forward by Kasteleyn (ref 16). The random walk method is a more attractive theory for the non-mathematician in that it is easier to understand the initial approach. Kasteleyn uses a self-avoiding random walk, in which the lattice is entirely covered with dimers, and the walker visits all lattice points once (i.e. it is a Hamiltonian walk, as opposed to an Euler walk which involves passing along all the lines once). The number of walks, which is also the number of close packed dimer arrangements per lattice point, tends to $\exp(G/\pi)$ where G is Catalan's constant, and hence, the number of arrangements per dimer again tends to $\exp(2G/\pi) = 1.791623$, giving $S = R \ln (1.791623)$ e.u. for the entropy resulting from the random orientation of the dimers.

Substances for Further Study

$Hg(NH_3)_2Br_2$ is isomorphous with the chloride (ref 19) and would be suitable for a similar study in which the entropy obtained from an equilibrium study and the third law entropies were compared. Here, however, it might be possible to arrive at S^o from measurements of the enthalpy of the reaction

$$Hg(NH_3)_2Br_2(c) \longrightarrow HgBr_2(c) + 2NH_3(g)$$

and from the dissociation pressure of ammonia in the system. With the chloride, this was not possible as dissociation proceeds via an intermediate $HgCl_2.^2/_3\ NH_3$ (refs 62, 73) and the dissociation pressures for the stages $HgCl_2.2NH_3 \longrightarrow HgCl_2.^2/_3\ NH_3$ and $HgCl_2.^2/_3\ NH_3 \rightarrow HgCl_2$ both of which must be measured, both appear from rough calculation to be belwo 10^{-6} mm Hg. This calculation was based on the value, measured by Biltz, for the enthalpy of formation of the complex, and therefore may be incorrect. For the bromide, no intermediate has ever been reported, and rough calculation gives a figure of $\sim 10^{-2}$ mm Hg for the dissociation pressure. This is capable of accurate, indirect, measurement in the following way. A suitable quantity of crystalline $Hg(NH_3)_2Br_2$, mixed with crystalline $HgBr_2$ could be allowed to fill an accurately calibrated 5 litre globe with ammonia at the equilibrium dissociation pressure. The globe could then be closed off from the mixture, and the ammonia condensed, using liquid nitrogen (at which temperature the vapour pressure of NH_3 is of the order of 10^{-10} mm Hg) in an accurately calibrated

vessel of 5 c.c. capacity, giving a 10^3 factor of magnification for the dissociation pressure. Cell measurements might prove difficult as the complex is less stable than the corresponding chloride complex, and the Hg/Hg^{2+} electrode might react to give mercurous bromide.

The iodide $Hg(NH_3)_2I_2$ would not be suitable for study of the following reasons i) it is unstable in air, decomposing within ½ minute. This would entail filling the sample container in a glove box, filled with ammonia at greater than the dissociation pressure, and correcting for the heat capacity of $NH_3(g)$ enclosed. ii) it decomposes via an intermediate phase $HgI_2.^4/_3$ (ref 74), which would complicate the calculation of S^o from dissociation pressure measurements, although a cell might be feasible. iii) it is <u>not</u> isomorphous with the chloride and bromide (ref 70) and a complete structure determination would have to be carried out to see whether disorder in the mercury positions was still present.

$Cu(NH_3)_2Cl_2$ and $Cu(NH_3)_2Br_2$ can exist in forms isomorphous with $Hg(NH_3)_2Cl_2$, and although these again have low dissociation pressures, some measurement of S^o using a suitable cell might be possible. Finally, the mixed salt $Cu(NH_4)_2Br_4.2NH_3$ is reported to show a similar type of disorder (ref 75).

CHAPTER VII

ANHYDROUS SODIUM CARBONATE

PREPARATION AND ANALYSIS OF ANHYDROUS Na_2CO_3.

As mentioned in the introduction, earlier workers in this laboratory had obtained unexpected results for the heat capacity of this substance, and in repeating the determination of heat capacity great care was taken in preparing the sample. The following transitions have been reported (refs 47, 48).

$$\alpha \xrightarrow[\text{2nd order}]{361^\circ C} \beta \xrightarrow[\text{1st order}]{489^\circ C} \gamma \xrightarrow{618^\circ C} \delta$$

c-centred,	P-centred
monoclinic	hexagonal

Care was taken to avoid the presence of the high temperature phases, and the following procedure was adopted.

A flexible-sided platinum boat was filled with A.R. Na_2CO_3 (which according to the makers, had not been heated to above $300^\circ C$ in its preparation) and placed in the middle of a silica tube, running through a muffle furnace, the temperature profile of which had been obtained with the use of a thermocouple inside the silica tube. (The use of a platinum boat is necessary as molten Na_2CO_3 attacks porcelain, silica and in fact even platinum after a time). The sample was heated under a stream of carbon dioxide, generated by heating cardice in a dewar with a fishtank heater, which could be regulated with a variac. The temperature reached 860° after about 1 hour, and was held there for 5 minutes. The muffle heater was then

switched off, and the sample allowed to cool overnight in the furnace. The fused mass of Na_2CO_3 was then transferred to a dessicator over P_2O_5, and the process repeated. Eleven repeats were necessary as a 50% contraction is experienced on fusion. The sample was then crushed into lumps, and heated slowly in a silica tube in the muffle furnace to 50° below the 2nd order transition temperature, at which temperature it was maintained for 6 hours, to give the sample the opportunity for passing over completely into the low-temperature form, if it had not done so already. It was stored over P_2O_5. No analysis was performed, as anhydrous sodium carbonate is a primary analytical standard.

Sodium Carbonate - Anhydrous.

Na_2CO_3 M.W. = 106.003

Wt of sample = 48.3709 gm

No. of Moles = 0.45632

Purity = 100% (assumed)

Corrections

Silver tube = +0.0061 gm.

Elect. solder = +0.2683 gm.

Indium solder = +0.5984 gm.

Contribution of Sample

T^oK	%
10	68.4
20	64.9
50	70.6
100	74.8
300	79.0

Experimental Heat Capacities of Anhydrous Na_2CO_3.

$T^{\circ}K$	C_p(cal/mole/$^{\circ}K$)	$T^{\circ}K$	C_p(cal/mole/$^{\circ}K$)
9.16	0.108	39.25	3.473
10.33	0.144	42.57	4.111
11.34	0.179	46.11	4.828
12.14	0.228	49.85	5.617
12.84	0.261	53.87	6.511
14.04	0.322	58.03	7.405
15.25	0.385	62.71	8.474
16.36*	0.437	67.81	9.301
18.17*	0.516	72.95	10.265
20.26*	0.694	78.15	11.319
22.07	0.874	83.33	12.106
23.79	1.081	80.29	11.604
25.68	1.293	85.70	12.493
21.54	0.814	91.74	13.379
23.24	1.003	98.29	14.352
25.23	1.234	105.36	15.191

Experimental Heat Capacities of Anhydrous Na_2CO_3 (Cont/d)

$T^\circ K$	Cp/cal/mole/$^\circ K$)	$T^\circ K$	Cp(Cal/mole/$^\circ K$)
27.58	1.527	112.67	16.066
30.16	1.909	120.27	16.864
33.01	2.354	132.02	18.038
36.13	2.899	137.95	18.520

• No refrigerant remaining; calorimeter spontaneously warming.

Experimental Heat Capacities of Anhydrous Na_2CO_3 (Cont/d)

$T^{\circ}K$	$Cp(Cal/Mole/^{\circ}K)$	$T^{\circ}K$	$Cp(cal/mole/^{\circ}K)$
146.07	19.181	223.60	23.657
~~154.90~~			
154.90	19.802	232.85	24.073
164.43	20.510	241.96	24.576
162.16	20.216	250.95	24.900
172.98	21.507	259.29	25.227
182.070	22.040	268.19	25.596
201.46	22.541	278.55	26.032
207.85	22.956	288.72	26.450
214.20	23.171	298.93	26.990

HEAT CAPACITIES OF Na_2CO_3 and its HYDRATES

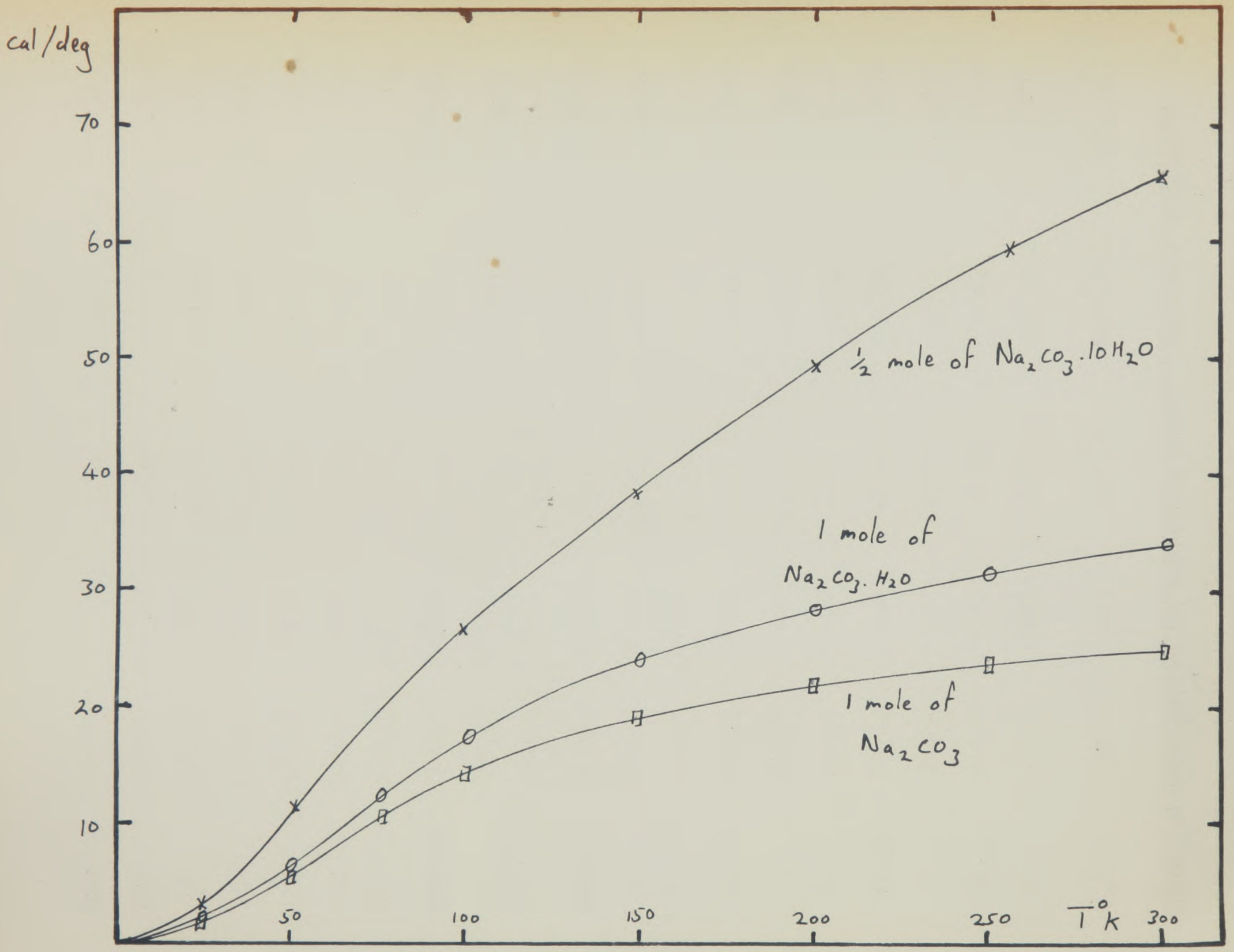

Molar Thermodynamics of Anhydrous Sodium Carbonate - Na_2CO_3.

T^oK	Cp	$\Phi(T)$	$(H-H^o_o)$	$(H-H^o_o)/T$	$-(G^o-H^o_o)/T$
10	0.135	0.045	0.36	0.04	0.01
20	0.675	0.277	4.05	0.20	0.08
30	1.870	0.753	16.04	0.53	0.22
40	3.610	1.525	42.84	1.07	0.45
50	5.662	2.555	88.7	1.77	0.78
60	7.820	3.781	156.3	2.61	1.18
70	9.788	5.137	244.5	3.49	1.64
80	11.560	6.561	351.4	4.39	2.17
90	13.141	8.016	475.1	5.28	2.74
100	14.541	9.475	613.6	6.14	3.34
110	15.777	10.920	765.3	6.96	3.96
120	16.865	12.340	928.7	7.74	4.60
130	17.827	13.729	1102.2	8.48	5.25
140	18.683	15.082	1284.9	9.18	5.90
150	19.451	16.397	1475.6	9.84	6.56
160	20.148	17.675	1673.6	10.46	7.22
170	20.791	18.916	1878.4	11.05	7.87
180	21.390	20.122	2089.3	11.61	8.51
190	21.956	21.294	2306.1	12.14	9.16
200	22.494	22.434	2528.3	12.64	9.79

Molar Thermodynamics of Anhydrous Sodium Carbonate - Na_2CO_3 (Cont/d)

$T^\circ K$	Cp	$S^\circ(T)$	$(H-H^\circ_o)$	$(H-H^\circ_o)/T$	$-(G^\circ-H^\circ_o)/T$
210	23.008	23.544	2755.9	13.12	10.42
220	23.500	24.626	2988.4	13.58	11.04
230	23.972	25.681	3225.8	14.03	11.66
240	24.422	26.710	3467.8	14.45	12.26
250	24.853	27.716	3714.2	14.86	12.86
260	25.268	28.699	3964.8	15.25	13.45
270	25.675	29.660	4219.5	15.63	14.03
280	26.089	30.601	4478.3	15.99	14.61
290	26.531	31.525	4741.4	16.35	15.17
300	27.035	32.432	5009.1	16.70	15.74
298.15	26.836	32.265	4959.2	16.63	15.63

Residual Entropy in the Hydrates of Sodium Carbonate.

The calorimetric standard entropy of anhydrous sodium carbonate was found in this work to have the value $S^{\circ}_{Na_2CO_3} = 32.26$ e.u.

If the assumption is made that the anhydrous salt is uniquely ordered at $0^{\circ}K$, then there is no residual entropy, and the calorimetric third law, standard entropy is equal to the standard entropy obtained from equilibrium measurements. This assumption is felt to be valid as there is no arrangement of hydrogen bonds here that could lead to different configurations of nearly equal energy.

We will compare the standard entropies found by the two methods for the monohydrate and decahydrate, using the above value for the standard entropy of the anhydrous salt, in conjunction with the data of Waterfield (ref |) and other, earlier, workers.

Residual Entropy in $Na_2CO_3.H_2O$.

a) 3rd law, calorimetric, S°.

Waterfield, using Goalby's measurements only for the range $14-55^{\circ}K$, found

$$S^{\circ}_{3rd\ law} = 40.19 \pm 0.2 \text{ e.u.}$$

b) S°, from equilibrium measurements.

This was found by considering the equilibrium

$$Na_2CO_3(S) + H_2O(g) \longrightarrow Na_2CO_3.H_2O(S)$$

where all substances are in their standard states. Then

$$S^{\circ}_{Na_2CO_3.H_2O(S)} = \Delta S^{\circ} + S^{\circ}_{Na_2CO_3(S)} + S^{\circ}_{H_2O(g)}$$

i) $S^{\circ}_{Na_2CO_3(S)}$ was found above to be 32.26 e.u.

ii) $S^{\circ}_{H_2O(g)}$ has been found from spectroscopic measurements (ref 49) to be 45.104 $\pm$ 0.01 e.u.

iii) ΔS° was found from the relation

$$\Delta G^{\circ}_{o/1} = -RT \ln ({}^{1}/P_{H_2O}) = \Delta H^{\circ}_{o/1} - T \Delta S^{\circ}_{o/1}$$

Elyard (ref 50) found P_{H_2O} = 5.28 $\pm$ 0.03 mm = 0.006947 atm

$$\therefore \Delta G^{\circ}_{o/1} = -2,944 \pm 3 \text{ cals.}$$

ΔH° was found from the heats of solution measured by Waterfield

$$Na_2CO_3(S) + aq = Na_2CO_3(aq); \Delta H^{\circ}_{o} = -5,421 \pm 5 \text{ cals}$$

$$Na_2CO_3.H_2O(S) + aq = Na_2CO_3.H_2O(AQ); \Delta H^{\circ}_{1} = -1,904 \pm 5 \text{ cals}$$

$$\therefore \Delta H^{\circ}_{o/1} = \Delta H^{\circ}_{o} - \Delta H^{\circ}_{1} - \Delta H^{\circ}_{W}$$

where ΔH°_{W} is the heat of vaporization of water. This important quantity hasbeen the subject of some of the most careful thermochemical measurements ever carried out, and is 10,419.5 $\pm$ 0.1 cal $mole^{-1}$ (ref 51).

$$\therefore \Delta H^{\circ}_{o/1} = -5,421 + 1,904 - 10,419.5 = -14,037 \pm 10 \text{ cals.}$$

$$\therefore \Delta S^{\circ} = \frac{(\Delta H^{\circ} - \Delta G^{\circ})_{o/1}}{T} = -37.21 \pm 0.04 \text{ e.u.}$$

Hence, $\underline{S^{\circ} = 40.15 \pm 0.2 \text{ e.u.}}$

(cf $S^{\circ}_{3rd\ law}$ = 40.19 $\pm$ 0.2 e.u.)

Hence, sodium carbonate monohydrate possess no residual entropy.

i.e. S_o, for $Na_2CO_3.H_2O = 0$

Residual Entropy in $Na_2CO_3.10H_2O$.

a) 3rd law, calorimetric, S°.

This was found by Waterfield to be 133.43 ± 0.2 e.u.

b) S° from equilibrium measurements.

This was found in the same way as for the monohydrate, by considering the equilibrium

$$Na_2CO_3.H_2O(S) + 9H_2O(g) = Na_2CO_3.10H_2O(S)$$

where all substances are in their standard states.

$$S^\circ_{Na_2CO_3.10H_2O(S)} = \Delta S^\circ_{1/10} + S^\circ_{Na_2CO_3.H_2O(S)} + 10\, S^\circ_{H_2O(g)}$$

$\Delta S^\circ_{1/10}$ was found from

$$\Delta G^\circ_{1/10} = \Delta H^\circ_{1/10} - T\Delta S^\circ_{1/10} = -RT \ln \left(\frac{1}{P_{1/10}}\right)$$

Waterfield, (ref 1) found

$$P_{1/10} = 16.46 \pm 0.02 \text{ mm} = 0.02166 \text{ atm}$$

$$\therefore \Delta G^\circ_{1/10} = -20{,}435 \pm 8 \text{ cals}$$

The standard enthalpy change is calculated as before, using Waterfield's data.

$$Na_2CO_3.H_2O(S) * aq = Na_2CO_3(aq);\ \Delta H^\circ_1 = -1{,}904 \pm 5 \text{ cals}$$

$$Na_2CO_3.10H_2O(S) + aq = Na_2CO_3.10H_2O(aq);\ \Delta H^\circ_{10} = +16634 \pm 8 \text{ cals}$$

$$\therefore \Delta H^\circ_{1/10} = \Delta H^\circ_1 - \Delta H^\circ_{10} - 9\Delta H^\circ_W = -113{,}218 \pm 13 \text{ cals}$$

$$\therefore \Delta S^{\circ}_{1/10} = \frac{(-113,218 \pm 13) - (-20,435 \pm 8)}{298.15}$$

$$= -311.20 \pm 0.05 \text{ e.u.}$$

Using $S^{\circ}_{Na_2CO_3 \cdot H_2O} = 40.19 \pm 0.2$ e.u.

$S^{\circ}_{H_2O} = 45.104 \pm 0.01$ e.u.

$S^{\circ}_{Na_2CO_3 \cdot 10H_2O} = (40.19 \pm 0.2) + (9 \times 45.104 \pm 0.01) - (311.20 \pm 0.05)$

$$= \underline{134.93 \pm 0.35 \text{ e.u.}}$$

(cf $S^{\circ}_{3rd\ law} = 133.43 \pm 0.2$ e.u.)

Hence, sodium carbonate decahydrate possesses residual entropy where

$$\underline{S_o = 1.50 \pm 0.5 \text{ e.u.}}$$

INTERPRETATION OF THE RESIDUAL ENTROPY IN SODIUM CARBONATE DECAHYDRATE

The value for S°, 1.50 ± 0.5 e.u. is significantly close to the value of R ln 2 = 1.38 e.u., which would be the entropy resulting from the presence of two configurations of almost identical energy at the absolute zero. The complete structure of $Na_2CO_3 \cdot 10H_2O$ has not been worked out, but recent work (ref 52) has shown that the space group is $C_{2/C}$ with four molecules in the unit cell, and that the dimensions of the monoclinic unit cell are a = 12.57 Å, b = 9.01 Å, C = 13.47 Å; β = 121°. There are four molecules per unit cell. Despite the difference in symmetry between CO_3^{2-} and SO_4^{2-}, it is considered quite probable (ref 53) that the structure of $Na_2CO_3 \cdot 10H_2O$ is quite closely related to that of $Na_2SO_4 \cdot 10H_2O$.

In $Na_2SO_4 \cdot 10H_2O$, for which Pitzer and Coulter found a residual entropy of 1.7 e.u., later shown by Brodale and Giauque to be 1.51 e.u., the structure was found (ref 54) to be monoclinic, space group $P2_{1/C}$, with four molecules in a unit cell dimensions a = 11.51 Å, b = 10.38 Å, C = 12.83 Å; β = 107°45'. Isomorphous replacement, using $Na_2SeO_4 \cdot 10H_2O$, and the corresponding tungstate, molybdate and chromate gave two-dimensional Fourier projections from which the structure was found to consist of layers, in which the cations are octahedrally surrounded by water molecules, the octahedra sharing edges to form zig-zag chains along the C-axis. Two water molecules per formula weight are not directly bonded to the sodium atoms, and are available for hydrogen bonding between the chains and the sulphate ions. One can explain

configurational residual entropy of Rln2 in this structure in the following way. To stabilize the layers, it is necessary for each of the two not-directly-bonded water molecules to make one hydrogen bond to the sodium hydrate sheath, and one to a sulphate oxygen atom. The possible environments of the two water molecules, relative to the two adjacent sulphate ions are shown below

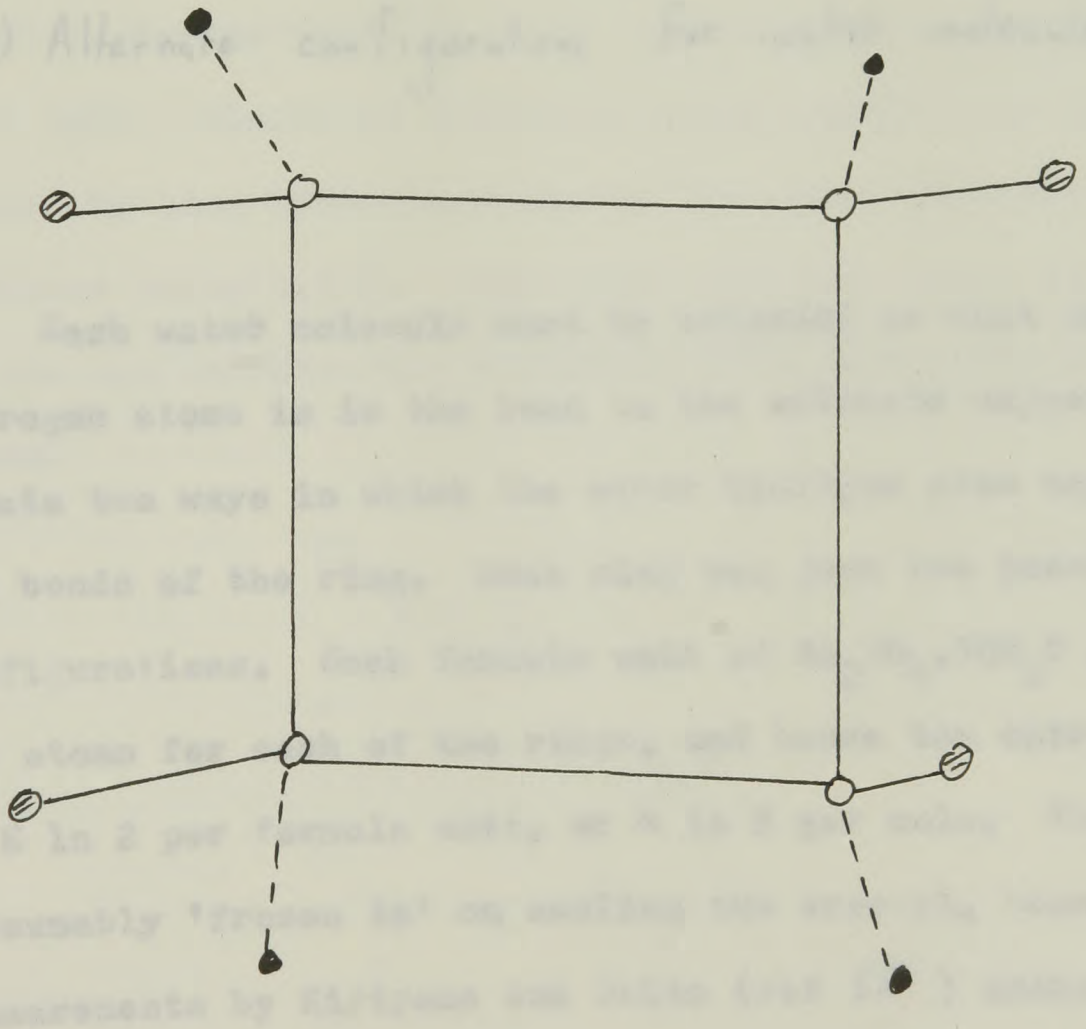

i) Bonding of water molecules, O, to sodium ions ●, and sulphate oxygens ◎. Solid lines represent hydrogen bonds. The above represents the overall picture; the two contributing configurations of water molecules are shown on the next page.

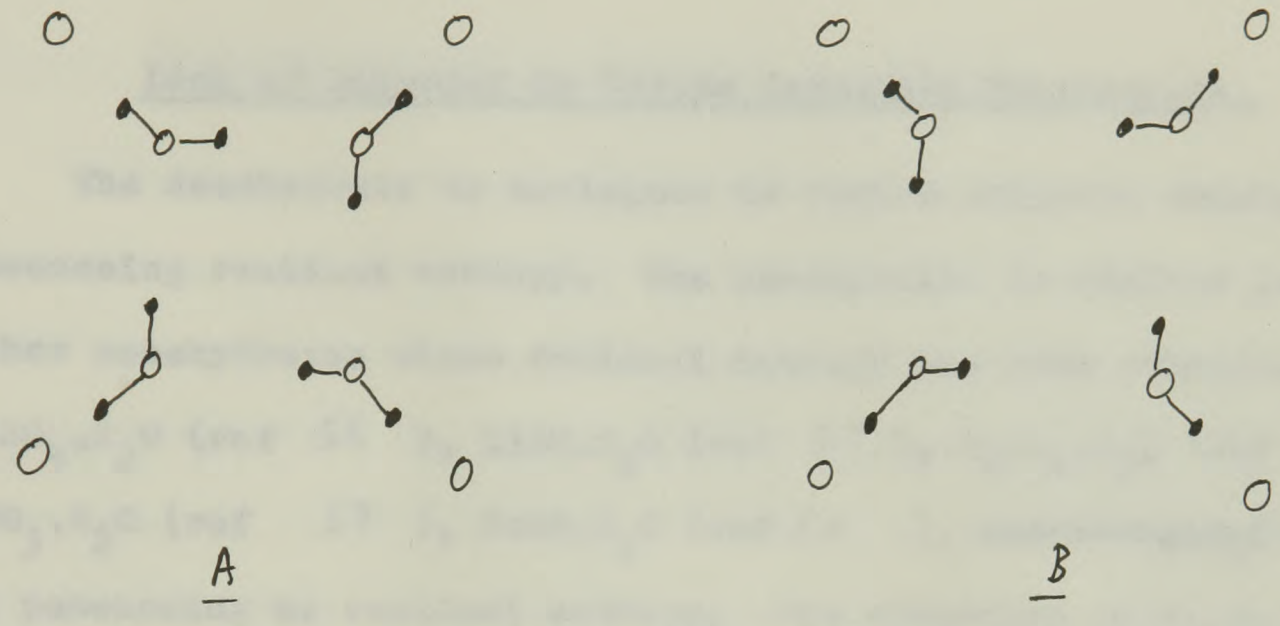

ii) Alternate configurations for water molecules in a ring

Each water molecule must be oriented so that one of its hydrogen atoms is in the bond to the sulphate oxygen, but there remain two ways in which the other hydrogen atom may be oriented in the bonds of the ring. Each ring has just two possible configurations. Each formula unit of $Na_2SO_4.10H_2O$ provides half the atoms for each of two rings, and hence the entropy of disorder is K ln 2 per formula unit, or R ln 2 per mole. The disorder is presumably 'frozen in' on cooling the crystal, because dielectric measurements by Kiriyama and Saito (ref 55) indicate that re-orientation of the water molecules probably occurs above 100°K.

If the structure of $Na_2CO_3.10H_2O$ is similar, in having octahedra of water surrounding the Na^+ ions, again sharing edges, and again leaving two water molecules per formula unit free to form hydrogen bonds as in $Na_2SO_4.10H_2O$, then a similar explanation would apply.

Lack of Disorder in Sodium Carbonate Monohydrate.

The decahydrate is analogous to sodium sulphate decahydrate in possessing residual entropy. The monohydrate is similar to the other monohydrates whose residual entropy has been studied, namely $CdSO_4.H_2O$ (ref 56), $LiOH.H_2O$ (ref 57), $H_2SO_4.H_2O$ (ref 58) $HNO_3.H_2O$ (ref 59), $NaOH.H_2O$ (ref 60), ~~and $CdSO_4.H_2O$ (ref)~~, in possessing no residual entropy. The structure of $Na_2CO_3.H_2O$ was found by Harper (ref 61) to be orthorhombic with four molecules per unit cell. Planes of carbonate ions, parallel to the 100 face are linked by long hydrogen bonds to the water molecules, the $CO_3^{2-} - H_2O$ distance being 2.6 Å. Each water molecule makes two hydrogen bonds to the two neighbouring carbonate ions, the structure being shown below.

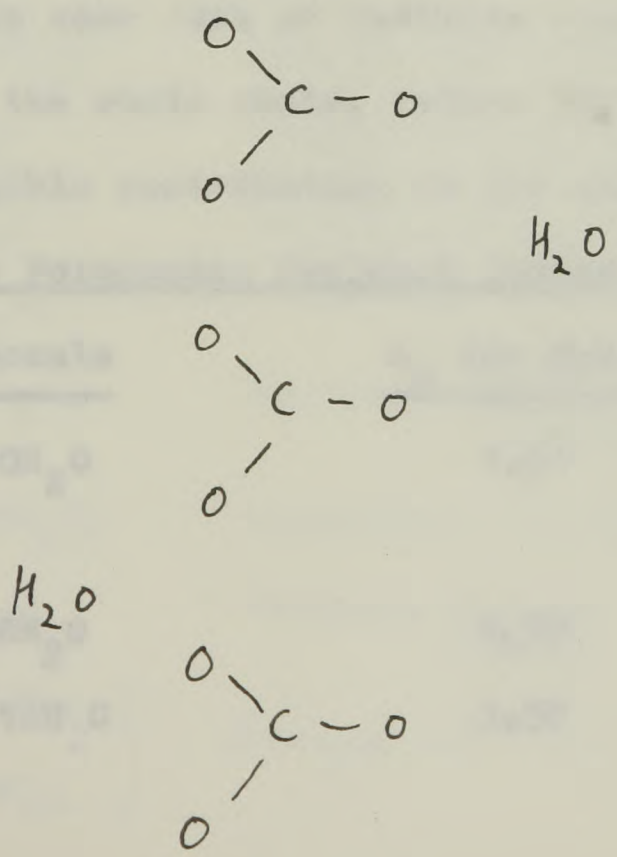

Residual Entropy in Hydrates - Summary

Comparatively few studies, and those mainly by Giauque and his co-workers, have been carried out on hydrate systems. This work has added two salts to those whose residual entropy has been studied, $Na_2CO_3.10H_2O$ which possesses residual entropy, and $Na_2CO_3.H_2O$ which does not. We summarize below firstly those hydrates which possess residual entropy, and secondly those that do not, given in order of increasing water content.

It will be noticed that those hydrates that possess residual entropy each have a large number of water molecules in the lattice, whereas in cases so far studied lower hydrates appear not to possess residual entropy. The conclusion that can perhaps be drawn from this is that in lower hydrates, the water molecules serve to link other groups in some form of infinite sheet or chain, and any disorder would involve the whole chain, rather than being local, and would thus make a negligible contribution to the molar entropy.

Hydrates Possessing Residual Entropy.

Formula	S_o (in e.u.)	Reference.
$Na_2SO_4.10H_2O$	1.51	Giauque and Brodale, J.A.C.S. 80 (1958) 2042
$Na_2CO_3.10H_2O$	1.50	This work
$Na_2HPO_4.12H_2O$	3.50	Waterfield and Staveley Trans. Farad. Soc. (in press)

Hydrates Possessing no Residual Entropy

Formula	Reference	
$2NH_3.H_2O$	Giauque and Hi	J.A.C.S. 75 (1953) 2811
$LiOH.H_2O$	Bauer, Johnston and Kerr.	J.A.C.S. 72 (1950) 5174
$NaOH.H_2O$	Giauque and Murch.	J. Phys. Chem. 66 (1962)2052
$Na_2CO_3.H_2O$	This Work	
$HNO_3.H_2O$	Giaque and Forsythe	J.A.C.S. 64 (1942) 48.
$H_2SO_4.H_2O$	Giauque and Rubin.	J.A.C.S. 74 (1952) 800
$NH_3.H_2O$	Giauque and Hi	J.A.C.S. 75 (1953) 2811
$CdSO_4.H_2O$	Giauque and Papadapoulos.	J.A.C.S. 77 (1955) 2740
$Na_2HPO_4.2H_2O$	Waterfield and Staveley.	Trans Farad. Soc (in press)
$H_2SO_4.2H_2O$	Giauque and Rubin	J.A.C.S. 74 (1952) 800
$NH_3.2H_2O$	Chan.	Diss. Abs 25 (1965) 6250
$CdSO_4.^8/_3H_2O$	Giauque and Papadapoulos.	J.A.C.S. 77 (1955) 2740
$HNO_3.3H_2O$	Giauque and Forsythe.	J.A.C.S. 64 (1942) 48
$H_2SO_4.3H_2O$	Giauque and Hornung	J.A.C.S. 77 (1955) 2883
$H_2SO_4.4H_2O.$	" " "	" " " "
$H_2SO_4.6\frac{1}{2}H_2O.$	Giauque, Hornung and Breckett	J.A.C.S. 78 (1956) 5747
$Na_2HPO_4.7H_2O.$	Waterfield and Staveley.	Trans Farad. Soc (in press)
$ZnSO_4.7H_2O$	Giauque, Baricau and Kunzler	J.A.C.S. 72 (1950) 5685
$CoSO_4.6H_2O$ } $CoSO_4.7H_2O$ }	Grauque and Rao	J. Phys. Chem. 69 (1965) 1272

APPENDIX

Appendix 1. Autocode Programme for calculating molar thermodynamic functions.

```
TITLE
FAJBN123456
CHAPTER o
A —> 10
B —> 10
C —> 10
H —> 100
X —> 100
D —> 10
W —> 10
Y —> 10
READ (N) - - - - - - - - - - N = No. sets of data
M = 1(1)N
1) READ (W) - - - - - - - - W = S50
READ (B) - - - - - - - - - B = (H50 - Ho°)
READ (I) - - - - - - - - - I = no terms in polynomial
K = o(1)I
READ (AK)- - - - - - - - - Ao, A1 etc = coeffs. of polynomial
REPEAT
CAPTION
....T.K..MOLCP.....S(T).....(H-Ho)....(H-Ho)/T...-(G-H)/T
NEWLINE
NEWLINE
```

```
NEWLINE
K = 50(10)300
Z = K  - - - - - - - - - -  Z = temperature at 10° intervals
2)F = ψ POLY(Z) Ao,I - - -  F = molar heat capacity
Co = 0
P = 1(1)I
CP = AP/P
REPEAT
H  = ψ POLY(Z)Co,I
H1 = Ao  LOG(Z)
XK = H + H1
X = XK - X50 + W - - - - -  X = Entropy
Do = o
R = I + 1
P = 1(1)R
O = P-1
DP = AQ/P
REPEAT
H2 = ψ POLY(Z)Do,P
H5 = H2 - H50 + B - - - - -  H5 = (H - H°o)
H6 = H5/Z  - - - - - -  H6 = (H-H°o)/T
H7 = X - H6  - - - - - -  H7 = -(G - H°o)/T
PRINT (Z) 3, 0
PRINT (F) 3, 3
PRINT (X) 3, 3
```

```
PRINT (H5) 5,1
PRINT (H6) 2, 2
PRINT (H7) 1, 3
JUMP 4, K ≠ 200
S = 1(1)5
NEWLINE
REPEAT
4) NEWLINE
NEWLINE
JUMP 3, Z = 298.15
REPEAT
NEWLINE
Z = 298.15
JUMP 2
3) NEWLINE
REPEAT
END
CLOSE
→
??
```

Appendix 2. Heat Capacities of Solder in cal/gm/deg.

$T^{o}K$	Elect. Solder	Indium solder	Silver Tube.
10	0.00246	0.00277	0.00053
15	0.00645	0.00662	0.00182
20	0.01080	0.01030	0.00454
30	0.01850	0.01750	0.01290
40	0.02410	0.0224	0.0223
50	0.02840	0.02610	0.03160
60	0.03150	0.02840	0.03900
100	0.03600	0.03780	0.04460
150	0.03900	0.04000	0.05100
200	0.04100	0.04100	0.05400
300	0.04300	0.04300	0.05600

Compositions.

Electrical Solder - commercially available, resin-covered flux, 40% Sn, 60% Pb.

Indium Solder - not commercially available, $ZnCl_2$ soln. flux, Bi 49%, Sn 15%, Pb 18%, In 18%; all by weight; all metals analar.

Silver tube - pure silver.

Appendix 3. Thermodynamic Symbols.

Energy gained by the system is POSITIVE.

∴ if work is done on the system, the system gains energy

If heat is put into the system, the system gains energy.

dq = incremental amount of heat

dw = " " " work.

U = Internal energy

P, V, T = Pressure, volume, temperature.

S = dq/T = Entropy

H = U + PV = Enthalpy = (dq)p

$C_p = (\partial H/\partial T)_p$ = Heat Capacity at const. pressure = $T(\partial S/\partial T)_p$

$C_v = (\partial U/\partial T)_v$ = " " " " volume

G = H - TS = Gibbs free energy (net work function) = $-w_{net}$

A = U - TS = Helmholtz free energy (Maximum work function = $-w_{gross}$

n_i = mole fraction

N = Avogadro's no.

Subscripts.

i) Lower subscript 'o', e.g. S_o. Value at T = 0°K = -273.15°C

ii) Upper subscript 'o', e.g. G^o. Value in standard state, i.e. at 25°C (298.15°K; also, for a liquid, at unit activity; also, for a gas, at unit (i.e. atmospheric) pressure

iii) Upper and lower subscripts 'o', e.g. H^o_o. Value for a substance in standard state as regards activity and pressure but at T = 0°K rather than T = 298.15°K.

iv) Lower subscript 'T', e.g. S_T. Value of function at temperature T°K.

Cells.

The potential of the solution is taken as 0. The electrode potential is the potential of the electrode w.r.t. the solution. (Hence electropositive metals, e.g. Na, have negative electrode potentials).

The reducing electrode is the more negative. It is written on the left hand side of the cell. It gives out electrodes into the solution. The oxidising electrode is positive, or less negative, is written on the right hand side of the cell, and takes up electrons.

REFERENCES

1.	Waterfield, C.G.	D. Phil Thesis, Oxford		(1967)	
2.	Dennison, D.M.	Proc. Roy. Soc.	115A	(1927)	483
3.	Clayton, J.O. and Giauque, W.F.	J. Am. Chem. Soc.	54	(1932)	2610
4.	Clusius, K.	Z. Electrochem.	40	(1934)	98
5.	Blue, R.W. and Giauque, W.F.	J. Am. Chem. Soc.	57	(1935)	991
6.	Newns, D.M. and Staveley, L.A.K.	Chem. Rev.	66	(1966)	267
7.	Buckingham A.D.	Laws and Applications of Thermodynamics. Pergamon		(1964)	44
8.	Giauque, W.F. and Stout J.W.	J. Am. Chem. Soc.	58	(1936)	1144
9.	Pitzer, K.S. and Coulter, L.V.	J. Am. Chem. Soc.	60	(1938)	1310
9.	Giauque, W.F. and Brodale	J. Am. chem. Soc.	80	(1958)	2042
10.	Nernst, Von W.	Sitzb. Konig Press Akad. Wiss		(1914)	355
11.	Gunther P.	Ann Phys.	51	(1916)	828
12.	Simon, F. and Swain, R.C.	Z. Phys. Chem.	28B	(1935)	189
13.	Anderson, C.T.	J. Am. Chem. Soc.	56	(1934)	340
14.	Backstrom, H.L.J.	J. Am. Chem. Soc.	47	(1925)	2441
15.	Bragg, W.L.	Proc. Roy. Soc.	A105	(1924)	16

16.	Kasteleyn P.W.	Physica	29	(1963)	1329
17.	Fisher, M.E. and Temperley, H.N.V.	Phys. Rev.	124	(1961)	1664
18.	Fowler, R.H. and Rushbrooke, G.S.	Trans. Farad. Soc.	33	(1937)	1272
19.	MacGillavry, C.H. and Bijvoet J.M.	Z. Krist.	94	(1936)	231
20.	Green, H.S. and Hurst, C.A.	'Order-Disorder Phenomena' Interscience		(1964)	ch 1.
21	Clay, R.M.	D. Phil. Thesis, Oxford.		(1965)	
22.	Van Kempen, H., Duffy Jr, W.T. Miedema, A.R. and Huiskamp W.J.	Physica	30	(1964)	1131
23.	Ukei, K. and Kanda, E.	J. Phys. Soc. Japan.	16	(1961)	2061
24.	Long, E.A. and Toettcher, F.C.	J. Am. Chem. Soc.	64	(1942)	629
25.	Zeigler, W.T.	J. Am. Chem. Soc.	63	(1941)	2700
26.	Chernayev, E.E., Sokolov, A., Smidt, N.E. and Mouraveskaya, G.S.	Doklady	62	(1948)	235
27.	Goalby B.B.	D. Phil. Thesis, Oxford		(1950)	
28.	Bates, T.R.	D. Phil. Thesis, Oxford.		(1958)	

29. Hall J.A. and Barber, C.R. — Nat. Phys. Lab. Notes on Applied Science, No. 12, 'Calibration of Temperature Measuring Instruments, p. 18.

30. Douglas, T.B. Furukawa, G.T. McCoskey R.E. and Ball, A.F. — J. Research. Nat. Bur. Stds. 53 (1954) 141

31. Furukawa, G.T. McCosky, R.E. and King, G.J. — J. Res. Nat. Bur. Stds. 47 (1951) 256

32. Skylankin, A.A. and Strelkov, P.G. — Zhur. Priklad. Mech. i Tech. Fiz. 2 (1960) 100

33. Stout, J.W., Cole, A.G. Huchens, J.O. and Robie R.A. — J. Am. Chem. Soc. 77 (1955) 2737

34. Korzhinskii, A.F. — Zapiski Vsesoyuz. Mineral Obshchestva (Chem. Abs. 51 7955f) 85 (1956) 535

35. Boettcher, A.L. and Wyllie, P.J. — Nature 213 (1967) 792

36. Hexter, R.M. — Spectrochim. Acta. 10 (1958) 281

37.	Gialotto, L. and Loinger, A.	Nuovo Cim.	8	(1951)	476
38.	Robie, R. A. Edwards, J.W.	J. Appl. Phys.	37	(1966)	2662
39.	Anderson, O.L.	Physical Acoustics and Mason W.P.; A. Press	3B	(1965)	89
40.	Betts, D.D., Bhatia, A.B. and Horton G.K.	Phys. Rev.	104	(1956)	43
41.	Cabannes, J.				
42.	Barron, T.H.K.	Lattice Dynamics, ed. R.F. Waller; Pergamon Press		(1965)	253
43.	Robie, R.A.	Private Communication			
44.	Peselnick, L., and Robie, R.A.	J. Appl. Phys.	34	(1963)	2494
45.	Jellinek, K.	Lehrbuch der Phys. Chem.	2	(1928)	303
46.	Kalinkina, I.N.	Soviet Physics, JETP	14	(1963)	1432
47.	Jaffray, J, and Martin, P.	J. Phys. Radium.	14	(1953)	553
	" " "	Compt. Rend.	236	(1953)	1755
48.	Brouns, E., Visser, J.W. and de Wolff, P.M.	Acta. Cryst.	17	(1964)	614
49.	Nat. Bureau of Standards	Circular 500			
50.	Elyard, C.A.	Part II thesis, Oxford.		(1954)	

51. Wagman, D.D., Kilpatrick, J.E. Taylor W.J. Pitzer, K.S., and Rossini F.D. — J. Res. Nat. Bur. Stds. 34 (1945) 143

52. Dunsmore, H.S. and Speakman, J.S. — Acta. Cryst. 16 (1963) 573

53. Murray-Rust, P. — Private communication to C. G. Waterfield.

54. Rubeo H.W. Templeton, D.H. Rosenstein, R.D. and Olovsson, I. — J. Am. Chem. Soc. 83 (1961) 820

55. Kiriyama, R. and Saito, Y. — Bull. Chem. Soc. Japan. 26 (1953) 531.

56. Giaque, W.F. and Papadapoulos, M.N. — J. Am. Chem. Soc. 77 (1955) 2740

57. Bauer, T.W. Johnston, H.L. and Kerr, E.C. — J. Am. Chem. Soc. 72 (1950) 5174

58. Rubin, T.R. and Giauque, W.F. — J. Am. Chem. Soc. 74 (1952) 800

59. Forsythe, W.R. and Giauque, W.F. — J. Am. Chem. Soc. 64 (1942) 48

60. Murch, L.E. and Giauque, W.F. — J. Phys. Chem. 66 (1962) 2052

61. Harper, J.P. — Z. Krist. (1953) 1493.

61. Harper, J.P. Z. Krist. 95 (1936) 266

62. Glasson, D.R. and Gregg, S.J. J. Chem. Soc. (1953) 1493

63. Pochon, M. Part II Thesis, Oxford. (1967)

64. Manolov, K.R. Russ. J. Inorg Chem. (1964) 111

65. Special Publication, Chemical Society of London, No. 7.

66. Latimer, W.M. Oxidation potentials. p. 179

67. Gmelin. Handbuch der Anorganischen Chemie 23 44

68. Overstreet, R, and Giauque, W.F. J. Am. Chem. Soc. 59 (1937) 254

69. Biltz, W. and Mau, C. Z. Anorg. Allgem. Chem. 148 (1925) 170

70. Linford, R.G. Part II thesis, Oxford (1965)

71. Van. Kempen, H, Gurofano, T, Meidema, A.R. and Huiskamp, W.J. Physica 31 (1965) 1096

72. Domb, C. Advances in Physics. 9 (1960) 149

73. Holmes, M.C.C. J. Chem. Soc. 113 (1911) 74

74. Francois, M. Ann. Chim. 11 (1929) 22

75. Silbersten, A. Compt. Rend 205 (1937) 909

ABSTRACT

ABSTRACT

One of the best methods of investigating disorder in crystals is the thermodynamic method, in which the calorimetric entropy calculated from a study of the heat capacity from low temperatures is compared with the entropy obtained by an independent method, such as statistical calculation or a study of some equilibrium involving the compound under co nsideration. In this work, the thermodynamic method has been used to investigate three distinct problems concerned with disorder.

The first problem is concerned with the size of the entropy difference between two forms of the same compound, having different crystal structures. The interest in this topic lies in its connection with t e entropy changein an order-disorder transition. A disordered phase of a substance possesses a configurational entropy of R ln W, where W is the number of energetically equivalent configurations that each formula unit can adopt, and a large part of the entropy change accompanying the transition to an ordered form of the same substance will be the configurational term, R ln W. The ordered and disordered forms will, however, differ slightly in their crystal structure, and consequently the lattice-vibrational frequency spectrum will not be the same for the two polymorphs. The configurational entropy term will therefore be accompanied by an entropy term arising from changes in thelattice-vibrational frequency

spectrum. The easiest way of assessing this last term would be to measure the entropy difference between two polymorphs of the same substance where questions of disorder do not arise, and any entropy difference is caused solely by differences in the lattice vibrations. Two such polymorphs are calcite and aragonite which are respectively the trigonal and orthorhombic forms of calcium carbonate, $CaCO_3$. The results and conclusions of this study are set out later in the abstract.

The second problem is one that has interested mathematicians, physicists and chemists for some time, and is to find the number of ways that dimers, occupying two lattice cells, can be arranged on a three-dimensional lattice. This problem has a bearing on theories of gas adsorption on solids and theories of theliquid state. The two dimensional case has been solved rigidly by topological algebra (refs 1 and 2) and by random walk methods (ref 3), the number of configurations being 1.791623 per dimer; an approximate solution has been found for the three dimensional case (ref 4) which suggests that the number of configurations should be about 2.38 per dimer, but no rigid mathematical solution has yet been put forward. A rather unusual chemical compound, fusible white precipitate, $Hg(NH_3)_2Cl_2$ has a structure in which 'rods' of NH_3-Hg^{2+}-NH_3 (corresponding to the dimers in the classical case) are randomly orientated parallel to three mutually perpendicular axes, on a cubic lattice of chloride ions. On cooling this compound

to low temperatures, there are in principle two things that can happen; either the structure will remain disordered, in which case comparison of the calorimetric entropy with that obtained by an equilibrium study will reveal residual entropy, or there will be an order-disorder transition, with an accompanying entropy change. From the entropy change, or residual entropy, the number of configurations can be obtained. The result of this investigation is given later in the appendix.

The final problem with which this work was concerned was part of an investigation into whether or not the hydrates of sodium carbonate were disordered. Comparison of the calorimetric entropies, and the entropies obtained from an equilibrium study, of $Na_2CO_3.H_2O$ and $Na_2CO_3.10H_2O$ measured by a previous worker (ref 5) appeared to show that the figure for S^o for anhydrous Na_2CO_3, on which the equilibrium study entropies of the hydrates depended, was too low, if the anhydrous salt was in fact completely ordered at room temperature. The calorimetric entropy of Na_2CO_3 was therefore remeasured and the results are summarised later in this abstract.

In order to obtain an accurate value of the calorimetric standard entropies of the substances mentioned above, namely calcite, aragonite, diammino mercuric chloride and anhydrous sodium carbonate, precise measurements of thelow temperature heat capacities of these substances had to be carried out. To enable this to be done, an

adiabatic, low-temperature calorimeter, capable of measuring heat capacities from a little above the boiling point of liquid helium to room temperature, was constructed. The construction, with the exception of some early stages in the wiring, was entirely carried out in the first year of this work.

The calorimeter is similar to those recently constructed in Oxford and elsewhere (no commercial model being, as yet, obtainable) but certain features are worthy of mention. The sample container is made of platinum-rhodium alloy, rather than the moreusual copper, to enable compounds that attack copper to be investigated. Adiabatic conditions aremaintained by a metal shield around the sample container, the temperature being controlled by automatic, rather than manual, control of the shield heater. It was found that this system functioned best when the shield was of light weight and consequently of small wall thickness. This precluded bringing the leads to the sample container into thermal equilibrium with the shield by carrying them in grooves in the shield wall, and instead they were carried in commercially available, alumina packed, metal sheathed tubes, soldered to the inside of the shield. The calorimeter is designed for use with liquid nitrogen, liquid hydrogen and liquid helium, and the whole of the temperature range is covered without the need to pump on the refrigerants.

The heat capacity of the empty sample container was measured, and also the heat capacity and standard entropy of benzoic acid. The latter values agreed with those found by other workers (refs 6, 7, 8)

to within 0.2% above 30°K and to 0.75% below 30°K. S° was found to be 40.05 e.u. compared with 40.054 e.u. (ref 6) and 40.04 e.u. (ref 7), showing that there does not seem to be any systematic error in the measurements.

The heat capacities, and standard calorimetric entropies of calcite and aragonite were measured and the values confirmed the early, rather imprecise measurements of Anderson (ref 9) who measured the heat capacities from 56°K upwards. The measurements in this work extended from 10°K in the case of calcite, agreeing with other early measurements (refs 10,11), and from 20°K for aragonite giving values that differed considerably from those of Güntlier (ref 12), whose results were also inconsistent with those of Anderson. The standard calorimetric entropies were found to be

Aragonite $S^{\circ} = 21.03$ e.u.

Calcite $S^{\circ} = 21.92$ e.u.

showing an entropy difference between the two polymorphs of 0.89 e.u. This agrees within experimental error with the difference found by the early calorimetric workers, and also with the value of 0.74 ± 0.2 e.u. found from an equilibrium study (ref 13), showing that the polymorphs are equally ordered.

The entropy difference between the polymorphs arises from differences in their lattice-vibrational spectra. An attempt was made to calculate the heat capacities of calcite and aragonite from spectral data, but this met with only partial success for several reasons. Although the lattice frequencies for calcite are well assigned, and indeed one spectroscopist has said that 'calcite is the touchstone in the application of modern theories of spectra to the solid state', even here, three frequencies are inactive in both the Raman and the i/r and use has had to be made of estimated values. For aragonite, only some of the modes of vibration have had frequencies assigned, and the information on lattice frequencies is too sketchy to form the basis of any calculations. The optical modes of vibration of calcite were treated as Einstein functions and the acoustic modes as Debye Functions, and although agreement with experimental heat capacities was satisfactory over most of the range, the calculated values were too low at very low temperatures and also above 200°K.

It is felt that the discrepancy at high temperatures arises from neglecting anharmonicity, and the low values at low temperatures are thought to arise because pure Einstein functions do not truely represent the relation between vibrational modes and heat capacity; Einstein functions very rapidly fall to low values as the temperature drops.

Although no values could be calculated for aragonite, to compare with the calculated calcite values, it is felt that such calculations would reveal that the modes of torsional oscillation of the carbonate ion in aragonite had higher frequencies and contributed less to the heat capacity than in calcite. In calcite, the carbonate ions lie in planes midway between adjacent planes of calcium ions, and the CO_3^{2-} oxygens do not lie directly over or under adjacent Ca^{2+} ions, whereas in aragonite, the carbonate ions are near the lower plane of Ca^{2+} ions, and the CO_3^{2-} oxygens lie directly under the calcium ions in the upper plane.

The heat capacity of $Hg(NH_3)_2Cl_2$ was measured from $3^{\circ}K$ to room temperature, measurements below $12^{\circ}K$ being carried out in a calorimeter built by another worker. No transition or thermal anomaly was observed which agrees with the behaviour predicted from the Ising model (ref 14). Hence disorder of the dimer units would appear to persist to the absolute zero, and no co-operative transition involving ammonia molecules would seem to have occurred. Here $Hg(NH_3)_2Cl_2$ is at variance with certain other ammines, the heat capacities of which have been studied; $Ni(NH_3)_6I_2$ for example has recently been shown (ref 15) to undergo a co-operative transition involving the ammonia molecules at $19.5^{\circ}K$, and also displays two other, superimposed transitions at $0.35^{\circ}K$, one an anti-ferromagnetic transition involving the unpaired nickel d electrons and the other a Schottky effect arising from

quantum mechanical tunnelling through the potential energy barrier to hindered rotation. The latter transition could in principle occur at a very low temperature in $Hg(NH_3)_2Cl_2$, in which case presumably each ammonia molecule would contribute R ln 2 to the transitional entropy, as is the case for the nickel salt.

If this transition does not occur, then ~~the difference between~~ the standard calorimetric entropy, found in this work to be 57.31 e.u. should be lower than the value for the standard entropy obtained by an equilibrium study by R ln W, where W is the number of configurations of the NH_3-Hg-NH_3 dimers on a three-dimensional lattice. Another worker is determining S^o from the temperature coefficient of the e.m.f. of the cell

$$\ominus \quad Hg(l) \;\big|\; Hg(NH_3)_2Cl_2(c) \;\big|\; NH_4Cl(aq),\ NH_3\ (aq) \;\big\|\; AgCl(c) \;\big|\; Ag(c) \quad \oplus$$

the cell reaction being

$$Hg(l) + 2AgCl(S) + 2NH_3\ (aq) \longrightarrow Hg(NH_3)_2Cl_2(S) + 2Ag(c)$$

and the standard entropies of the other reactants are known. These measurements are not yet complete.

Although many studies of this type, where S^o obtained from heat capacity measurements is compared with S^o obtained from an equilibrium study, have been carried out on hydrate systems, this is believed to be the first study of this type on an ammoniate.

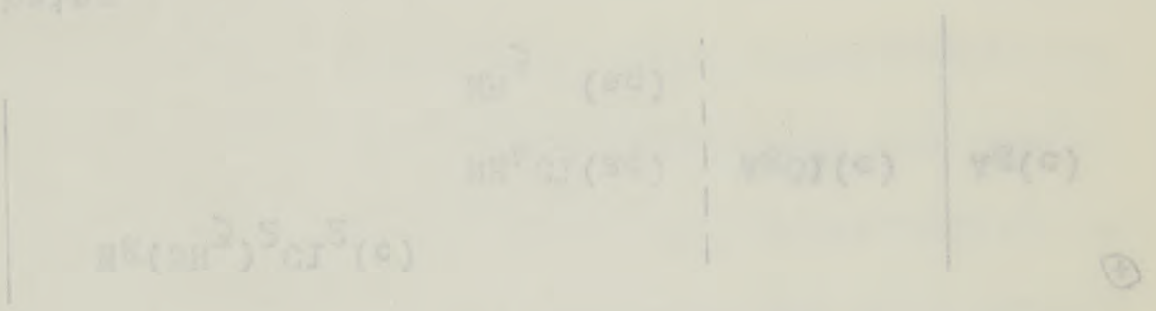

The calorimetric standard entropy of anhydrous sodium carbonate was found to be 32.26 e.u. Taken in conjunction with Waterfield's values (ref 5) for the standard entropies of the mono- and deca-hydrate, this determination shows that the monohydrate is completely ordered at the absolute zero, and that the decahydrate possesses residual entropy of 1.50 ± 0.5 e.u. The results are best summarized in a table.

Compound.	Standard Entropy	Calorimetric Entropy
Na_2CO_3		32.26 ± 0.2 e.u.
$Na_2CO_3.H_2O$	40.16 ± 0.2 e.u.*	40.19 ± 0.2 e.u.
$Na_2CO_3.10H_2O$	134.93 ± 0.3 e.u.*	133.43 ± 0.2 e.u.

* Obtained from measuring the enthalpy changes and dissociation pressures of water in the reactions

$$Na_2CO_3(c) + H_2O(g) \longrightarrow Na_2CO_3.H_2O(c)$$

$$Na_2CO_3.H_2O(c) + 9H_2O(g) \longrightarrow Na_2CO_3.10H_2O(c)$$

The residual entropy in the decahydrate is interpreted in terms of disorder in someof the hydrogen bonding. The thesis concludes with a brief summary of studies of residual entropy in hydrates.

References to the Abstract.

1. Fisher, M.E. Phys. Rev. 124. (1961) 1664
2. Kasteleyn, P.W. Physica 27 (1961) 1209
3. " " 29 (1963) 1329
4. Fowler, R.H. and Rushbrooke G.S., Trans. Farad. Soc. 33 (1937) 1272
5. Waterfield, C.G. D.Phil Thesis. Oxford (1967)
6. Furukawa, G.T. et al. J.R.N.B.S. 47 (1951) 256.
7. Sklyankin, A.A. and Strelkov P.G. Zhw. Priklad. Mech. i Tech. Fiz. 2 (1960) 100
8. Suga, H and Seki, S Bull Chem. Soc. Japan. 38 (1965) 1000
9. Anderson C.T., J. Am. Chem. Soc. 56 (1934) 340
10. Nernst, W and Schwess Sitzb. Konig press Aked. Wiss (1914) 353
11. Simon, F and Swain, R.C. Z. Phys. Chem. 28B (1935) 189.
12. Güntler, P Ann. Phys. 51 (1916) 828
13. Backstrom, H.L.J. J. Am. Chem. Soc. 47 (1925) 2441.
14. 'Order-Disorder Phenomena' by H. S. Green and C. A. Hurst, Interscience, (1964), ch. 1.
15. van Kempen et al. Physica 30 (1964) 1131.